

RESISTIVE AND REACTIVE ELEMENTS

BASED ON

GALVANOMAGNETIC EFFECTS

---

A Thesis

Presented to

The Faculty of Graduate Studies and Research

The University of Manitoba

---

In Partial Fulfillment

of the Requirements for the Degree of

MASTER OF SCIENCE

in

Electrical Engineering

---

by

KOHEI JOKURA

May, 1971.



## ABSTRACT

A new method of producing variable solid state elements for inductance, capacitance, positive or negative resistance, or the combination of them has been developed on the basis of the galvanomagnetic effects. The elements are versatile and can provide pure resistance or pure reactance with a wide range of magnitude or impedance of any quality factors; and they can be easily miniaturized for integrated microelectronic circuits.

Experimental results obtained from prototype elements indicate that the experiment agrees well with the theoretical model and that the elements will be useful not only for microelectronics, but also for many other applications.

## ACKNOWLEDGEMENTS

The author wishes to acknowledge the assistance given by Dr. K.C. Kao, who suggested the project and supervised the work throughout.

The financial support of the National Research Council of Canada under Grant A-3339 is deeply appreciated.

## CONTENTS

	Page
CHAPTER I INTRODUCTION .....	1
CHAPTER II THE PRINCIPLES OF PASSIVE MAGNETO- REACTIVE ELEMENT .....	5
2.1 The Hall Effect .....	6
2.2 Equivalent Circuit of a Hall Specimen	17
2.3 Magnetoreactive Elements .....	23
2.4 The Experimental Performance of the Magnetoreactive Elements .....	30
CHAPTER III THE PRINCIPLES OF ACTIVE MAGNETORE- ACTIVE ELEMENTS .....	30
3.1 Equivalent Impedance of An Active Network .....	31
3.2 Equivalent Impedance of An Active Hall Element .....	37
CHAPTER IV RESISTIVE AND REACTIVE ELEMENTS .....	44
4.1 Fabrication of The Element and General Requirements .....	44
4.2 Analysis of the Resistive and Reactive Element Based on Galvanomagnetic Effect (R.R.E.G.).....	51
4.3 The Electrical Characteristics of the Resistive and Reactive Element Based on Galvanomagnetic Effect (R.R.E.G.).....	54

	Page
CHPATER V EXPERIMENTAL RESULTS AND DISCUSSION ..	72
5.1 Equivalent Impedance with D.C. power Source and D.C. Active Hall Load .....	72
5.2 Equivalent Impedance with A.C. Source and A.C. Active Hall Load .....	79
5.3 Resistive and Reactive Element Based on Galvanomagnetic Effect (R.R.E.G.)	85
5.4 The Use of R.R.E.G. in An Experi- mental Tuned Circuit .....	98
CHPATER VI CONCLUSION .....	109
APPENDIX A THE TIME DEPENDENCE OF EQUIVALENT IMPEDANCE .....	112
APPENDIX B THE PHYSICAL MEANING OF Q .....	116
BIBLIOGRAPHY .....	117

## LIST OF FIGURES

		Page
Fig. 2.1	Charge carrier movement in the semiconductor under a steady magnetic field $B$ and a d.c. electric field $F$ which is perpendicular to $B$ .	7
Fig. 2.2	The Hall specimen under the magnetic field $B_z$ and electric field $F_x$ .	7
Fig. 2.3	The effect of the specimen dimension on the Hall voltage. (after Hausler, 1968)	9
Fig. 2.4 (a)	Charge carrier concentration in silicon samples containing boron as a function of reciprocal absolute temperature.	13
Fig. 2.4 (b)	Hall mobility of holes in silicon samples containing boron as a function of absolute temperature.	13
Fig. 2.4 (c)	Charge carrier concentration in silicon samples containing arsenic as a function of reciprocal absolute temperature.	14
Fig. 2.4 (d)	Hall mobility of electrons in silicon samples containing arsenic as a function of absolute temperature.	14

		Page
Fig. 2.4 (e)	Hall coefficient of silicon samples containing boron as a function of reciprocal absolute temperature.	15
Fig. 2.4 (f)	Hall coefficient of silicon samples containing arsenic as a function of reciprocal absolute temperature.	15
Fig. 2.5	Temperature dependence of the Hall coefficient, resistivity and electron mobility of InAs.	16
Fig. 2.6	Frequency dependence of the Hall field ( after Keith, 1960).	19
Fig. 2.7	Four-terminal Symmetrical Hall specimen and its equivalent circuit.	20
Fig. 2.8	Three terminal un-symmetrical Hall specimen and its equivalent circuit.	22
Fig. 2.9	Hall specimen consisting of multi-Hall terminals and its equivalent circuit.	24
Fig. 2.10	Magnetoreactive element with mono-pair Hall terminals.	25
Fig. 2.11	Magnetoreactive element with multi-pair Hall terminals.	25
Fig. 2.12	Experimental results of four-pair Hall terminal magnetoreactive element.	29

		Page
Fig. 3.1	An active network and its equivalent circuit.	33
Fig. 3.2	An active Hall element consisting of an active Hall load.	39
Fig. 3.3	Equivalent circuit of Fig. (3.2).	39
Fig. 4.1	The resistive and reactive element based on galvanomagnetic effect (R.R.E.G.).	46
Fig. 4.2	Circuit diagram of R.R.E.G..	49
Fig. 4.3	Equivalent circuit of R.R.E.G.	50
Fig. 4.4	R, X and Q as functions of $\gamma$ for $H = 0$ and $ p(\omega) G = 10$ .	55
Fig. 4.5	R, X and Q as functions of $\gamma$ for $H = 6 \Omega$ and $ p(\omega) G = 10$ .	56
Fig. 4.6	R, X and Q as functions of $\gamma$ for $H = 10 \Omega$ and $ p(\omega) G = 10$ .	57
Fig. 4.7	R, X and Q as functions of $\gamma$ for $H = 12 \Omega$ and $ p(\omega) G = 10$ .	58
Fig. 4.8	Simple phase shifter for current source.	60
Fig. 4.9	Frequency dependence of real and imaginary parts of $P(\omega)$ for current source.	61
Fig. 4.10	Frequency dependence of real and imaginary parts of $P'(\omega)$ for current source.	62

Fig. 4.11	Simple phase shifter for voltage source.	64
Fig. 4.12	Frequency dependence of real and imaginary parts of $P'(\omega)$ for a voltage source.	66
Fig. 4.13	Frequency dependence of real and imaginary parts of $P'(\omega)$ for a voltage source.	67
Fig. 4.14	Frequency dependence of R and X for various G with $H = 10 \Omega$ .	68
Fig. 4.15	Frequency dependence of R and X for various G with $H = 30 \Omega$ .	69
Fig. 4.16	Frequency dependence of R and X for $H = 10, 20$ and $30 \Omega$ with $G = 10,000$ .	69
Fig. 4.17	Frequency dependence of R and X for $H = 10, 20$ and $30 \Omega$ with $G = 10,000$ .	71
Fig. 5.1	Experimental set-up (a) and its equivalent circuit (b).	73
Fig. 5.2	V as a function of $I_H$ for the case $R_0 \gg R_1$ and $E_0 \gg K_H B I_H$ .	75
Fig. 5.3	I and Z as functions of $I_H$ for the case $R_0 \sim 0$ and $V = E_0$ .	76
Fig. 5.4	V, I and Z as functions of $I_H$ for $R_0$ having the same order of the value of $R_1$ .	78

		Page
Fig. 5.5	Experiment set-up for measuring the values of $Z$ as a function of $\phi$ ( $= \tan^{-1} \frac{X}{R}$ ) and $\left  \frac{I_H}{I} \right $ for $\omega_0 = 2\pi \cdot 10\text{KH}_z$ and $\omega_0 - \omega_1 = 0.2 \text{ H}_z$ .	82
Fig. 5.6	$Z$ as a function of $\phi = \tan^{-1} \frac{X}{R}$ and $\left  \frac{I_H}{I} \right $ for $\omega_0 = 2\pi \cdot 10\text{KH}_z$ and $\omega_0 - \omega_1 = 0.2\pi \text{H}_z$ .	83
Fig. 5.7	$Z$ and $\phi$ as functions of time.	84
Fig. 5.8	Experimental set-up for measuring $Z$ as a function of $\gamma$ between $I$ and $I_H$ .	88
Fig. 5.9	$ Z $ and $\phi$ as functions of $\gamma$ and $\left  \frac{I_H}{I} \right $ .	89
Fig. 5.10	$R$ and $X$ as functions of frequency.	90
Fig. 5.11	$X$ as a function of frequency and phase shifter capacitance.	91
Fig. 5.12	$R$ as a function of frequency and phase shifter capacitance.	92
Fig. 5.13	$R$ and $X$ as functions of frequency.	93
Fig. 5.14	$X$ as a function of frequency and phase shifter capacitance.	94
Fig. 5.15	$R$ as a function of frequency and phase shifter capacitance.	95
Fig. 5.16	$R$ and $X$ as functions of frequency and direction of Hall current.	96
Fig. 5.17	$R$ and $X$ as functions of frequency and phase shifter capacitance.	97

		Page
Fig. 5.18	Z $G_1 = 0.583 \times 10^4$ ( $R_{I2} = 1K \Omega$ ) and $G_2 = 1.23 \times 10^4$ ( $R_{I2} = 567 \Omega$ ).	99
Fig. 5.19	The use of a (R.R.E.G.) in an oscillator circuit.	100
Fig. 5.20	Experimental results of current oscillation.	102
Fig. 5.21	The use of R.R.E.G. in a tuned circuit (parallel resonance).	103
Fig. 5.22	The use of R.R.E.G. in a tuned circuit (series resonance).	104
Fig. 5.23	Experimental result of parallel resonance.	105
Fig. 5.24	Experimental result of series resonance.	106
Fig. 5.25	Parallel resonance and series resonance for different values of capacitance $C_r$ ( $C_r = 0.91\mu F$ , $0.174\mu F$ , $0.555\mu F$ , $0.385\mu F$ and $0.185\mu F$ ).	107
Fig. 5.26	$\phi_p$ for parallel resonance and $\phi$ for series resonance for different values of capacitance $C_r$ .	108
Fig. A.1	Phase relation between $E_0$ and $E_1$ for the case $ E_0  =  E_1 $ .	114
Fig. A.2	Variation of the real part and imaginary part of $E_1/E_0$ .	115

## NOMENCLATURE

A	Current gain of an amplifier.
$A_1$	Current gain of the first stage of an amplifier.
$A_2$	Current gain of the second stage of an amplifier.
B	Applied magnetic field (flux density).
$B_3$	Magnetic field in z direction.
C	Capacitance.
$C_p$	Phase shifter capacitance.
$C_{p1}, C_{p2}$	Phase shifter capacitances in the first stage and the second stage of an amplifier, respectively.
$C_r$	Resonance capacitance.
d	Thickness of Hall specimen
$E_d$	The voltage of driving source for $I_H$ .
$E_g$	Intrinsic ionization energy or energy gap between the edges of conduction band and valence band.
$E_2, E_{21}, E_{22}, \dots, E_{2m}$	Potential of Hall terminals.
$E_0$	Thévenin potential of a power source.
$E_1$	Thévenin potential of an active load.
$E_2$	Internal Hall voltage across the Hall terminals.
F	Electric field strength.

$F_{x1}$	Electric field in x direction.
$F_y$	Hall field strength.
$f_H$	Geometrical influence factor.
$f_0, f_1$	Reference frequencies.
G	Current gain and generation constant.
H	Thévenin impedance of an active load. across the terminals, a and b.
I	Current passing the current terminals of Hall specimen.
$I_{A1}$	Output current of first stage of an amplifier.
$I_H$	Hall current passing through the Hall terminals.
$I_x$	Current in x direction.
$i_{A1}, i_{A2}$	Input current of first and second stage of an amplifier, respectively.
$J_x$	Electric current density in x direction in a semiconductor.
j	$= \sqrt{-1}$
$K_H, K_{H1}, K_{Hm}$	Hall sensitivities.
k	Boltzman constant.
l	Length of the Hall specimen.
m	Number of Hall terminals pairs.
n	Carrier concentration in a semi- conductor.

P, P'	Phase shift and attenuation factor.
Q	Quality factor of an impedance which is equal to the absolute value of the imaginary part divided by the value of the real part.
q	Elementary electronic charge.
R	Real part of the impedance Z, across the terminals a to b.
R <sub>b</sub>	Bypass resistance across the input terminals of the amplifier and phase shifter unit.
R <sub>H</sub>	Hall coefficient.
R <sub>I1</sub> , R <sub>I2</sub>	Real part of Z <sub>I1</sub> and Z <sub>I2</sub> respectively.
R <sub>s</sub>	Resistance connected in series to the current terminals of the Hall specimen.
R <sub>1</sub>	Real part of Z, and also internal resistance across the current terminals of the Hall specimen.
R <sub>2</sub> , R <sub>21</sub> ....R <sub>2m</sub>	Internal resistances across the Hall terminals of the Hall specimen.
S	Hall specimen.
T	Absolute temperature.
Tr <sub>1</sub> Tr <sub>s</sub>	Transistors
t	Time (secs).
V	Terminal voltage across the terminals a and b.

$V_{A1}$	Output voltage of the first stage of an amplifier.
$V_H$	Hall voltage across the Hall terminals.
$v$	Average velocity of charge carriers in a semiconductor.
$w$	Width of the Hall specimen.
$X$	Imaginary part of $Z$
$X_c$	Reactance of capacitor.
$X_{cr}$	Reactance of capacitor at resonance.
$X_d$	Imaginary part of $Z_d$ .
$X_{p1}, X_{p2}$	Imaginary part of the first phase shifter and the second phase shifter, respectively.
$X_1$	Imaginary part of $Z_1$ .
$x, y, z$	
$Z$	Impedance across the terminals a and b.
$Z_d$	Thévenin impedance of an active Hall load.
$Z_{I1}, Z_{I2}$	Input impedance of the first stage excluding $R_S$ , and the second stage of the amplifier and phase shifter unit respectively.
$Z_{rp}, Z_{rs}$	Parallel and series resonance impedance across the terminals a and b respectively.
$Z_0, Z_1$	Thévenin impedance of a power source and an active load, respectively.
$Z_{11}, Z_{22}$	Input impedance and output impedance of the $Z$ parameter, respectively.

$Z_{12}, Z_{21}$	Reverse and forward transfer impedance of the Z parameter, respectively.
$\alpha$	Phase angle between $E_0$ and I.
$\beta$	Phase angle between $E_1$ and I.
$\gamma$	Phase angle between $I_H$ and I.
$\xi$	Magnitude of $E_0 / E_1$ .
$\epsilon_r$	Relative permittivity.
$\epsilon_0$	Permittivity of vacuum.
$\theta$	Hall angle between $E_x$ and E.
$\mu_e$	Electron mobility in a semiconductor.
$\sigma$	Electrical conductivity.
$\tau$	Collision relaxation time.
$\phi$	Phase angle between the imaginary part and the real part of an impedance Z.
$\phi_{rp}, \phi_{rs}$	Phase angle between the imaginary part and the real part of $Z_{rp}$ and $Z_{rs}$ , respectively.
$\psi$	Phase angle between $E_0$ and $E_1$ .
$\psi_0$	Initial phase angle between $E_0$ and $E_1$ at $t = 0$ .
$\omega$	Angular frequency.
$\omega_c$	Angular collision frequency.
$\omega_d$	Angular frequency corresponding to the dielectric relaxation time $t_d$ .
$\omega_p$	Angular plasma frequency.
$\omega_0$	Angular frequency of power source.
$\omega_1$	Angular frequency of active Hall load.

## CHAPTER I

## INTRODUCTION

In the past ten years a number of different techniques have been proposed for the fabrication of monolithic resistors and capacitors for microcircuits. These elements still have some limitations from the view point of their applications, but they do accomplish some desired functions (Lin, 1967; Gandhi, 1968). However, monolithic or miniaturized inductors with high values of quality factor,  $Q$ , have not yet been successfully achieved. Although considerable effort has been made to develop a method to represent an inductance by means of an active circuit, such as the use of transistorized gyrators, impedance convertors or operational amplifiers (Laxpati and Mitra, 1962; Josephs, George and Billette, 1965; Capparelli, 1967), they are quite inferior in electrical characteristics to commonly available conventional inductors and take up considerably more space than active elements (Barnwell, 1970). This is why in practice their use is generally avoided whenever possible and why in most practical integrated circuits desired functions are accomplished by means of special circuits without the use of inductance.

The trend toward miniaturization makes it desirable to fabricate circuit elements using semiconductors. In 1965 Kataoka et al were the first to produce a solid state inductor based on the magneto-reactive characteristics of the Hall effect. They connected a capacitor to the Hall terminals of an InSb specimen so that the current flowing through this capacitor will produce a potential across the current terminals, which is not in phase with the applied voltage; and therefore the impedance across the current terminals is not purely resistive, but consists of both resistive and reactive components. This method is quite limited and there are many disadvantages associated with it. The major disadvantages are:

- (1) it is difficult to obtain a high inductance because this would require a high magnetic field or a high capacitance across the Hall terminals,
- (2) it is difficult to vary the impedance across the current terminals to any values desired, and
- (3) it is difficult to obtain a practical value of  $Q$ .

They reported that the highest value of  $Q$  for a mono-Hall terminal InSb element at 10 k-Gauss is 0.19

(Kataoka et al, 1965) and that for a five-Hall terminal one is 0.64 (Toda, 1966). The multi-Hall terminal method proposed by Kataoka et al (1966) does not increase appreciably the value of  $Q$ . They also suggested a P-D-N (P-type semiconductor-dielectric material-N-type semiconductor) structure for the magnetoreactive elements but the value of  $Q$  still could not be increased to a value higher than unity. Because of the inherent shortcomings of the models of Kataoka et al, the present project being described in this thesis has been carried out to study the shortcomings and to find a method to overcome them.

In this thesis Chapter II describes the basic principle of the magnetoreactive elements proposed by Kataoka et al and their shortcomings. Chapter III describes a new element developed in the Materials Research Laboratory of the University of Manitoba. In this element an active source instead of a passive element is connected across the Hall terminals so that the input impedance of the element is a function of both the magnitude and phase of the current passing through the Hall terminals. The method of producing an active source derived from the circuit to be connected to the current terminals of the element and the electrical characteristics of this new element are described in Chapter IV, and some experimental results showing the

good agreement between the theory and experiments are given in Chapter V. General conclusions are given in Chapter VI.

## CHAPTER II

## THE PRINCIPLES OF PASSIVE MAGNETOREACTIVE ELEMENTS

It is well known that the resistance of a Hall semiconductor specimen can be varied by varying either the magnetic field or the external resistance connected across the Hall terminals. (Motto, 1962; Weiss, 1968). The Hall voltage between the Hall terminals produces a current flowing through the external resistance and hence creates a second Hall voltage across the current terminals. It is this second Hall voltage which oppose the external applied voltage across the current terminals so as to increase the resistance between these two terminals. This effect is generally referred to as the "magnetoresistive effect" and its validity does not depend on the form of applied fields; that is, the same effect can be observed either with d.c. voltages or with a.c. voltages.

If a reactance instead of the pure resistance is connected to the Hall terminals, the Hall current will produce a second Hall voltage across the current terminals, which is no longer in phase with the applied a.c. voltage so that the impedance across the current terminals will consist of a reactive component as well as a resistive component. The element which

can produce a reactance in a magnetic field is called the magnetoreactive element. In the following the principle and characteristics of such an element fabricated in various ways are discussed.

## 2.1 The Hall Effect

Before considering the a.c. electric field, let us review some basic phenomena of the Hall effect in a semiconductor under a steady applied magnetic field  $\vec{B}$  and a d.c. electric field  $\vec{F}$  which is perpendicular to  $\vec{B}$ . In this case the electrons will move circularly until they suffer a collision with imperfections, the average time between two collisions being called "the relaxation time". After one collision the electrons will start to move again under the influence of  $\vec{B}$  and  $\vec{F}$  as shown in Fig. (2.1). The angle  $\theta$  between  $\vec{F}$  and the current  $\vec{I}$  is called the "Hall angle", which is positive for electrons and negative for holes. For a fixed direction of  $\vec{B}$  and  $\vec{F}$  the Lorentz force  $|q(\vec{F} + \vec{v} \times \vec{B})|$  acting on the electrons is in the same direction as that acting on the holes although the general direction of the current due to electrons may differ very little from that due to holes ---- mainly due to the difference between the mobilities of electrons and holes.

When the applied electric field  $F_x$  is in the

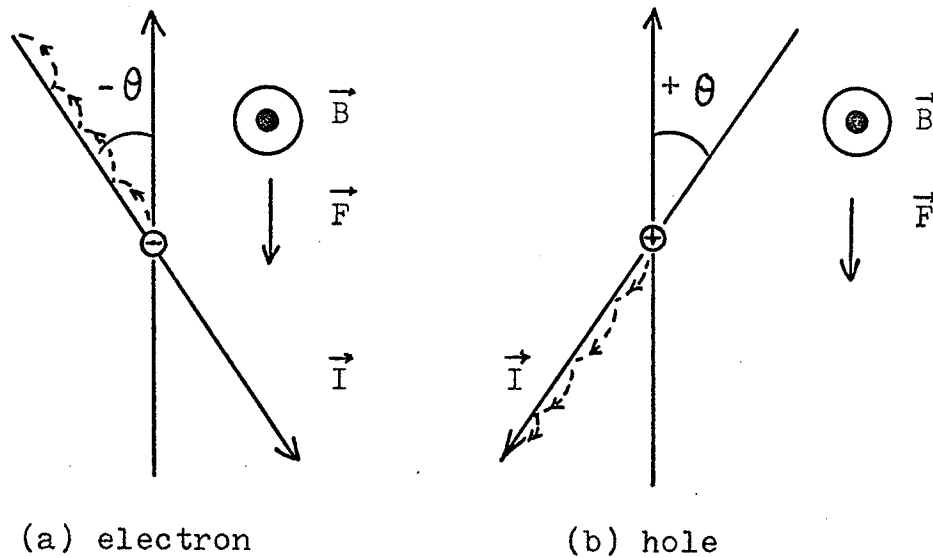


Fig. (2.1) Charge carrier movement in the semiconductor under a steady magnetic field  $B$  and a d.c. electric field  $F$  which is perpendicular to  $B$ .

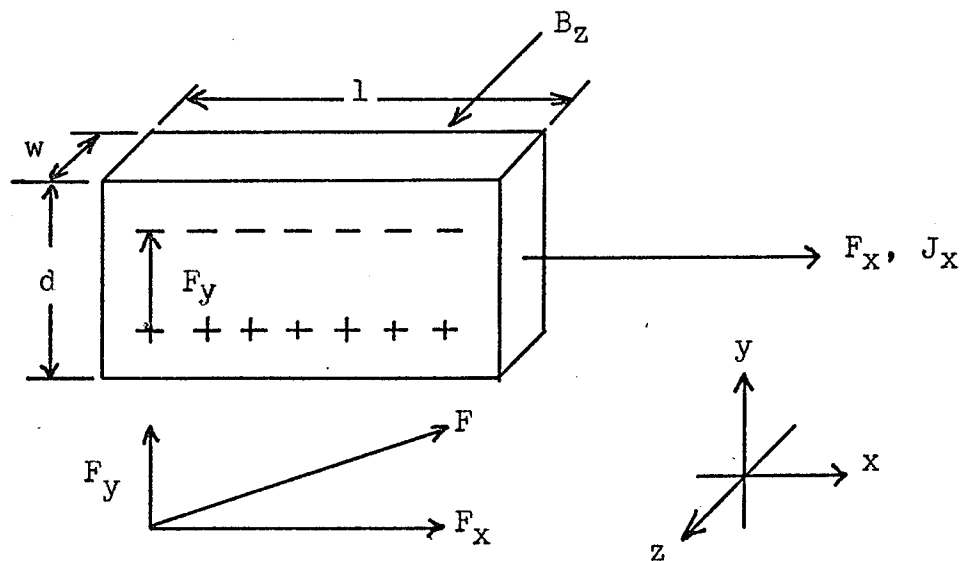


Fig. (2.2) The Hall specimen under the magnetic field  $B_z$  and electric field  $F_x$ .

$x$  -direction, and the applied magnetic field  $B_z$  in the  $z$ -direction, the Hall field  $F_y$  will be in  $y$  -direction as shown in Fig. (2.2). The Hall angle is thus defined by

$$\tan \theta = \frac{F_y}{F_x} \quad (2.1)$$

and the Hall field by

$$F_y = R_H J_x B_z \quad (2.2)$$

where  $R_H$  is the Hall coefficient. Since in the steady state the Lorentz force must balance the electrostatic force due to the Hall field, thus  $F_y$  can also be written as

$$\begin{aligned} F_y &= v_x B_z \\ &= \mu_e F_x B_z \\ &= \frac{J_x B_z}{n q} \end{aligned} \quad (2.3)$$

where  $J_x$  and  $v_x$  are the current density and electron velocity in the  $x$ -direction, respectively;  $\mu_e$  is the electron mobility, and  $n$  is the density of mobile electrons. Thus,

$$R_H = \frac{1}{n q} \quad (2.4)$$

If Hall element has the thickness  $d$  and the width  $w$ , then the Hall voltage is

$$\begin{aligned} V_H &= F_y w \\ &= R_H J_x B_z w \end{aligned}$$

Geometrical influence factor  $f_H$

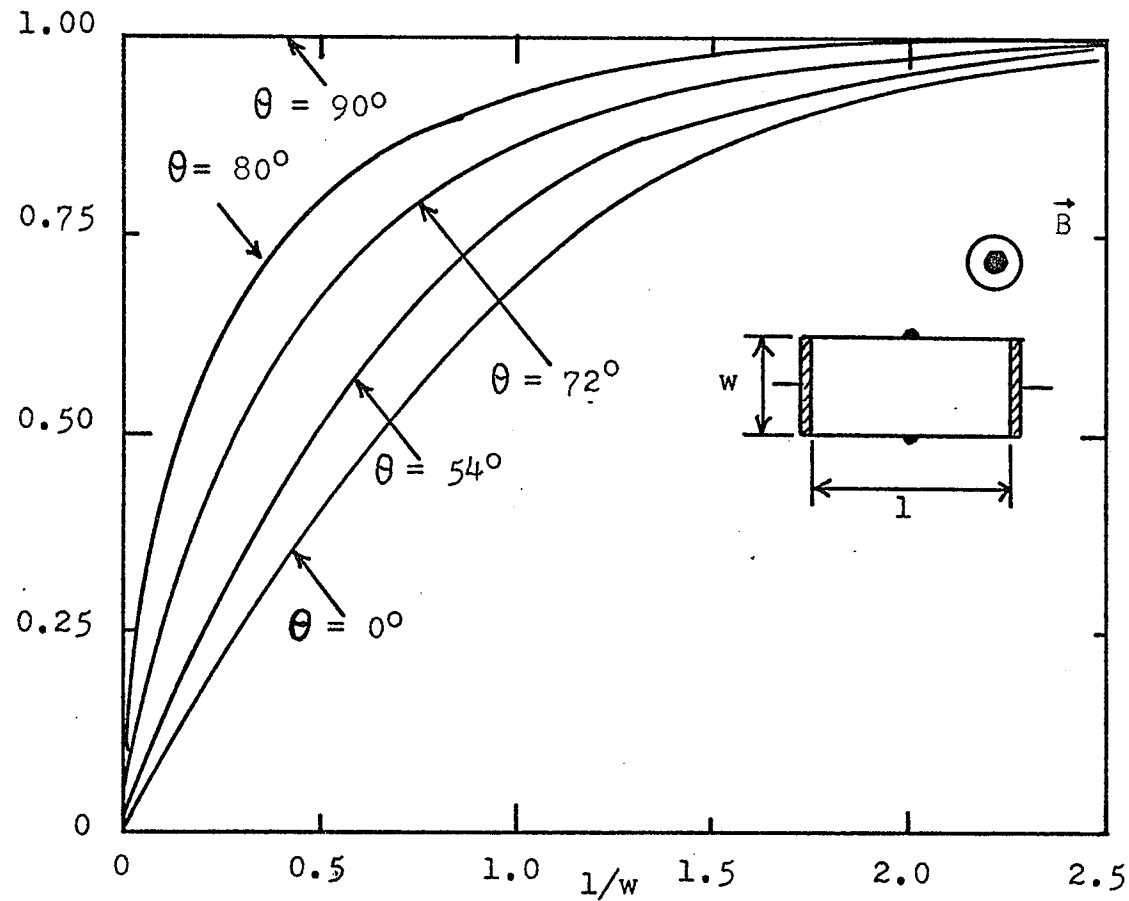


Fig. (2.3) The effect of the specimen dimension on the Hall voltage. (after Hausler, 1968)

$$\begin{aligned}
 &= \frac{R_H}{d} (J_x d w) B_z \\
 &= \frac{R_H}{d} I_x B_z \\
 &= K_H I_x B_z \quad (2.5)
 \end{aligned}$$

where  $I_x$  is the total current in the  $x$ -direction, and  $K_H$  is the Hall sensitivity which is defined by

$$K_H = \frac{R_H}{d} \quad (2.6)$$

The geometrical shape and dimension affect the Hall voltage. The Hall voltage taking into account the geometrical influence is given by (Wick, 1954; Haeusler, 1968).

$$V_H = K_H I B f_H\left(\frac{l}{w}, \theta\right) \quad (2.7)$$

where  $f_H$  is the geometrical influence factor which is a function of the Hall angle  $\theta$ , and the ratio of the length to the width of the Hall specimen. For rectangular Hall specimens Haeusler (1968) has calculated  $f_H$  as a function of  $\frac{l}{w}$  and  $\theta$  and their results are shown in Fig. (2.3). It can be seen that the geometrical influence can be ignored if the ratio  $\frac{l}{w}$  is larger than 2.

The Hall field, the Hall coefficient and the conductivity of a semiconductor depend upon temperature (Debye, 1954; Morin and Maita, 1954; Harman,

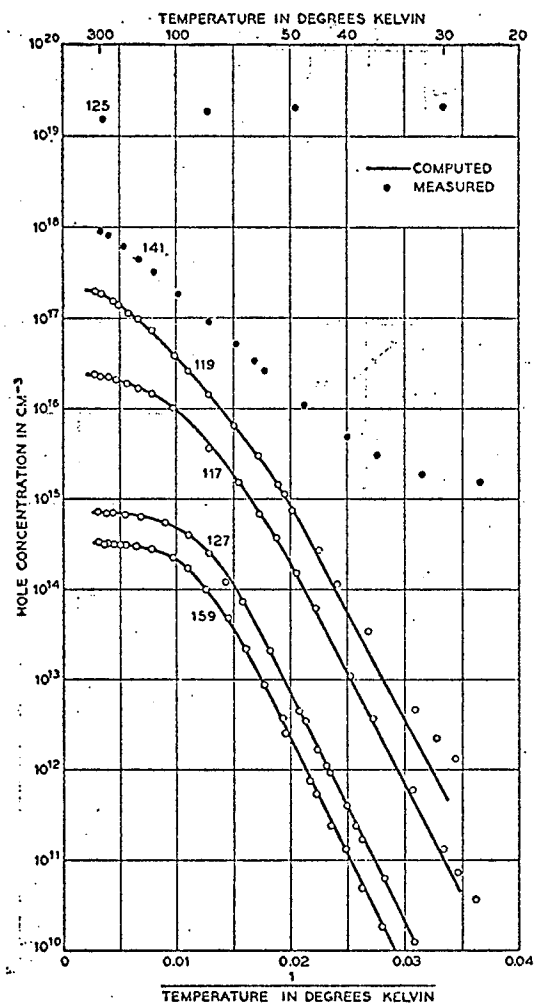
Georing and Beer, 1956). From Equations (2.3) and (2.4) the Hall field and hence the Hall coefficient are proportional to mobility of carrier and are inversely proportional to carrier concentration. The mobility generally increases with decreasing temperature because of the effects of scattering by lattice, ionized, impurity and dislocation. For intrinsic semiconductors the mobility is approximately proportional to  $T^{-3/2}$  and the carrier concentration is approximately proportional to  $T^{3/2} \exp\left(\frac{E_g}{2kT}\right)$  where  $T$  is the absolute temperature,  $E_g$  is the forbidden gap and  $k$  is the Boltzman constant (Debye 1954; Morin and Maita 1954). The temperature dependence of both carrier mobility and carrier concentration for extrinsic semiconductors containing impurities is far more complicated. However, in general, the mobility decrease, while the carrier concentration increases with increasing temperature for a certain temperature range. Fig. (2.4) shows the temperature dependence of the Hall coefficient, electron mobility and concentration of Si containing Arsenic and Boron, and Fig. (2.5) shows the temperature dependence of the Hall coefficient and resistivity of InAs.

If the magnetic field remains steady but the applied electric field is alternating and sinusoidal, the Hall field and the Hall coefficient will not be

The following data are for Figs. (2.4) (a), (b), (c), (d), (e), (f). The results shown in these are obtained by Morin et al (1954).

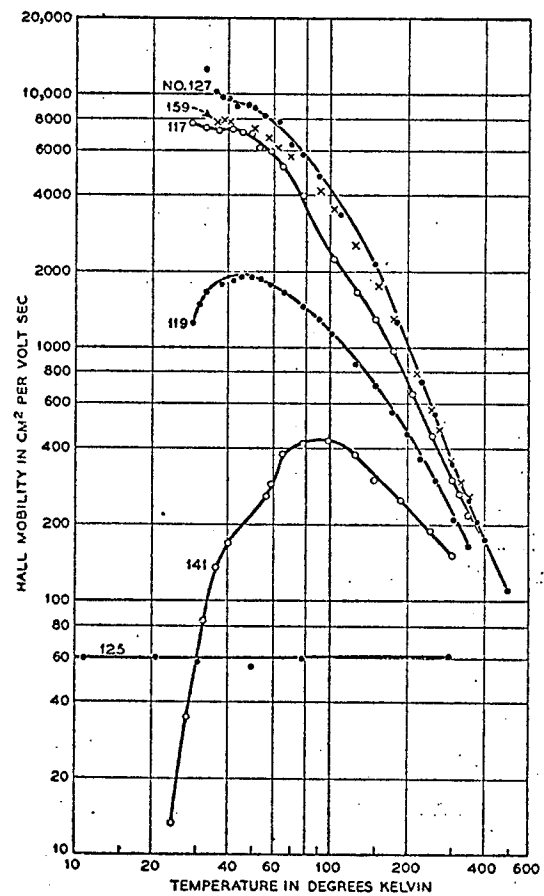
The Composition of samples and summary of extrinsic range results.

Sample No.	Majority impurity ionization energy ev	Net impurity concentration $\text{cm}^{-3}$	Minority impurity concentration $\text{cm}^{-3}$	Mass parameter	Added impurity
n type					
131	0.056	$1.75 \times 10^{14}$	$1.0 \times 10^{14}$	0.5	arsenic
130	0.049	$2.1 \times 10^{15}$	$5.25 \times 10^{14}$	1.0	arsenic
129	0.048	$1.75 \times 10^{16}$	$1.43 \times 10^{15}$	1.2	arsenic
139	0.046	$1.3 \times 10^{17}$	$2.2 \times 10^{15}$	1.0	arsenic
126	?	$2.2 \times 10^{18}$	...	...	arsenic
140	degenerate	$2.7 \times 10^{19}$	...	...	arsenic
p type					
159	0.045	$3.1 \times 10^{14}$	$4.1 \times 10^{14}$	0.4	none
127	0.045	$7.0 \times 10^{14}$	$2.2 \times 10^{14}$	0.4	boron
117	0.043	$2.4 \times 10^{16}$	$2.3 \times 10^{15}$	0.6	boron
119	0.043	$2.0 \times 10^{17}$	$4.9 \times 10^{15}$	0.7	boron
141	?	$1 \times 10^{18}$	...	...	boron
125	degenerate	$1.5 \times 10^{19}$	...	...	boron



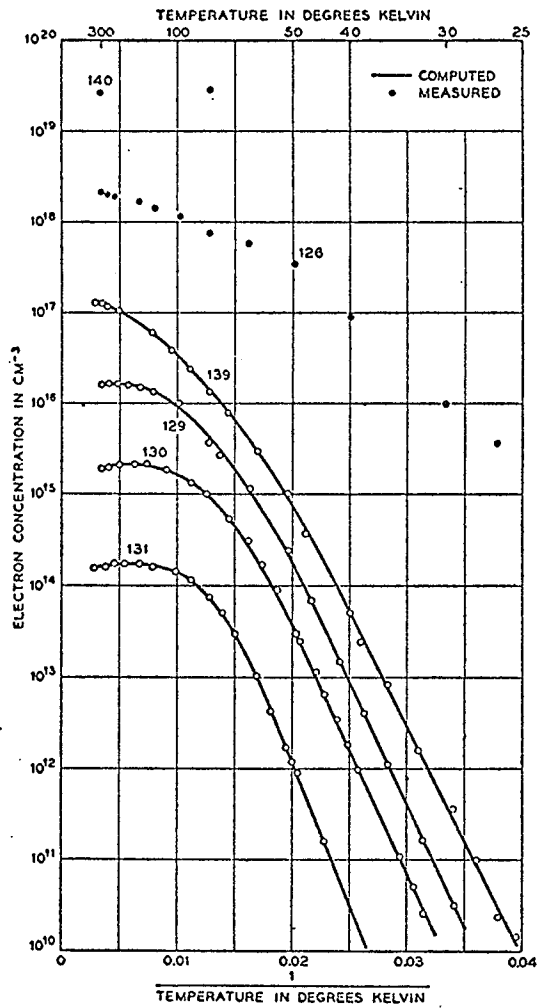
Charge carrier concentration in silicon samples containing boron as a function of reciprocal absolute temperature.

Fig. (2.4) (a)



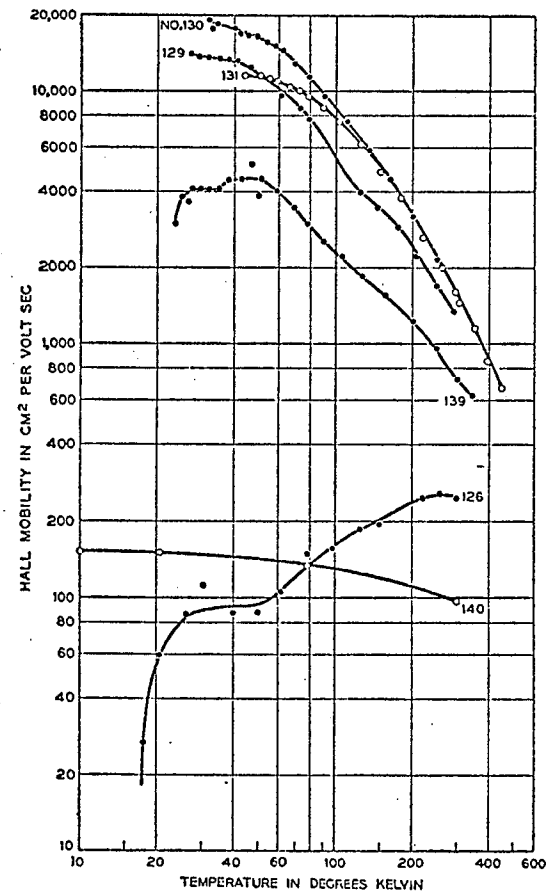
Hall mobility of holes in silicon samples containing boron as a function of absolute temperature.

Fig. (2.4) (b)



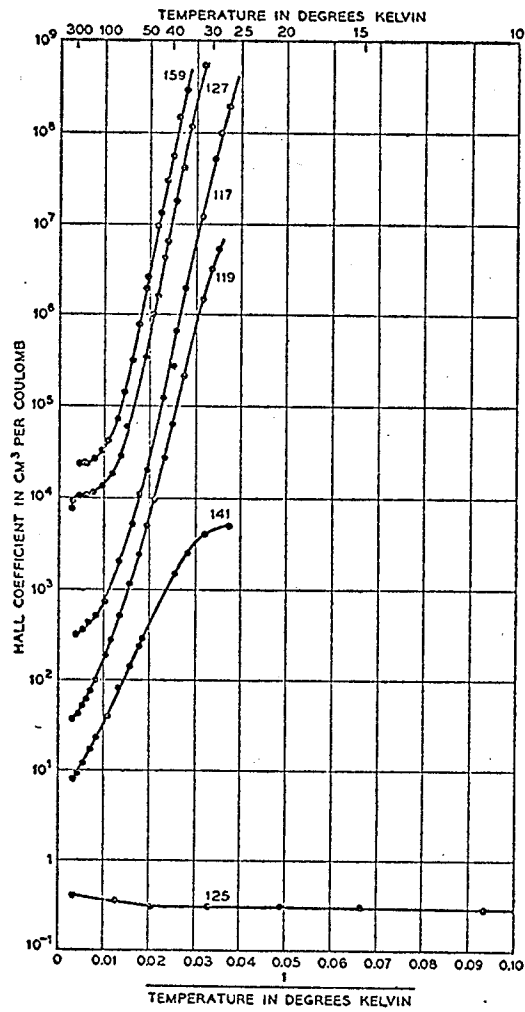
Charge carrier concentration in silicon samples containing arsenic as a function of reciprocal absolute temperature.

Fig. (2.4) (c)



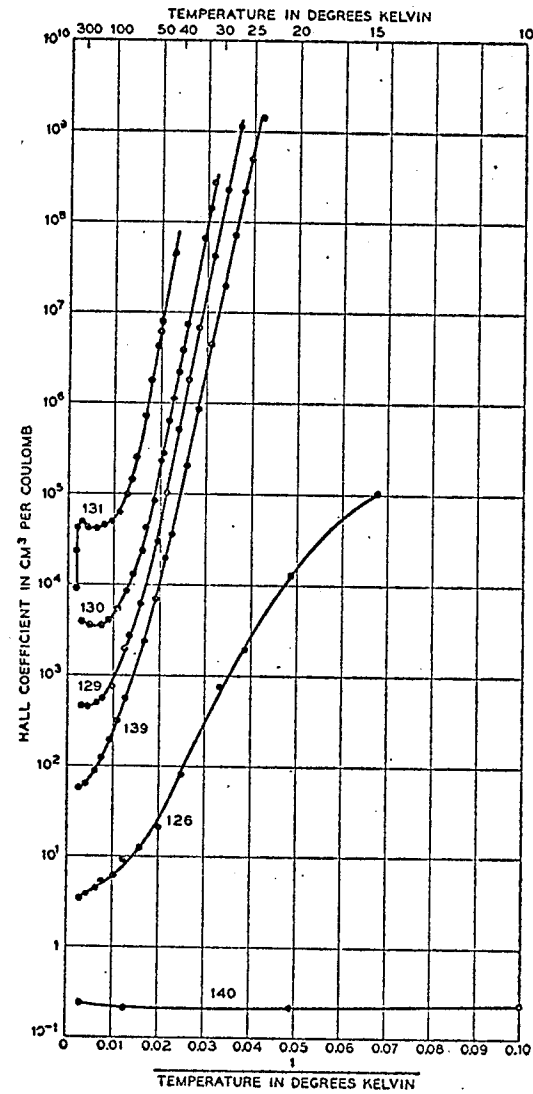
Hall mobility of electrons in silicon samples containing arsenic as a function of absolute temperature.

Fig. (2.4) (d)



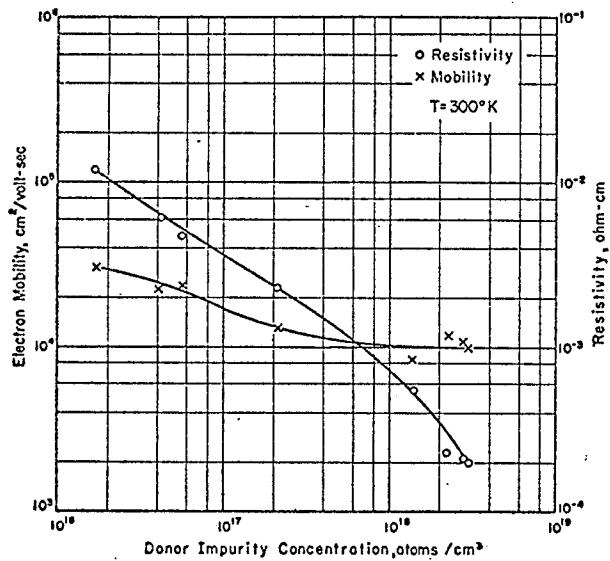
Hall coefficient of silicon samples containing boron as a function of reciprocal absolute temperature. Composition of samples given in page 12

Fig. (2.4) (e)



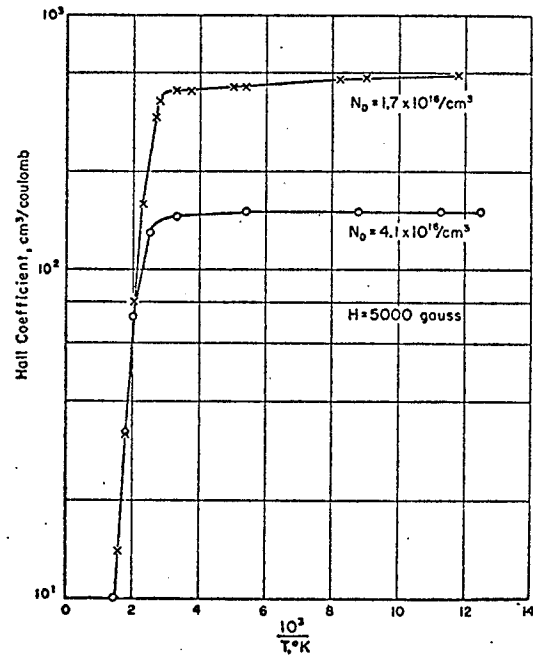
Hall coefficient of silicon samples containing arsenic as a function of reciprocal absolute temperature. Composition of samples given in page 12

Fig. (2.4) (f)



Mobility and resistivity at room temperature as a function of donor concentration.

Fig. (2.5) (a)



Hall coefficient as a function of reciprocal temperature for two InAs specimens.

Fig. (2.5) (b)

Fig. (2.5) Temperature dependence of the Hall coefficient, resistivity and electron mobility of InAs.

affected unless the frequency of the electric field approaches the value corresponding to dielectric relaxation time  $\tau_d$ . The frequency dependence of the Hall field plotted in ratio of  $F_y$  at frequency  $\omega$  to  $F_y$  at d.c. field is shown in Fig. (2.6) in which  $\omega_d = \frac{\sigma}{\epsilon_r \epsilon_0}$ ,  $\omega_c = \frac{1}{\tau}$  and  $\omega_p = \sqrt{\omega_c \omega_d}$  angular plasma frequency;  $\sigma$ ,  $\tau$ ,  $\epsilon_r$  and  $\epsilon_0$  are respectively the d.c. conductivity, collision relaxation time, relative permittivity, and permittivity in vacuum. The value of  $\omega_d$  for germanium is of the order of  $2\pi \cdot 10^{10}$  radians/sec. and for most semiconductors  $\omega_d$  is much higher than what are concerned in this thesis. However, the effect of frequency on the Hall field and Hall coefficient have been reported by many investigators (Champlin, 1960; Nishina and Spry, 1958; Barlow and Kataoka, 1958; Barlow 1962; Miller, 1961).

From Equations (2.3), (2.4) and (2.6) the higher the carrier mobility, and the lower the carrier concentration, the higher are the Hall field and the Hall coefficient. Table (2.1) gives some semiconductors which are generally used for Hall devices.

## 2.2 Equivalent Circuit of a Hall Specimen

If the current terminals are considered as two input terminals, and the Hall terminals as two output terminals as shown in Fig. (2.7) a Hall specimen can be treated as a four-terminal network. Thus

Table (2.1) Representative values of materials parameters at 300°K†

Material	$R$ cm <sup>3</sup> /C	$\rho$ Ω-cm	$n$ † cm <sup>-3</sup>	$\mu$ † cm <sup>2</sup> /V-sec	$R/\rho^{1/2}$	$k_1\mu^2$ §	$k_2(R/\rho^{1/2})$ §	$\left \frac{1}{R} \frac{dR}{dT}\right $ %/°C
n-Si	360,000	200	$2 \times 10^{13}$	1500	25,000	0.09	120	<0.01
	7000	4.5	$1 \times 10^{15}$	1300	3300	0.07	16	<0.01
n-Ge	87,000	25	$5 \times 10^{13}$	3600	17,000	0.5	85	4
	21,000	5	$3.5 \times 10^{14}$	3600	9000	0.5	45	0.3
	4250	1	$1.7 \times 10^{15}$	3500	4000	0.5	20	<0.01
GaAs	1700	0.2	$3.7 \times 10^{15}$	8500	3800	3	17	0.1
	15	0.0045	$4.2 \times 10^{17}$	3300	220	0.4	1.1	0.01
InAs	3700	0.1	$1.7 \times 10^{15}$	35,000	12,000	50	60	3
	570	0.02	$1.1 \times 10^{16}$	28,000	4000	30	20	0.1
	115	0.005	$5.5 \times 10^{16}$	23,000	1600	20	8	<0.01
InSb	380	0.005	$2 \times 10^{16}$	75,000	5400	225	27	2
	19	0.0006	$3.3 \times 10^{17}$	32,000	770	40	3.8	0.01
Bi	5-10	~0.002	~ $6 \times 10^{17}$	~5000	200	1	1	~0.4

† Data from Ross *et al.*<sup>(14)</sup> and from unpublished results at Battelle.

‡ Hall coefficient factors of approximately 1.18 were used for Si and Ge; lower values for the III-V materials.

§ The normalization factors  $k_1$  and  $k_2$  are chosen so that the values of the respective figure of merits are unity in the case of bismuth.

|| Denotes that specimen is intrinsic or nearly intrinsic.

After Beer (1966)

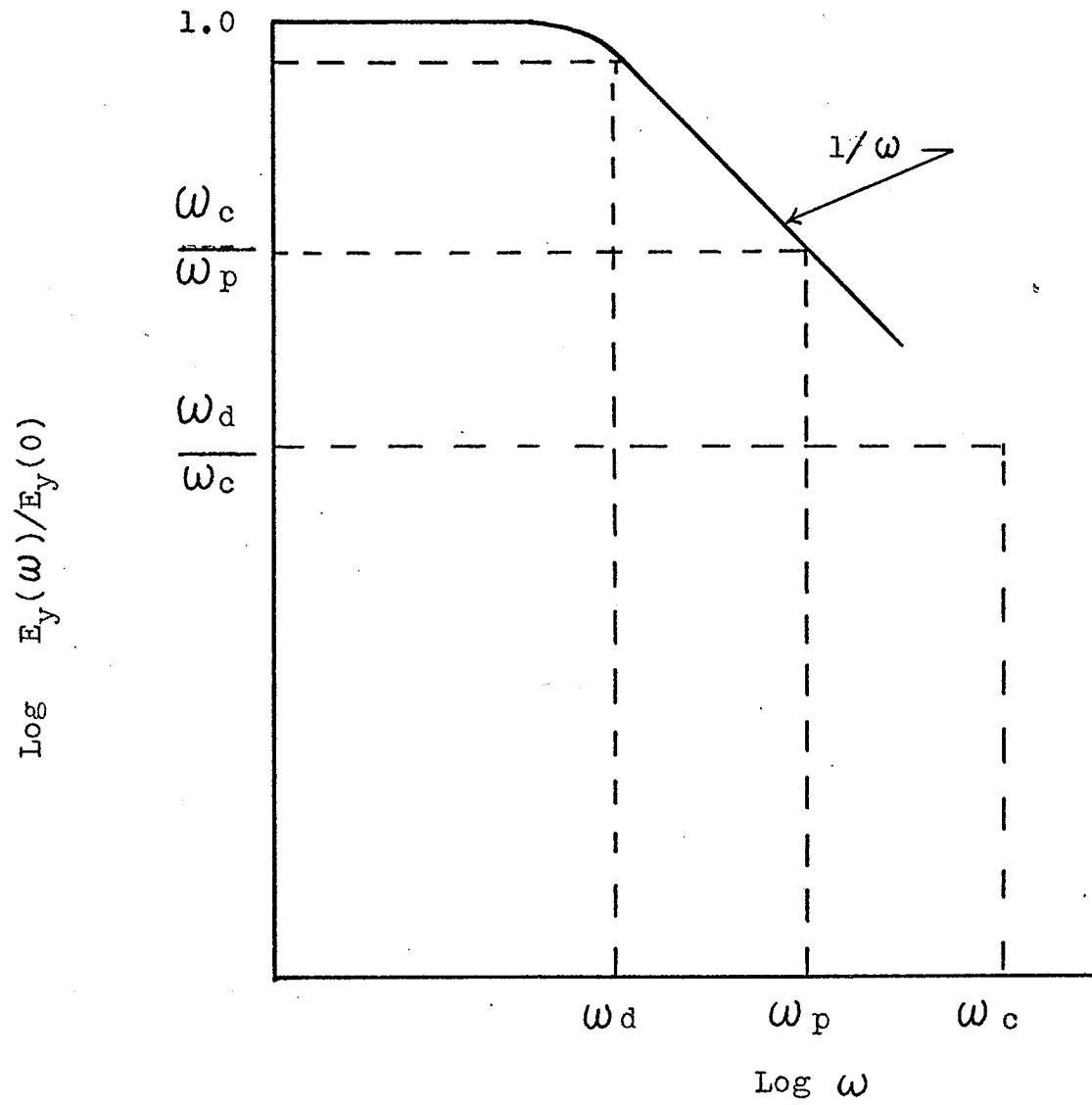


Fig. (2.6) Frequency dependence of the Hall field (after Keith, 1960)

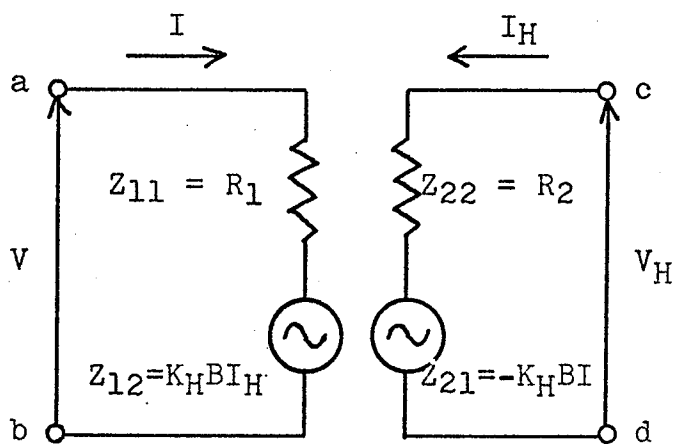
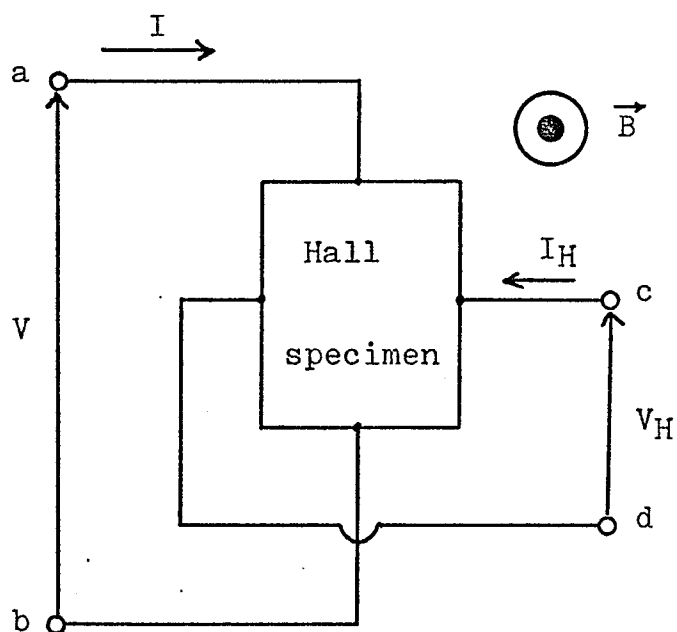


Fig. (2.7) Four-terminal Symmetrical Hall specimen and its equivalent circuit.

the input voltage  $V$  and the output voltage  $V_H$  can be expressed in terms of input current  $I$  and output current  $I_H$  as

$$\begin{aligned} V &= I Z_{11} + I_H Z_{12} \\ V_H &= I Z_{21} + I_H Z_{22} \end{aligned} \quad (2.8)$$

where  $Z_{11}$ ,  $Z_{12}$ ,  $Z_{21}$  and  $Z_{22}$  are the  $Z$ -parameters which define the characteristics of the network. The  $Z$ -parameters are given by

$$\begin{aligned} Z_{11} &= \text{input impedance} = \left. \frac{V}{I} \right|_{I_H=0} \\ Z_{22} &= \text{output impedance} = \left. \frac{V_H}{I_H} \right|_{I=0} \\ Z_{12} &= \text{reverse transfer impedance} = \left. \frac{V}{I_H} \right|_{I=0} \\ Z_{21} &= \text{forward transfer impedance} = \left. \frac{V_H}{I} \right|_{I_H=0} \end{aligned} \quad (2.9)$$

For a Hall specimen, these  $Z$ -parameters are:

$$\begin{aligned} Z_{11} &= R_1 \\ Z_{22} &= R_2 \\ Z_{12} &= K_H B \\ Z_{21} &= -K_H B \end{aligned} \quad (2.10)$$

where  $R_1$  and  $R_2$  are in fact the resistance of the Hall semiconductor specimen measured from the current terminals, and from the Hall terminals, respectively.

For a three terminal rectangular Hall specimen, the equivalent circuit is shown in Fig. (2.8).

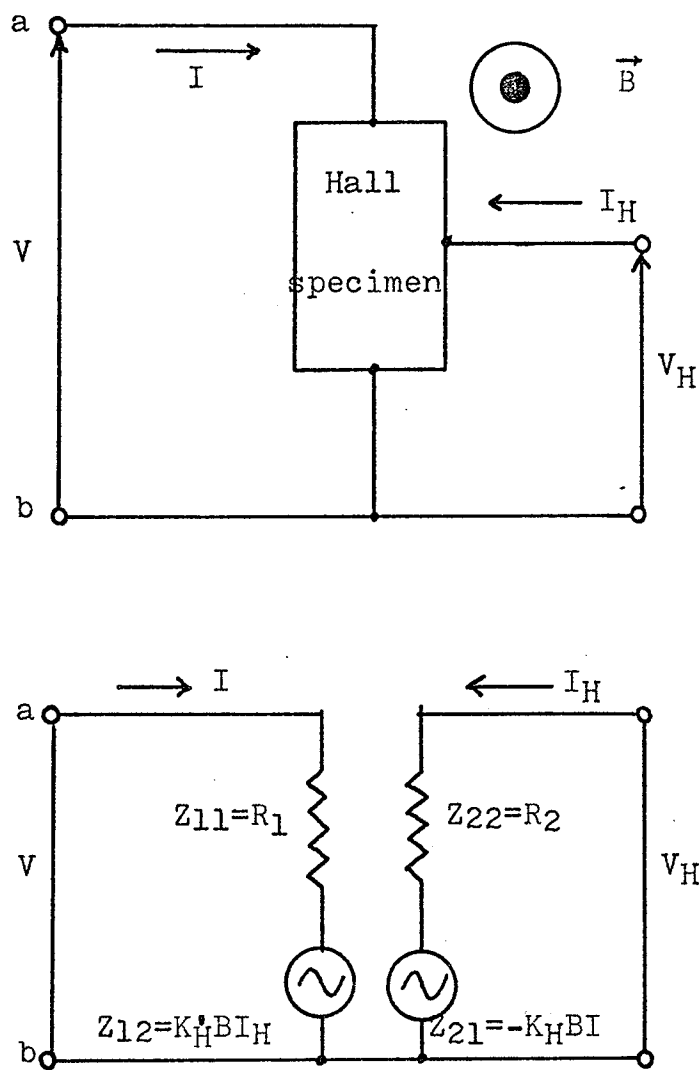


Fig. (2.8) Three terminal un-symmetrical Hall specimen and its equivalent circuit.

In this case  $R_2$  is the resistance of the Hall specimen measured between one Hall terminal and the common terminal.

For the Hall specimen consisting of multi-Hall terminals, the equivalent circuit is shown in Fig. (2.9). In this case  $R_{21}$  ----  $R_{2m}$  represents the resistances of the specimen measured between the corresponding two Hall terminals. If the Hall sensitivity is the same for each pair of Hall terminals, we have

$$E_1 = K_H B (I_{H1} + I_{H2} + \dots + I_{Hm}) \quad (2.11)$$

and  $E_{21} = E_{22} = E_{23} = \dots = E_{2m} = K_H B I$

### 2.3 Magnetoreactive Elements

The fundamental configuration of the magnetoreactive element developed by Kataoka et al (1965) is shown in Fig. (2.10). They connected a passive reactive element  $X_d$  across the Hall terminals. The electrical characteristics can be expressed by a four-terminal network, as

$$\begin{aligned} V &= R_1 I + K_H B I_H \\ V_H &= K_H B I - R_H I_H = j X_d I_H \end{aligned} \quad (2.12)$$

where all parameters have the usual meaning as given in the previous sections. From Equation (2.12) the input impedance of the element is given by

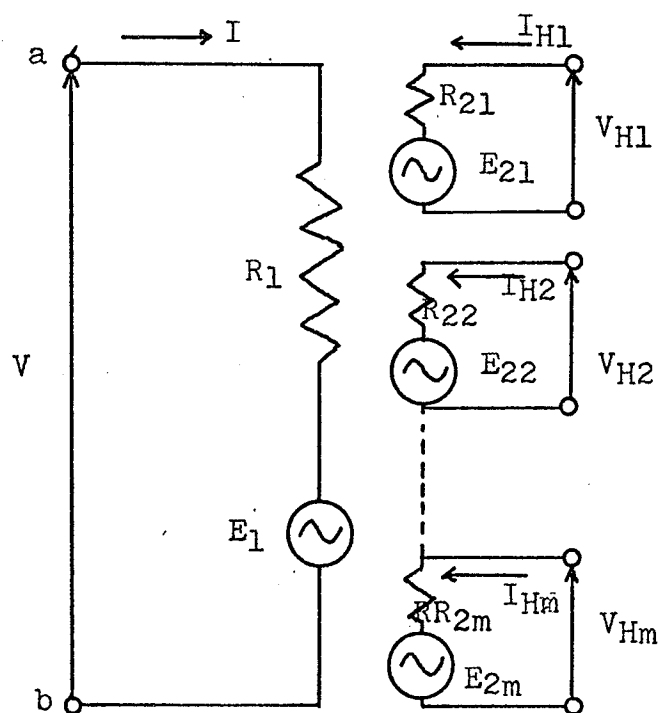
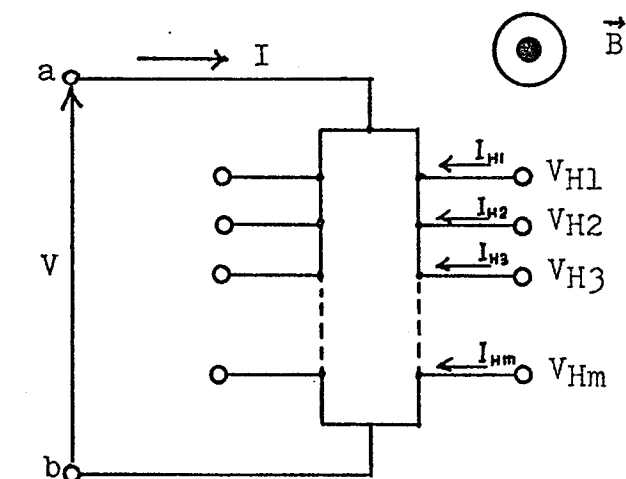


Fig. (2.9) Hall specimen consisting of multi-Hall terminals and its equivalent circuit.

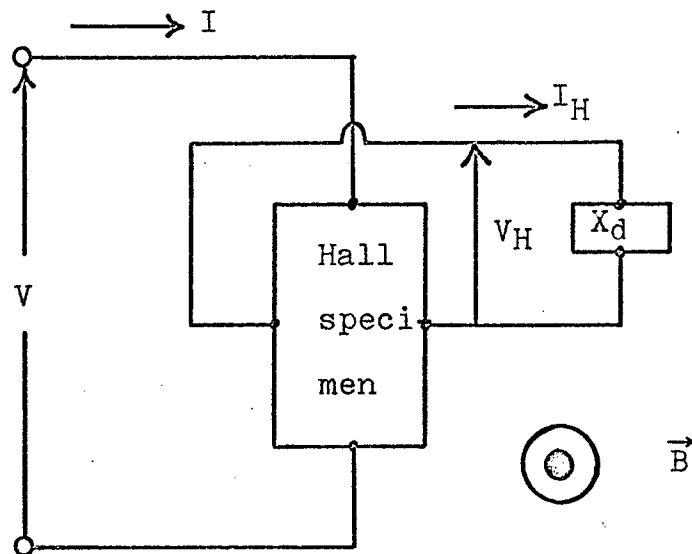


Fig. (2.10) Magnetoreactive element with mono-pair Hall terminals.

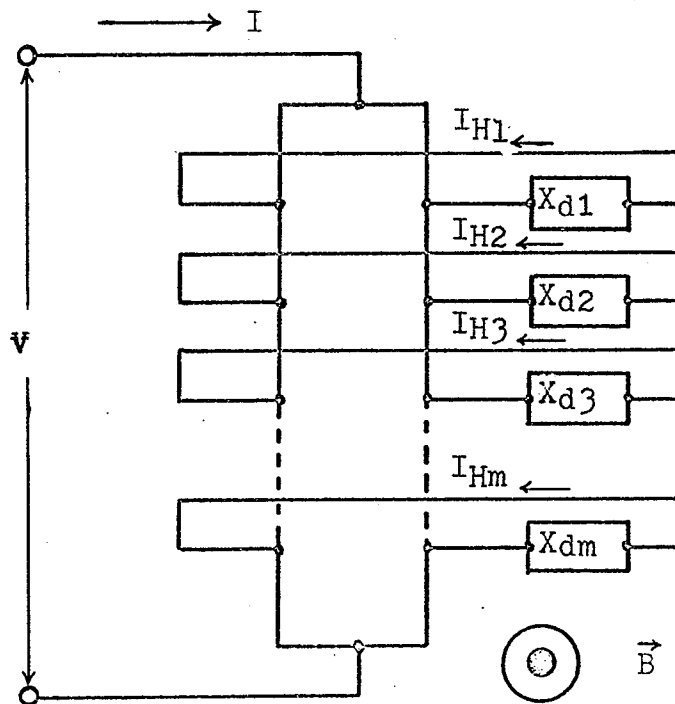


Fig. (2.11) Magnetoreactive element with multi-pair Hall terminals.

$$\begin{aligned}
 Z &= \frac{V}{I} = R_1 + \frac{K_H^2 B^2}{R_2 + jX_d} \\
 &= R_1 + \frac{K_H^2 B^2 R_2}{R_2^2 + X_d^2} - j \frac{K_H^2 B^2 X_d}{R_2^2 + X_d^2} \quad (2.13) \\
 &= R + jX
 \end{aligned}$$

Thus the impedance  $Z$  may be divided into two parts, the real component  $R$  and the reactive component  $X$ ; and they are

$$R = R_1 + \frac{K_H^2 B^2 R_2}{R_2^2 + X_d^2} \quad (2.14)$$

$$X = - \frac{K_H^2 B^2 X_d}{R_2^2 + X_d^2} \quad (2.15)$$

It can be seen that the sign of  $X$  is just opposite to the sign of  $X_d$ . This implies that if passive load connected to the Hall terminals is a capacitor the input reactance  $X$  will behave like an inductive reactance. The magnitude of  $X$  is proportional to the square of the magnetic field as long as the magneto resistance effect of  $R_2$  is relatively small.

The quality factor  $Q$  of this element is given by

$$Q = \frac{X}{R} = \frac{K_H^2 B^2 X_d}{R_1 R_2^2 + R_1 X_d^2 + K_H^2 B^2 R_2} \quad (2.16)$$

The value of  $Q$  depends on the magnetic field. For a magnetic field of 10 kilogauss at room temperature the maximum value of  $Q$  is only 0.2. For such a low value of  $Q$ , the application of this element is limited.

To increase the value of  $Q$ , Kataoka et al (1968) has suggested to use the multi-Hall terminals specimen, as shown in Fig. (2.11). Using the equivalent circuit for this element shown in Fig. (2.9), we can write

$$\begin{aligned}
 V &= R_1 I + K_H B (I_{H1} + I_{H2} + \dots + I_{Hm}) \\
 V_{H1} &= K_{H1} B I - R_{21} I_{H1} = j X_{d1} I_{H1} \\
 V_{H2} &= K_{H2} B I - R_{22} I_{H2} = j X_{d2} I_{H2} \\
 &\vdots \\
 V_{Hm} &= K_{Hm} B I - R_{2m} I_{Hm} = j X_{dm} I_{Hm}
 \end{aligned} \tag{2.17}$$

The input impedance is then given by

$$\begin{aligned}
 Z &= \frac{V}{I} = R_1 + \frac{(K_H B)(I_{H1} + I_{H2} + \dots + I_{Hm})}{I} \\
 &= R_1 + K_H B \left[ \frac{K_{H1} B}{R_{21} + j X_{d1}} + \frac{K_{H2} B}{R_{22} + j X_{d2}} + \dots \right. \\
 &\quad \left. \dots + \frac{K_{Hm} B}{R_{2m} + j X_{dm}} \right] \tag{2.18}
 \end{aligned}$$

If  $X_{d1} = X_{d2} = \dots = X_{dm} = X_d$ ,  $R_{21} = R_{22} = \dots = R_{2m} = R_2$   
and  $K_{H1} = K_{H2} = \dots = K_{Hm} = K_H$ ; then Equation

(2.18) can be written as

$$\begin{aligned}
 Z &= R_1 + \frac{m (K_H B)^2}{R_2 + j X_d} \\
 &= R_1 + \frac{m (K_H B)^2 R_2}{R_2^2 + X_d^2} \\
 &\quad - j \frac{m (K_H B)^2 X_d}{R_2^2 + X_d^2} \\
 &= R + j X \tag{2.19}
 \end{aligned}$$

From Equation (2.19) we obtain

$$R = R_1 + \frac{m(K_H B)^2 R_2}{R_2^2 + X_d^2} \quad (2.20)$$

$$X = - \frac{m(K_H B)^2 X_d}{R_2^2 + X_d^2} \quad (2.21)$$

and

$$Q = \frac{X}{R} = \frac{m(K_H B)^2 X_d}{R_1 R_2^2 + R_1 X_d^2 + m(K_H B)^2 R_2} \quad (2.22)$$

Although the multi-Hall terminals specimen increases slightly the value of the reactive component, it does not appreciably improve the value of  $Q$ . The reasons for the small  $Q$  are that the second term on the right hand side of Equation (2.20) can not be made negative because the direction of the Hall current  $I_H$  depends only on the polarity of the Hall generator which is proportional to  $K_H B I$  and it tends to increase the effective input resistance. Furthermore, the phase of the Hall current  $I_H$  can not exceed  $\pm 90^\circ$  with respect to Hall generator voltage. It should be noted that the load connected to each pair of Hall terminals may be made identical, but  $R_2$ 's and  $K_H$ 's are not identical because the positions of the Hall terminals are different. However, because of the physical limitation of the size of Hall specimens and electrodes, both  $Q$  and  $X$  can not be greatly increased by this method.

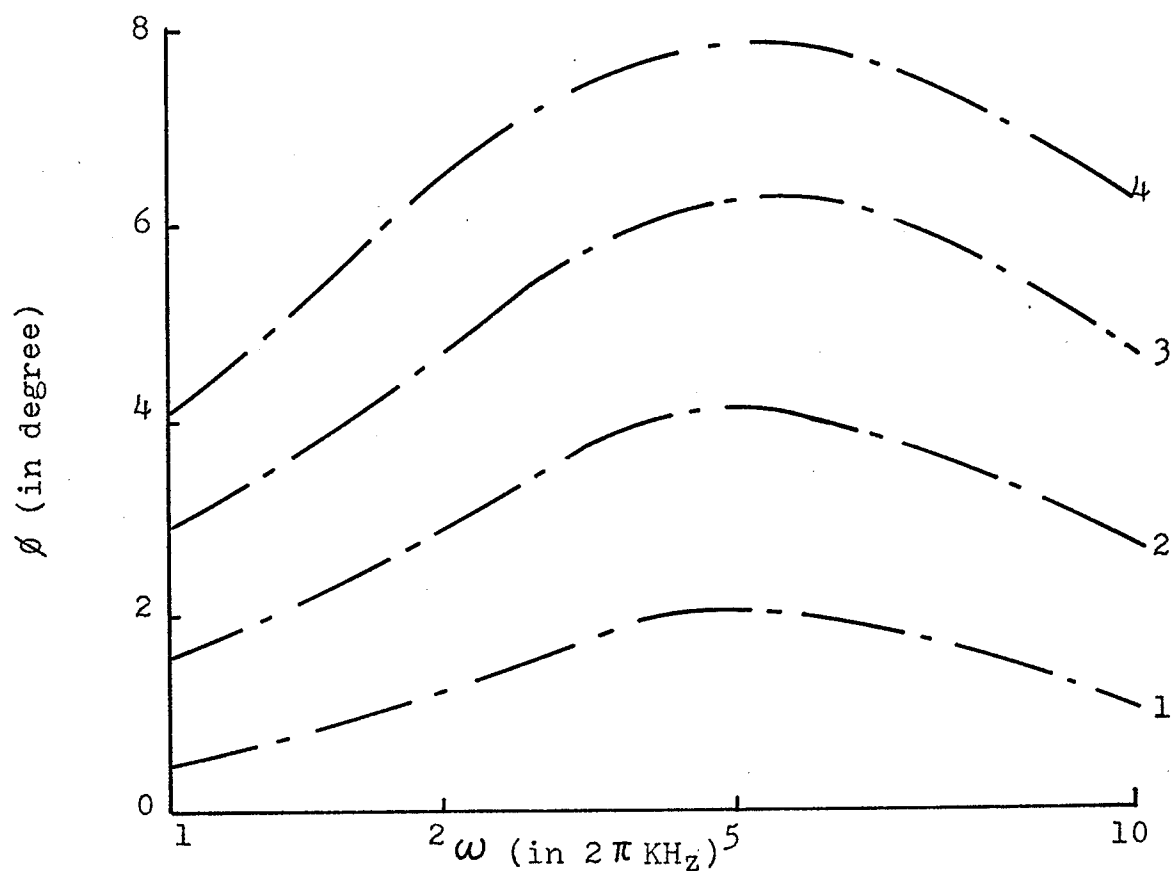
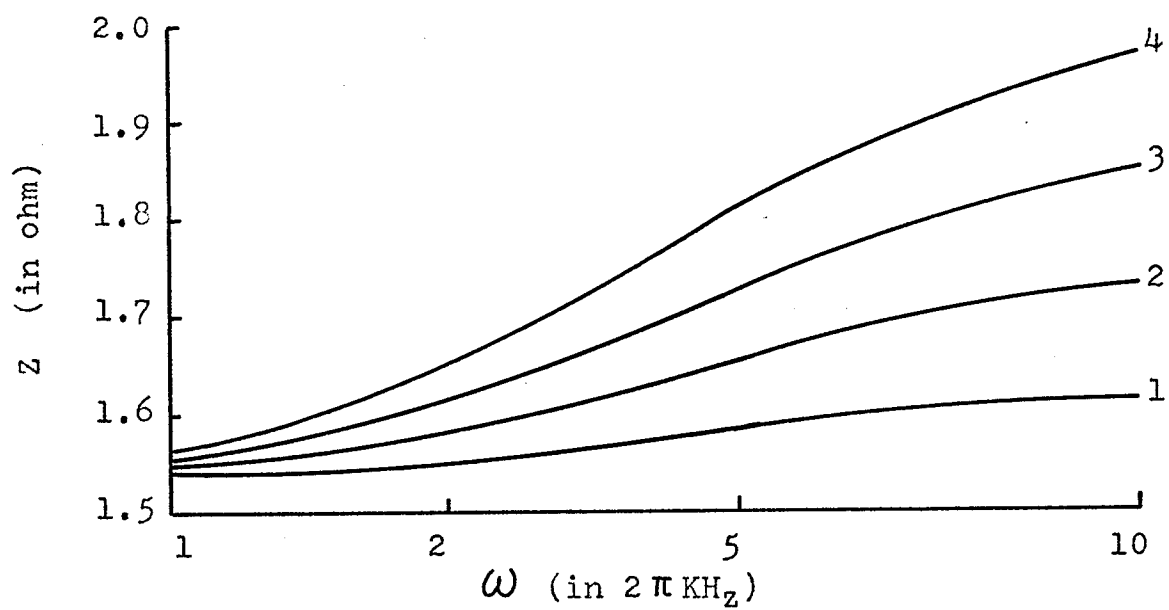


Fig. (2.12) Experimental results of four-pair Hall terminal magnetoreactive element, 1, 2, 3 and 4 indicate the number of Hall terminals.

#### 2.4 The Experimental Performance of the Magneto - reactive Elements

Kataoka et al (1968) and Toda (1965) have reported that the quality factor for a mono-pair Hall terminal element is 0.2 and that for a five-pair Hall terminal element is 0.63. An experiment using a four-pair Hall terminal element fabricated on a  $InSb$  Hall specimen with a  $10 \mu F$  capacitor connected to each pair of Hall terminals has also been performed in the Material Research Laboratory of the University of Manitoba. The results shown in Fig. (2.12) are in good agreement with the theory. However, the value of  $Q$  is too small, the magnetoreactive element to represent an inductance is not practical.

## CHAPTER III

## THE PRINCIPLES OF ACTIVE MAGNETOREACTIVE ELEMENTS

We have pointed out that the passive magneto-reactive elements with only passive reactors connected to the Hall terminals proposed by Kataoka et al (1968) can not provide an inductance with a quality factor high enough for practical applications. Although many other methods are also available (Josephs et al, 1965; Capparelli 1967) for representing inductance for microelectronic circuits, the equivalent inductors with the performance close to that of conventional coil inductors have not yet been achieved. In this chapter we propose a new method to produce high inductive reactance with high quality factor. Before doing so, we explain the basic concept of this new method.

### 3.1 Equivalent Impedance of An Active Network

Consider a simple active network consisting of a power source and an active load, and its equivalent circuit as shown in Fig. (3.1). The equivalent impedance of the active load is defined as the ratio of the voltage across the active load to the current flowing into it. Since the voltage and the frequency of the power source may not be the same as those of the active

load, we have to use the superposition theorem to solve this problem. From Fig. (3.1), the current flowing into the active load (see Appendix I) is

$$\begin{aligned} I(\omega_o, \omega_i, t) &= I_o(\omega_o) - I_i(\omega_i) \\ &= \frac{E_o(\omega_o)}{Z_o(\omega_o) + Z_i(\omega_o)} - \frac{E_i(\omega_i)}{Z_o(\omega_i) + Z_i(\omega_i)} \end{aligned} \quad (3.1)$$

and the voltage across the terminals a and b is

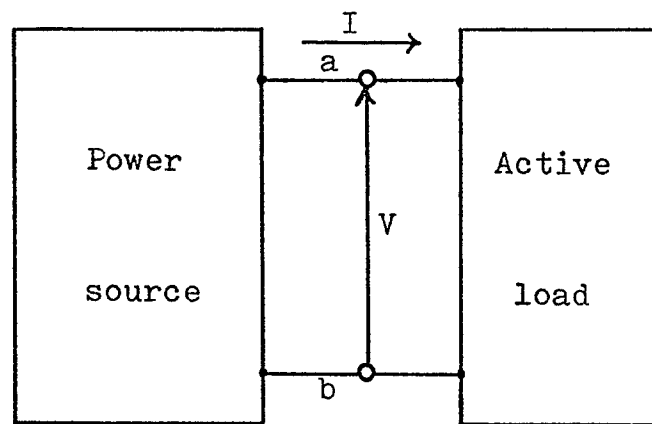
$$\begin{aligned} V(\omega_o, \omega_i, t) &= Z_i(\omega_o) I_o - Z_i(\omega_i) I_i + E_i(\omega_i) \\ &= \frac{Z_i(\omega_o) E_o(\omega_o)}{Z_o(\omega_o) + Z_i(\omega_o)} + \frac{Z_o(\omega_i) E_i(\omega_i)}{Z_o(\omega_i) + Z_i(\omega_i)} \end{aligned} \quad (3.2)$$

Thus the equivalent impedance of the active load can be written as

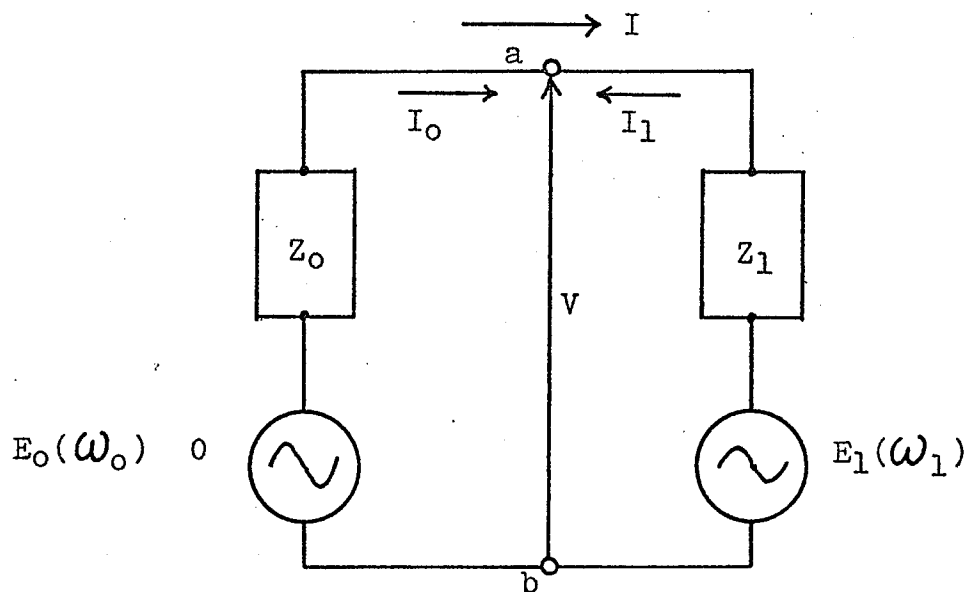
$$\begin{aligned} Z(\omega_o, \omega_i, t) &= \frac{V(\omega_o, \omega_i, t)}{I(\omega_o, \omega_i, t)} \\ &= Z_i(\omega_o) + \frac{E_i(\omega_i)}{I(\omega_o, \omega_i, t)} \left\{ \frac{Z_i(\omega_o) + Z_o(\omega_i)}{Z_o(\omega_i) + Z_i(\omega_i)} \right\} \end{aligned} \quad (3.3)$$

Case 1:

If  $Z_o$  and  $Z_i$  are independent of frequency, then Equation (3.3) becomes



(a) An active network consisting of power source and active load.



(b) The equivalent circuit.

Fig. (3.1) An active network and its equivalent circuit.

$$\begin{aligned}
 Z(\omega_0, \omega_1, t) &= Z_1 + \frac{E_1(\omega_1)}{I(\omega_0, \omega_1, t)} \\
 &= Z_1 + \frac{(Z_1 + Z_0)}{\frac{E_0(\omega_0)}{E_1(\omega_0)} - 1} \quad (3.4)
 \end{aligned}$$

If  $E_0(\omega_0)/E_1(\omega_1)$  is expressed (see Appendix I) as

$$\begin{aligned}
 \frac{E_0(\omega_0)}{E_1(\omega_0)} &= \varepsilon \angle \psi(\omega_0, \omega_1, t, \psi_0) \\
 &= \varepsilon \cos \psi(\omega_0, \omega_1, t, \psi_0) \\
 &\quad + j \varepsilon \sin \psi(\omega_0, \omega_1, t, \psi_0) \quad (3.5)
 \end{aligned}$$

where  $\psi(\omega_0, \omega_1, t, \psi_0) = (\omega_0 - \omega_1)t - \psi_0$

then Equation (3.4) becomes

$$Z(\omega_0, \omega_1, t) = Z_1 + \frac{(Z_1 + Z_0) \{ \varepsilon \cos \psi(\omega_0, \omega_1, t, \psi_0) - 1 \}}{\varepsilon^2 - 2 \varepsilon \cos \psi(\omega_0, \omega_1, t, \psi_0) + 1} \quad (3.6)$$

where  $\psi(\omega_0, \omega_1, t, \psi_0) = (\omega_0 - \omega_1)t - \psi_0$  with  
 $t \leq \frac{2\pi}{\omega_0 - \omega_1}$  and with this as the assumption that  
the voltage of the power source is  $E_0 \angle 0$  and the voltage  
of the source in the active load is  $E_1 \angle \psi_0$ , both angles  
referring to  $t = 0$ .

Case 2:

If the frequency of the power source is identical to that of the active load, i.e.  $\omega_0 = \omega_1 = \omega$ ,

Equation (3.3) becomes

$$\begin{aligned} Z(\omega) &= Z_1(\omega) + \frac{E_1(\omega)}{I(\omega)} \\ &= Z_1(\omega) + \frac{Z_1(\omega) + Z_0(\omega)}{\frac{E_0(\omega)}{E_1(\omega)} - 1} \end{aligned} \quad (3.7)$$

Let us now write  $Z_1$  and  $Z_0$  as

$$\begin{aligned} Z_1(\omega) &= R_1(\omega) + jX_1(\omega) \\ Z_0(\omega) &= R_0(\omega) + jX_0(\omega) \end{aligned} \quad (3.8)$$

and take  $I$  as reference

$$\begin{aligned} I(\omega) &= |I| e^{j0} \\ E_0(\omega) &= |E_0| e^{j\alpha} \\ E_1(\omega) &= |E_1| e^{j\beta} \end{aligned} \quad (3.9)$$

Substitution of Equation (3.9) into (3.1) gives

$$\begin{aligned} I(\omega) &= \frac{|E_0| e^{j\alpha} - |E_1| e^{j\beta}}{(R_0 + R_1) + j(X_0 + X_1)} \\ &= \frac{(R_0 + R_1)[|E_0| \cos \alpha - |E_1| \cos \beta] + (X_0 + X_1)[|E_0| \sin \alpha + |E_1| \sin \beta]}{(R_0 + R_1)^2 + (X_0 + X_1)^2} \\ &\quad + j \frac{(X_0 + X_1)[-|E_0| \cos \alpha + |E_1| \cos \beta] + (R_0 + R_1)[|E_0| \sin \alpha - |E_1| \sin \beta]}{(R_0 + R_1)^2 + (X_0 + X_1)^2} \end{aligned} \quad (3.10)$$

Since we take  $I(\omega)$  as reference, the imaginary part of  $I(\omega)$  must be set zero. We thus have

$$\frac{X_0 + X_1}{R_0 + R_1} = \frac{E_0 \sin \alpha - E_1 \sin \beta}{E_0 \cos \alpha - E_1 \cos \beta} \quad (3.11)$$

Substituting Equation (3.11) into Equation (3.10), we obtain

$$\begin{aligned} I(\omega) &= \frac{|E_0| \cos \alpha - |E_1| \cos \beta}{(R_0 + R_1)^2 + (X_0 + X_1)^2} \\ &\quad \left\{ (R_0 + R_1) + (X_0 + X_1) \left[ \frac{|E_0| \sin \alpha - |E_1| \sin \beta}{|E_0| \cos \alpha - |E_1| \cos \beta} \right] \right\} \\ &= \frac{|E_0| \cos \alpha - |E_1| \cos \beta}{(R_0 + R_1)^2 + (X_0 + X_1)^2} \left\{ (R_0 + R_1) + \frac{(X_0 + X_1)^2}{R_0 + R_1} \right\} \\ &= \frac{|E_0| \cos \alpha - |E_1| \cos \beta}{R_0 + R_1} \\ &= \frac{|E_0| \sin \alpha - |E_1| \sin \beta}{X_0 + X_1} \end{aligned} \quad (3.12)$$

and hence Equation (3.3) becomes

$$\begin{aligned} Z(\omega) &= \frac{V(\omega)}{I(\omega)} \\ &= R_1(\omega) + jX_1(\omega) + \frac{|E_1| e^{j\beta}}{|I| e^{j\theta}} \\ &= R_1(\omega) + jX_1(\omega) + \frac{|E_1|}{|I|} \cos \beta + j \frac{|E_1|}{|I|} \sin \beta \end{aligned}$$

$$= R(\omega) + jX(\omega) \quad (3.13)$$

The real and imaginary part of  $Z(\omega)$  are

$$\begin{aligned} R(\omega) &= R_1(\omega) + \frac{|E_1|}{|I|} \cos \beta \\ &= R_1(\omega) + \frac{\{R_0(\omega) + R_1(\omega)\} |E_1| \cos \beta}{|E_0| \cos \alpha - |E_1| \cos \beta} \\ &= R_1(\omega) + \frac{R_0(\omega) + R_1(\omega)}{\frac{|E_0| \cos \alpha}{|E_1| \cos \beta} - 1} \quad (3.14) \end{aligned}$$

and

$$\begin{aligned} X(\omega) &= X_1(\omega) + \frac{|E_1|}{|I|} \sin \beta \\ &= X_1(\omega) + \frac{\{X_0(\omega) + X_1(\omega)\} |E_1| \sin \beta}{|E_0| \sin \alpha - |E_1| \sin \beta} \\ &= X_1(\omega) + \frac{X_0(\omega) + X_1(\omega)}{\frac{|E_0| \sin \alpha}{|E_1| \sin \beta} - 1} \quad (3.15) \end{aligned}$$

From Equation (3.14) and (3.15) we can express the quality factor (see Appendix II) as

$$\begin{aligned} Q(\omega) &= \frac{|X(\omega)|}{R(\omega)} \\ &= \frac{|X_1(\omega) + \frac{|E_1|}{|I|} \sin \beta|}{R_1(\omega) + \frac{|E_1|}{|I|} \cos \beta} \quad (3.16) \end{aligned}$$

$Q$  is positive when  $R(\omega)$  is positive and  $Q$  is negative when  $R(\omega)$  is negative.

$$= R(\omega) + jX(\omega) \quad (3.13)$$

The real and imaginary part of  $Z(\omega)$  are

$$\begin{aligned} R(\omega) &= R_1(\omega) + \frac{|E_1|}{|I|} \cos \beta \\ &= R_1(\omega) + \frac{\{R_0(\omega) + R_1(\omega)\} |E_1| \cos \beta}{|E_0| \cos \alpha - |E_1| \cos \beta} \\ &= R_1(\omega) + \frac{R_0(\omega) + R_1(\omega)}{\frac{|E_0| \cos \alpha}{|E_1| \cos \beta} - 1} \quad (3.14) \end{aligned}$$

and

$$\begin{aligned} X(\omega) &= X_1(\omega) + \frac{|E_1|}{|I|} \sin \beta \\ &= X_1(\omega) + \frac{\{X_0(\omega) + X_1(\omega)\} |E_1| \sin \beta}{|E_0| \sin \alpha - |E_1| \sin \beta} \\ &= X_1(\omega) + \frac{X_0(\omega) + X_1(\omega)}{\frac{|E_0| \sin \alpha}{|E_1| \sin \beta} - 1} \quad (3.15) \end{aligned}$$

From Equation (3.14) and (3.15) we can express the quality factor (see Appendix II) as

$$\begin{aligned} Q(\omega) &= \frac{|X(\omega)|}{R(\omega)} \\ &= \frac{|X_1(\omega) + \frac{|E_1|}{I} \sin \beta|}{R_1(\omega) + \frac{|E_1|}{I} \cos \beta} \quad (3.16) \end{aligned}$$

$Q$  is positive when  $R(\omega)$  is positive and  $Q$  is negative when  $R(\omega)$  is negative.

From this simple analysis it can be seen that  $R(\omega)$ ,  $X(\omega)$ , and  $Q(\omega)$  can be varied to any desired value by adjusting either the ratio  $\left| \frac{E_o}{E_i} \right|$  or the relative difference  $\alpha$  and  $\beta$ .

### 3.2 Equivalent Impedance of An Active Hall Element

An active Hall element can be considered as a Hall specimen with an active load connected between the Hall terminals as shown in Fig. (3.2). This element can be considered as an active network similar to the active load described in Section (3.1). Since the current flowing at the current terminal  $I$  produces a Hall potential between the Hall terminals  $E_2$ , and the current flowing at the Hall terminals,  $I_H$  produces a second Hall potential across the current terminals  $E_1$ , the equivalent circuit of Fig. (3.2) is shown in Fig. (3.3).  $E_2$  is proportional to  $I$  and  $E_1$  proportional to  $I_H$ .  $E_o(\omega)$  and  $Z_o$  are respectively the Thévenin source and impedance of the power source,  $R_1$  and  $R_2$  are the resistances of the Hall element measured respectively between the current terminals a and b, and between the Hall terminals c and d. The active load connected across the Hall terminals can be considered as consisting of an impedanceless power source  $E_d(\omega)$  and a series impedance  $Z_d$ .

Referring to Section (3.1), and assuming that

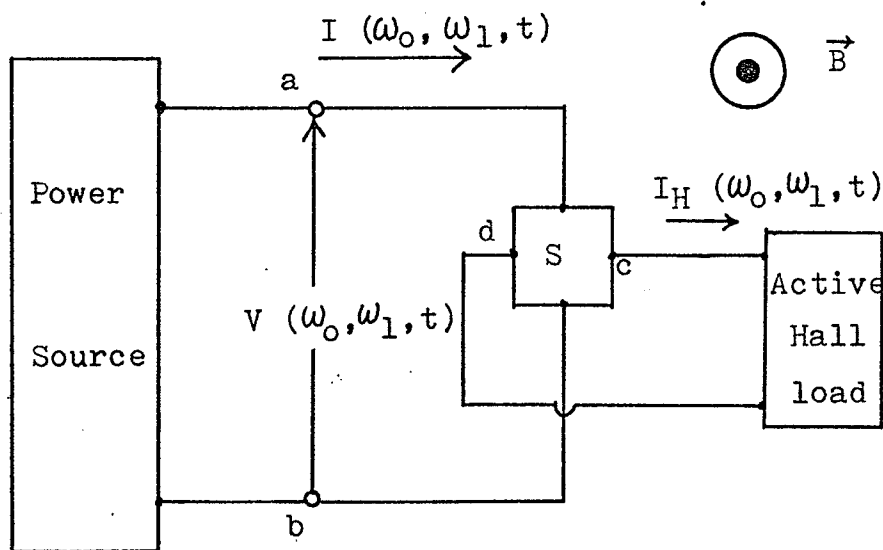


Fig. (3.2) An active Hall element consisting of an active Hall load.

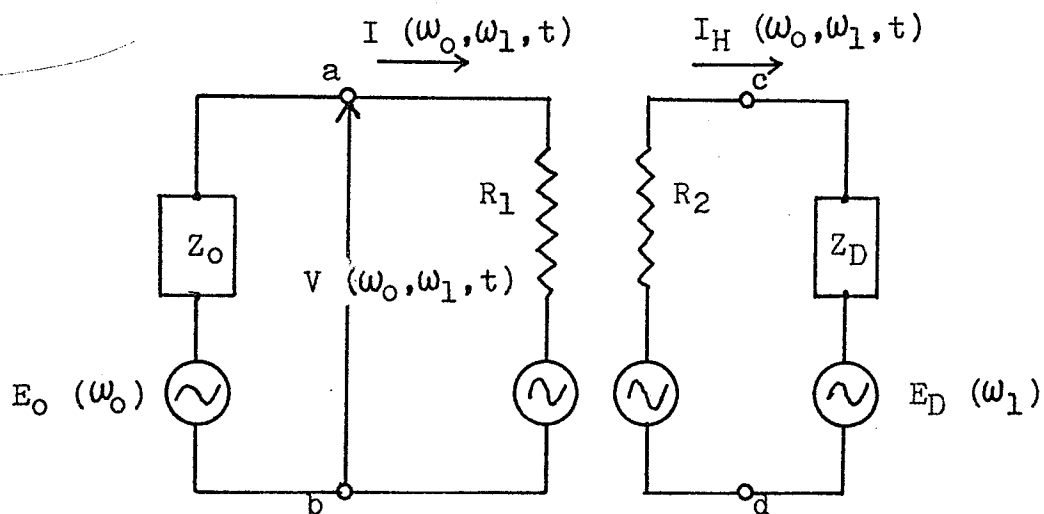


Fig. (3.3) Equivalent circuit of Fig. (3.2).

the difference between frequencies  $\omega_0$  and  $\omega_1$  is small, then  $Z_0(\omega_0) \simeq Z_0(\omega_1)$  and  $Z_d(\omega_0) \simeq Z_d(\omega_1)$ , we can write

$$E_2(\omega_0, \omega_1) = K_H B I(\omega_0, \omega_1) \quad (3.17)$$

$$E_1(\omega_0, \omega_1) = K_H B I(\omega_0, \omega_1) \quad (3.18)$$

$$I_H(\omega_0, \omega_1) = \frac{E_2(\omega_0, \omega_1) - E_d(\omega_1)}{R_2 + Z_d} \quad (3.19)$$

$$I(\omega_0, \omega_1) = \frac{E_0(\omega_1) - E_1(\omega_0, \omega_1)}{R_1 + Z_0} \quad (3.20)$$

and the voltage between a and b is

$$V(\omega_0, \omega_1) = R_1 I(\omega_0, \omega_1) + E_1(\omega_0, \omega_1) \quad (3.21)$$

Similar to Equation (3.3), the equivalent impedance of the active Hall element between a and b can thus be written as

$$\begin{aligned} Z(\omega_0, \omega_1) &= \frac{V(\omega_0, \omega_1)}{I(\omega_0, \omega_1)} \\ &= R_1 + \frac{E_1(\omega_0, \omega_1)}{I(\omega_0, \omega_1)} \\ &= R_1 + \frac{R_1 + Z_0}{\frac{E_0(\omega_0)}{E_1(\omega_0, \omega_1)} - 1} \quad (3.22) \end{aligned}$$

Substituting Equations (3.17) - (3.20) into Equation (3.22), we obtain

$$Z(\omega_0, \omega_1) = R_1 + \frac{(K_H B)^2}{R_2 + Z_d} - \frac{E_d(\omega_1) K_H B}{I(\omega_0, \omega_1) [R_2 + Z_d]} \quad (3.23)$$

This equation degenerates into Equation (2.13) when  $E_d = 0$ .

Now consider the case in which  $\omega_0 = \omega_1 = \omega$ . Then Equation (3.23) becomes

$$Z(\omega, \omega) = R_1 + \frac{(K_H B)^2}{R_2 + Z_d} - \frac{E_d(\omega) K_H B}{I(\omega) [R_2 + Z_d]} \quad (3.24)$$

Again by taking  $I(\omega)$  as reference in phase, we then define the phase relations as

$$\begin{aligned} I(\omega) &= |I| e^{j0} \\ I_H(\omega) &= |I_H| e^{j\delta} \\ E_0(\omega) &= |E_0| e^{j\alpha} \\ E_1(\omega) &= |E_1| e^{j\beta} \\ E_d(\omega) &= |E_d| e^{j\gamma} \\ Z_d(\omega) &= R_d(\omega) + jX_d(\omega) \end{aligned} \quad (3.25)$$

Introducing Equation (3.25) into Equation (3.24)

and writing  $Z(\omega) = R(\omega) + jX(\omega)$ , we obtain the real part of  $z(\omega)$

$$R(\omega) = R_1 + \frac{(K_H B)^2 (R_2 + R_d)}{(R_2 + R_d)^2 + X_d^2} - \frac{K_H B \left| \frac{E_d}{I} \right| \{ (R_2 + R_d) \cos \varphi + X_d \sin \varphi \}}{(R_2 + R_d)^2 + X_d^2} \quad (3.26)$$

and the imaginary part of  $Z(\omega)$

$$X(\omega) = \frac{-(K_H B)^2 X_d + K_H B \left| \frac{E_d}{I} \right| \{ (R_2 + R_d) \sin \varphi - X_d \cos \varphi \}}{(R_2 + R_d)^2 + X_d^2} \quad (3.27)$$

and the quality factor

$$Q(\omega) = \frac{|X(\omega)|}{R(\omega)} = \frac{-(K_H B)^2 X_d + K_H B \left| \frac{E_d}{I} \right| \{ (R_2 + R_d) \sin \varphi - X_d \cos \varphi \}}{R_1 (R_2 + R_d)^2 + R_1 X_d^2 + (K_H B)^2 (R_2 + R_d) - K_H B \left| \frac{E_d}{I} \right| \{ (R_2 + R_d) \cos \varphi + X_d \sin \varphi \}} \quad (3.28)$$

In practice,  $X_d$  can be made zero i.e.  $X_d = 0$ .

Under this condition  $\varphi = \gamma$ , then Equations (3.26) - (3.28) become

$$R(\omega) = R_1 + \frac{(K_H B)^2}{R_2 + R_d} - \frac{K_H B |E_d| \cos \gamma}{|I| (R_2 + R_d)} \quad (3.29)$$

$$X(\omega) = - \frac{K_H B |E_d| \sin \gamma}{|I| (R_2 + R_d)} \quad (3.30)$$

$$Q(\omega) = \frac{1 - K_H B \sin \gamma}{\left| \frac{I}{E_d} \right| [R_1(R_2 + R_A) + (K_H B)^2] - K_H B \cos \gamma} \quad (3.31)$$

Equations (3.29) - (3.31) can be further simplified by making  $E_d(\omega) \gg E_2(\omega)$  and  $R_d \gg K_H B$ . These conditions can be easily satisfied in practice. With these conditions these equations become

$$R(\omega) = R_1 - \frac{K_H B |I_H|}{|I|} \cos \gamma \quad (3.32)$$

$$X(\omega) = - \frac{K_H B |I_H|}{|I|} \sin \gamma \quad (3.33)$$

and

$$Q(\omega) = \frac{|-\sin \gamma|}{\frac{R_1}{K_H B} \left| \frac{I}{I_H} \right| - \cos \gamma} \quad (3.34)$$

where  $|I_H| = |E_d|/R_d$ , since  $|E_d| \gg |E_2|$  and  $R_d \gg K_H B$ .

These equations imply that  $R$ ,  $X$ , and  $Q$  can be adjusted to any desired values simply by adjusting the ration  $\frac{|I|}{|I_H|}$  and the angle  $\gamma$ .

## CHAPTER IV

## RESISTIVE AND REACTIVE ELEMENTS

On the basis of the concept of the equivalent impedance of an active Hall element (with an active load connected between the Hall terminals), such an element can be considered as one of the methods to synthesize a given impedance. In this chapter the fabrication principles and the electrical characteristics of such elements will be discussed. For simplicity, the time dependent elements which involve two or more different frequencies will not be included.

#### 4.1 Fabrication of The Element and General Requirements

For a time-independent element, the frequency of the power source must be the same as that of the active Hall element. This rules out the possibility of using a separate source for  $E_d$  in the active Hall element (see Figs. (3.2) and (3.3)), because it is impossible in practice to make the frequency of  $E_d$  the same as that of the other active network (we consider it as power source in Section (3.1)) to be connected to this element without an automatic synchronizing system connected in between. The latter is complicated and not practical. For this reason,

we derive  $E_d$  from the active network to be connected to this element. Fig. (4.1) shows the basic arrangement of the resistive and reactive element using Galvanomagnetic effect (R.R.E.G.) in which  $B$  is the constant applied magnetic field,  $S$  represents the semiconductor Hall specimen,  $A$ , the amplifier and  $P$ , the phase shifter. For a desirable element the equivalent impedance  $Z(\omega)$  should be independent of the current  $I(\omega)$ . To satisfy this requirement,  $|I_H|$  must be proportional to  $|I|$ . This means that the amplifier must be linear i.e. its output current must be proportional to its input current. (cf Equations (3.32) to (3.34)).

The type of the active network to be connected to the element and required characteristics of R.R.E.G. determine the choice of the Hall specimen, amplifier and phase shifter. In general the following factors are important for choosing these components:

(a) Hall sensitivity  $K_H$  must be high so that smaller magnetic field and smaller amplification are required to produce the required magnitude of  $Z(\omega)$ .

(b) The amplifier must have high current gain and must be isolated from both the input and output to avoid any possible oscillations of the amplifier caused by the

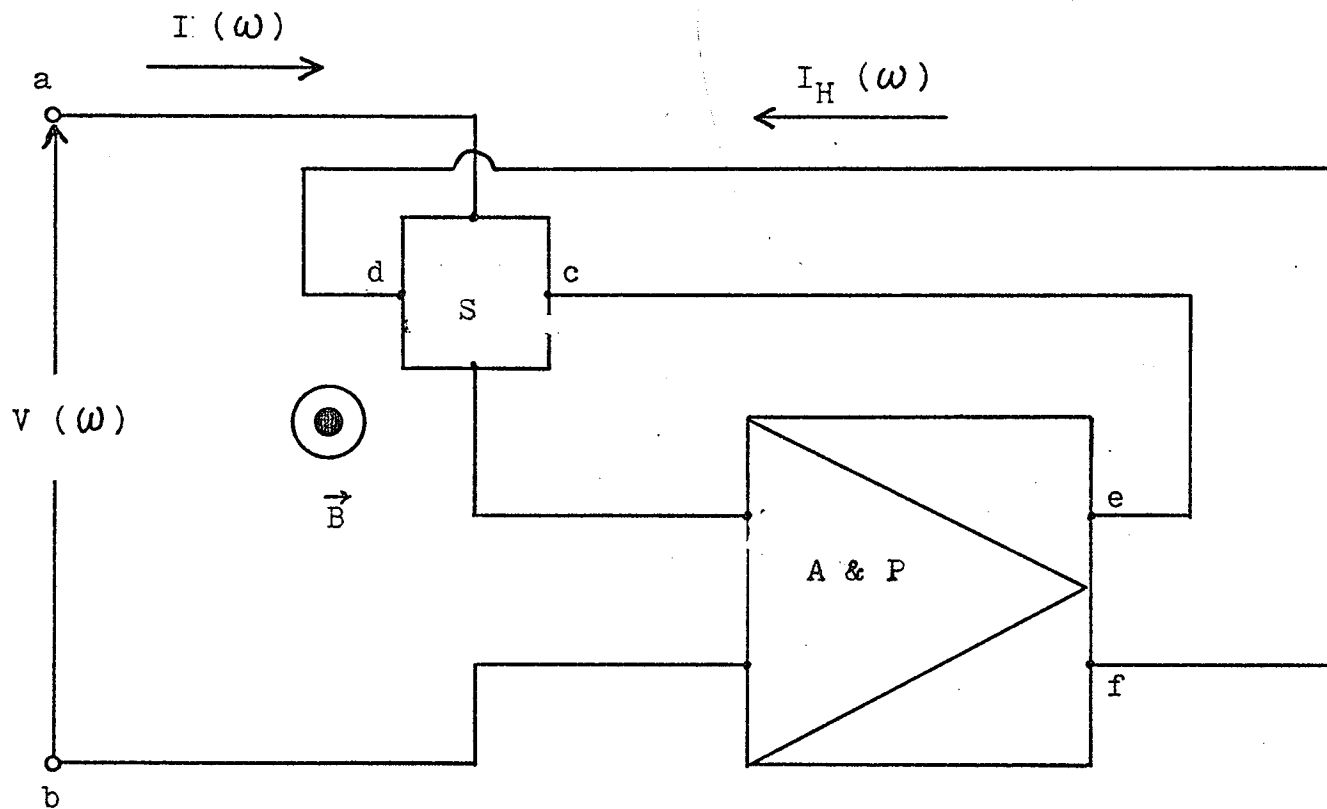


Fig. (4.1) The resistive and reactive element based on galvanomagnetic effect (R.R.E.G.).

feedback through the Hall specimen.

(c) The phase shifter should be designed in such a way that the attenuation of the amplification is as small as possible.

(d) The magnetic field can be produced by permanent magnetic films deposited on the surfaces of the Hall specimen. Since most magnetic films are conductive or semiconductive, it is desirable to deposit first a dielectric film on the Hall sample surface before a magnetic film is deposited to isolate the Hall specimen from the magnetic films.

Some typical values of input impedance, output impedance, current gain and voltage gain of transistor amplifiers are given in Table (4.1). According to the requirements given in (b) we use the common emitter configuration for the amplifier and differential amplifier arrangement to isolate the input and output of the amplifier. Fig. (4.2) shows the circuit diagram of R.R.E.G. in which  $C_p$  is the phase shifting capacitor,  $T_{r1}$  to  $T_{r5}$  are the transistors and  $R_b$  is a bypass resistor of very low value which should be so small that its disturbance to  $I(\omega)$  is negligibly small. Fig. (4.3) is the equivalent circuit of Fig. (4.2) in which  $A_1$  and  $A_2$  are respectively the current gains of the first stage and the

Table (4.1) after Ghausi (1965)

	Common base configuration	Common collector configuration	Common emitter configuration
Input impedance	3.5 ohms	237 K-ohms	1.620 ohms
Output impedance	138 K-ohms	55 ohms	72 K-ohms
Current gain	0.98	50	-.44
Voltage gain	127	0.99	-124

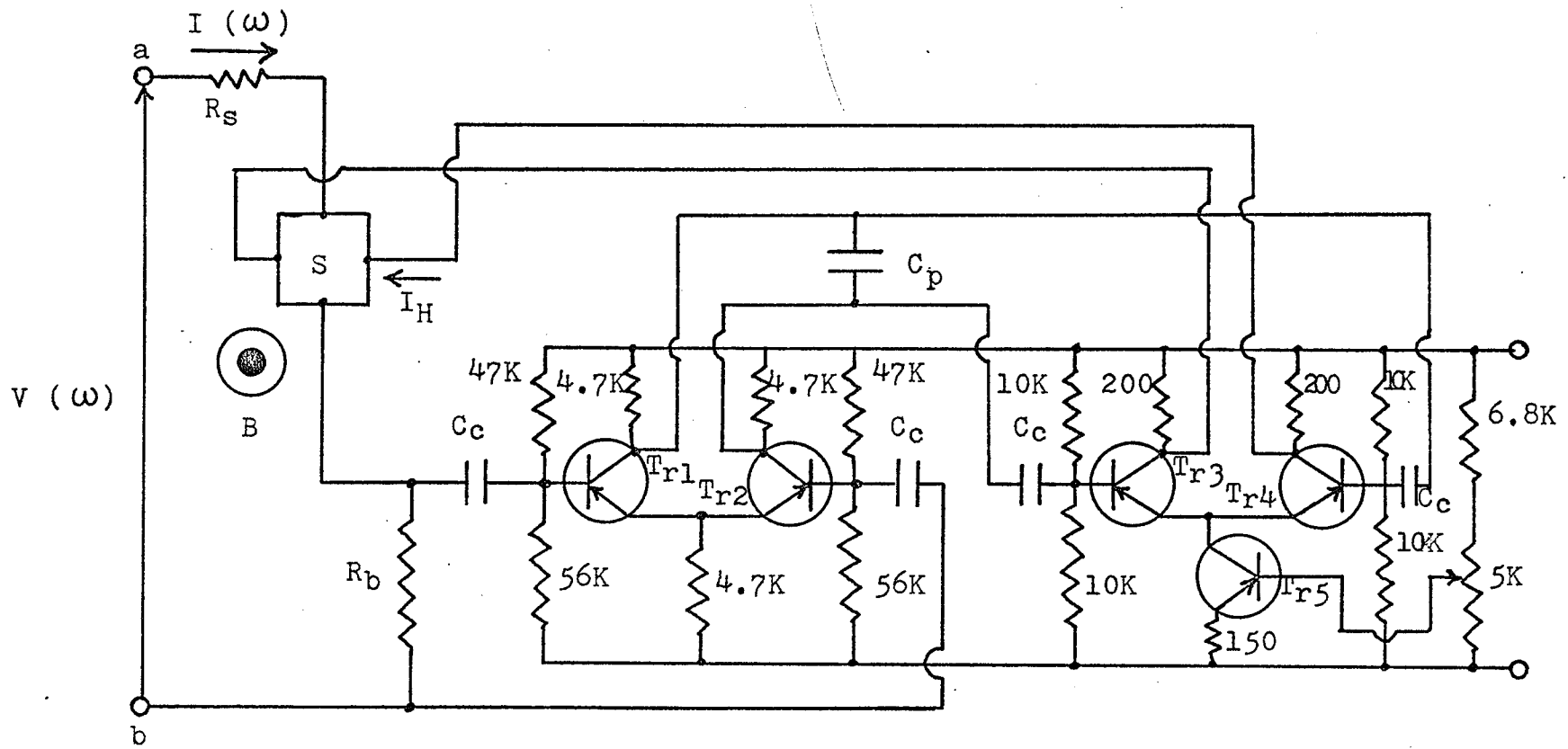


Fig. (4.2) Circuit diagram of R.R.E.G.

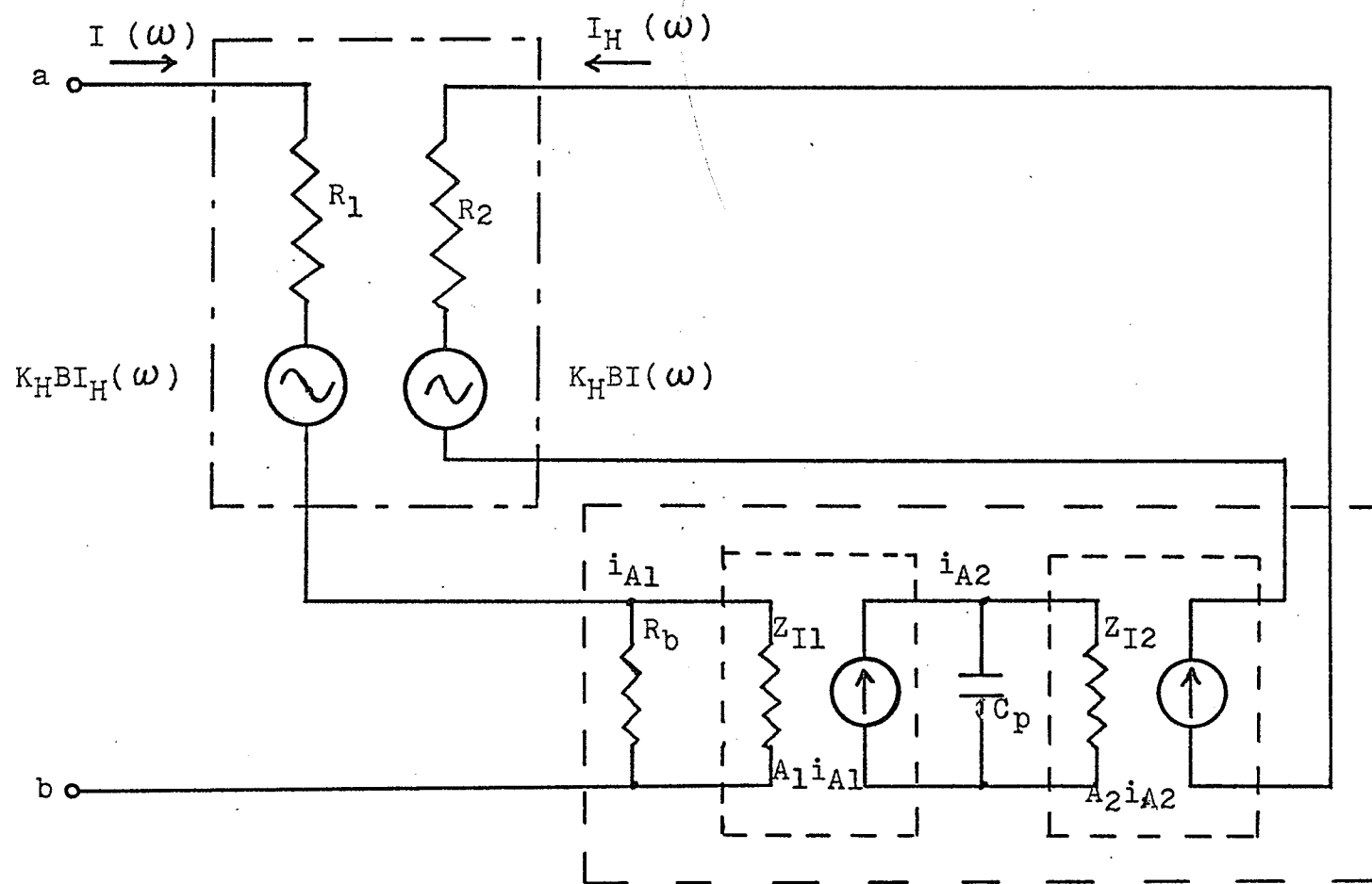


Fig. (4.3) Equivalent circuit of R.R.E.G.

second stage of the amplifier,  $Z_{I1}$  and  $Z_{I2}$  are respectively the input impedances of the first and the second stages of the amplifier. The output impedances of both stages of the amplifier are assumed to be large enough for a constant current output.

#### 4.2 Analysis of the R.R.E.G.

To simplify the analysis we first define the three parameters  $H(\omega)$ ,  $G(\omega)$ , and  $P(\omega)$ . The Thévenin impedance  $H(\omega)$  across the terminal a, and b in Fig. (4.1) consists of the internal resistance  $R_i$  between the current terminals of the Hall specimen, the combination of the bypass resistor  $R_b$ , the input impedance of the amplifier  $Z_{I1}$  and series resistance  $R_s$ . Thus

$$H(\omega) = R_s + R_i + \frac{R_b Z_{I1}}{R_b + Z_{I1}} \quad (4.1)$$

The current gain and generation constant,  $G(\omega)$  is defined as the ratio of the magnitude of the second Hall potential to the magnitude of the current flowing into current terminals of the Hall specimen when the phase shift and the attenuation factor  $P(\omega)$  is unity. It is

$$G(\omega) = \frac{|K_H B I_H(\omega)|}{|I(\omega)|} \Big|_{P(\omega) = 1} \quad (4.2)$$

The phase shift and attenuation factor,  $P(\omega)$  is defined as the functional variable which indicates the phase shift  $\gamma$  of the output current  $I_H(\omega)$  from the in-

put current  $I(\omega)$ , and also indicates the attenuation of the current gain of the A and P unit, and it is expressed as

$$P(\omega) = |P(\omega)| (\cos \gamma + j \sin \gamma) \quad (4.3)$$

The value of  $P(\omega)$  can be positive, or negative, or complex.

Using the three parameters, we can write the equivalent impedance of the R.R.E.G. as

$$\begin{aligned} Z(\omega) &= H(\omega) + G(\omega) P(\omega) \\ &= H(\omega) + G(\omega) |P(\omega)| (\cos \gamma + j \sin \gamma) \\ &= R(\omega) + j X(\omega) \end{aligned} \quad (4.4)$$

The equivalent impedance can also be expressed as the ratio of the voltage across the terminals a and b to the current flowing at the current terminals of the Hall specimen.

Thus

$$\begin{aligned} Z(\omega) &= \frac{V(\omega)}{I(\omega)} \\ &= \frac{R_s I(\omega) + R_l I(\omega) + \frac{R_b Z_{I1}}{R_b + Z_{I1}} I(\omega)}{I(\omega)} \\ &\quad + \frac{K_H B I(\omega) \frac{R_b}{R_b + Z_{I1}} A_1 - \frac{1}{j\omega C_p} A_2}{I(\omega)} \end{aligned}$$

$$= R_s + R_i + \frac{R_b Z_{I1}}{R_b + Z_{I1}} + K_H B A_1 A_2 \frac{R_b}{R_b + Z_{I1}} \cdot \frac{1}{1 + j\omega C_p Z_{I2}} \quad (4.5)$$

By comparing Equations (4.4) and (4.5) we get

$$H(\omega) = R_s + R_i + \frac{R_b Z_{I1}}{R_b + Z_{I1}} \quad (4.6)$$

and

$$G(\omega) = K_H B A_1 A_2 \quad (4.7)$$

$$P(\omega) = \frac{R_b}{R_b + Z_{I1}} \cdot \frac{1}{1 + j\omega C_p Z_{I2}} \quad (4.8)$$

If  $Z_{I1}$  and  $Z_{I2}$  are expressed as

$$Z_{I1} = R_{I1}(\omega) + jX_{I1}(\omega)$$

$$Z_{I2} = R_{I2}(\omega) + jX_{I2}(\omega)$$

then from  $P(\omega) = |P(\omega)| (\cos \gamma + j \sin \gamma)$

we obtain

$$|P(\omega)| \cos \gamma = \frac{(R_b^2 + R_b R_{I1})(1 - \omega C_p X_{I2}) - R_b X_{I1} \omega C_p R_{I2}}{\{(R_b + R_{I1})^2 + X_{I1}^2\} \{(1 + \omega C_p X_{I2})^2 + (\omega C_p R_{I2})^2\}} \quad (4.9)$$

$$|P(\omega)| \sin \gamma = - \frac{\omega C_p R_{I2} (R_b^2 + R_b R_{I1}) + R_b X_{I1} (1 - \omega C_p X_{I2})}{\{(R_b + R_{I1})^2 + X_{I1}^2\} \{(1 + \omega C_p X_{I2})^2 + (\omega C_p R_{I2})^2\}} \quad (4.10)$$

If  $Z_{I1}$  and  $Z_{I2}$  are real only, then  $X_{I1} = X_{I2} = 0$ .

Equation (4.6), (4.9), (4.10) become

$$H(\omega) = R_s + R_1 + \frac{R_b R_{I1}}{R_b + R_{I1}} \quad (4.11)$$

$$|P(\omega)| \cos \gamma = \frac{R_b}{(R_b + R_{I1}) [1 + \omega C_p R_{I2}]^2} \quad (4.12)$$

$$|P(\omega)| \sin \gamma = - \frac{R_b \omega C_p R_{I2}}{(R_b + R_{I1}) [1 + \omega C_p R_{I2}]^2} \quad (4.13)$$

In practice  $R_b$  can be made very small as compared with  $R_{I1}$ . If  $R_b \ll R_{I1}$  then Equation (4.11) to (4.13) become

$$H(\omega) = R_s + R_1 + R_b \quad (4.14)$$

$$|P(\omega)| \cos \gamma = \frac{R_b}{R_{I1} [1 + \omega C_p R_{I2}]^2} \quad (4.15)$$

$$|P(\omega)| \sin \gamma = \frac{- R_b \omega C_p R_{I2}}{R_{I1} [1 + \omega C_p R_{I2}]^2} \quad (4.16)$$

#### 4.3 The Electrical Characteristics of R.R.E.G.

The electrical characteristics of the R.R.E.G. are determined by the characteristics of  $H(\omega)$ ,  $G(\omega)$  and  $P(\omega)$ . For low frequencies  $H(\omega)$  and  $G(\omega)$  can be assumed to be constant. The frequency characteristics of  $R(\omega)$ ,  $X(\omega)$  and  $Q(\omega)$  are dependent only on  $P(\omega)$ . Figs (4.4), (4.5), (4.6), and (4.7) show the variation of  $R$ ,  $X$ , and  $Q$  with the phase angle  $\gamma$  for  $H = 0$ ,

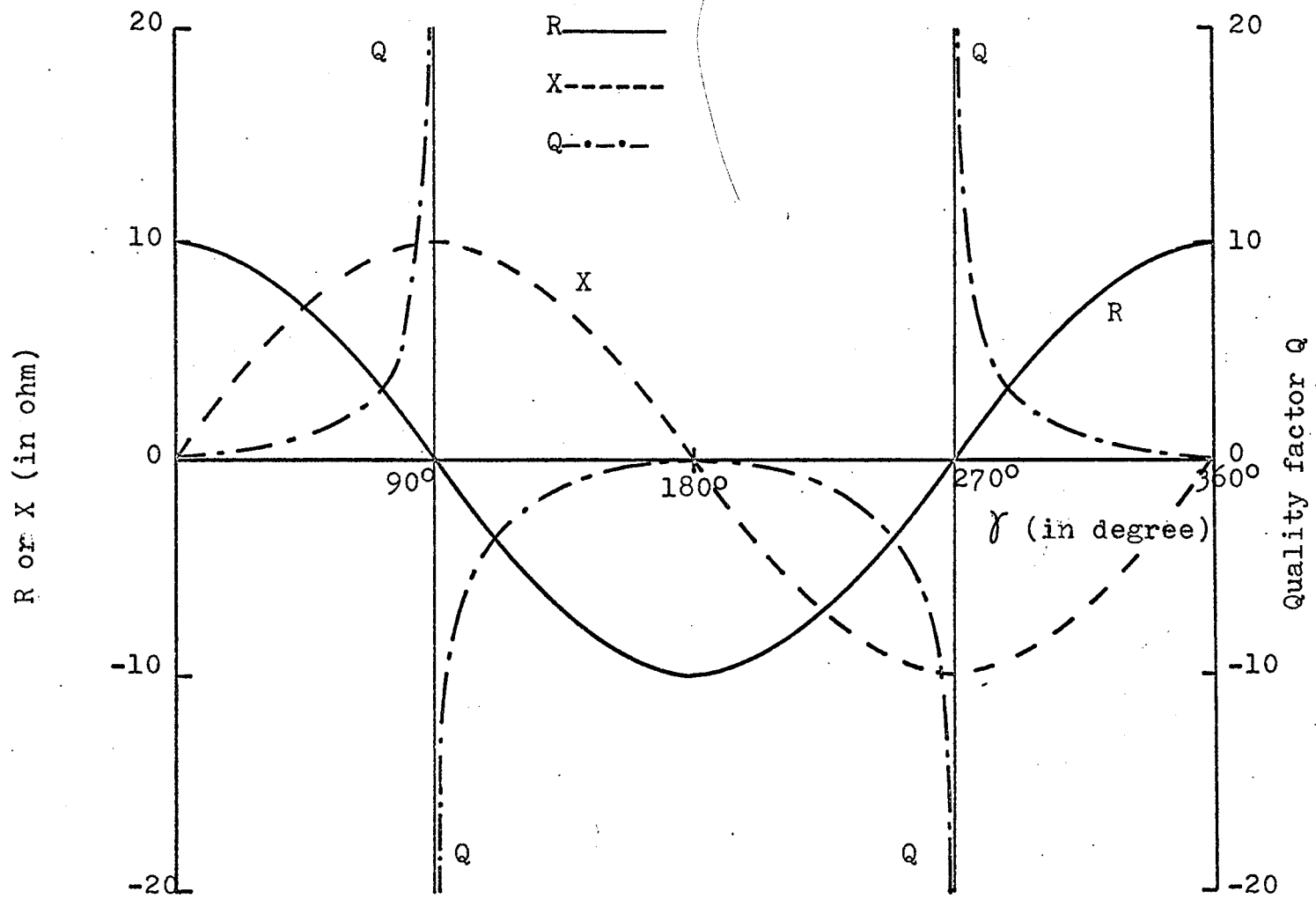


Fig. (4.4) R, X and Q as functions of  $\gamma$  for  $H = 0$  and  $|p(\omega)G| = 10$ .

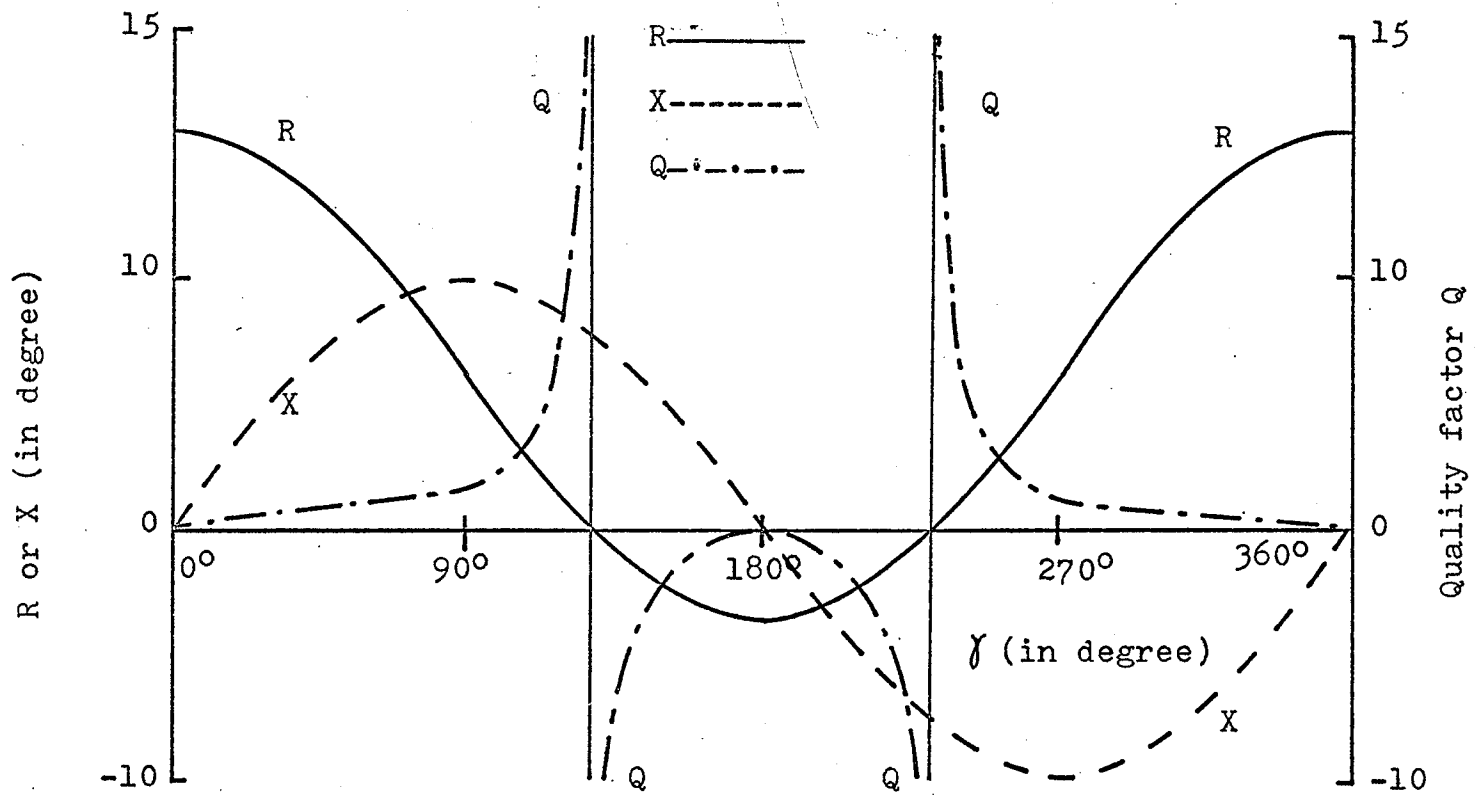


Fig. (4.5) R, X and Q as functions of  $\gamma$  for  $H = 6\Omega$  and  $|p(\omega)|G = 10$

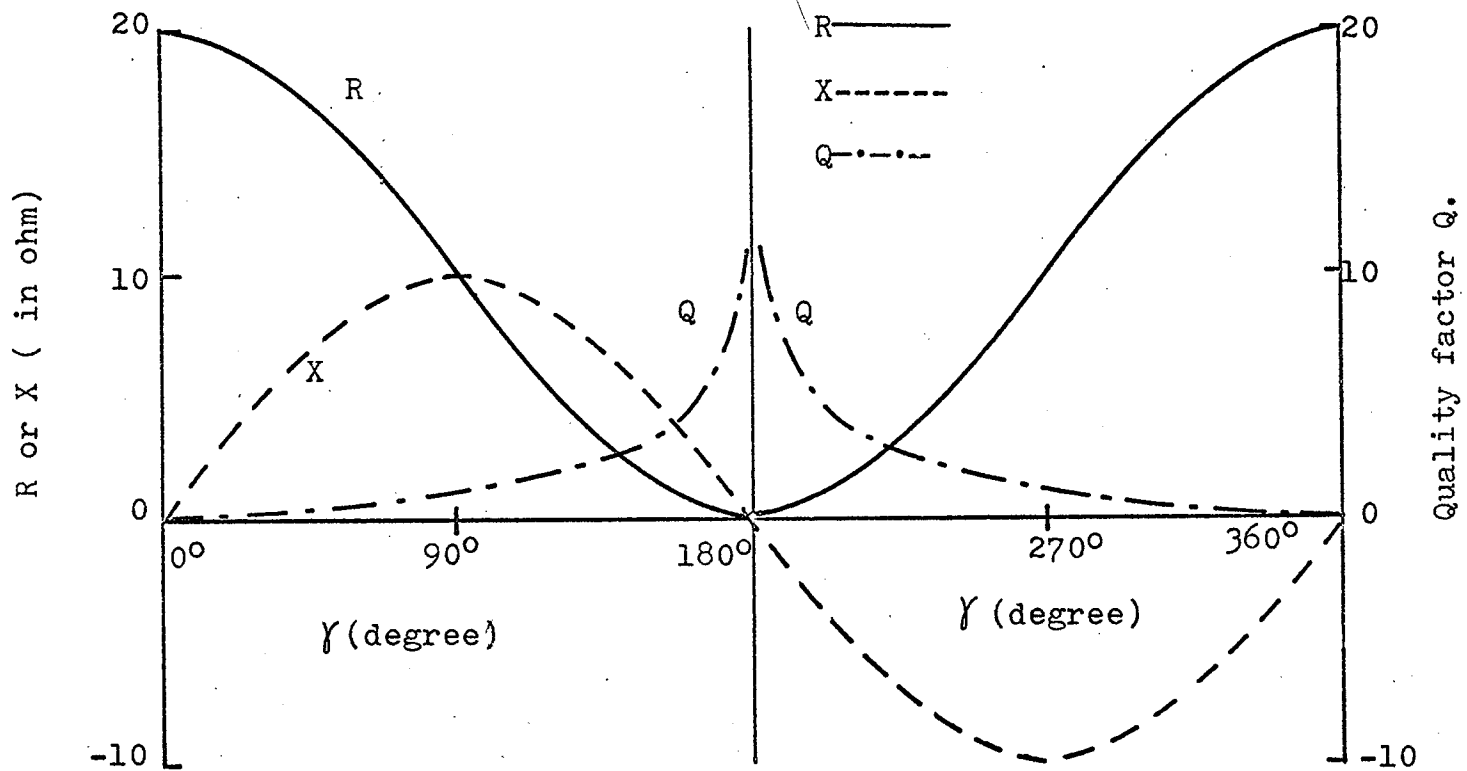


Fig. (4.6) R, X and Q as functions of  $\gamma$  for  $H = 10 \Omega$  and  $|p(\omega)|G = 10$ .

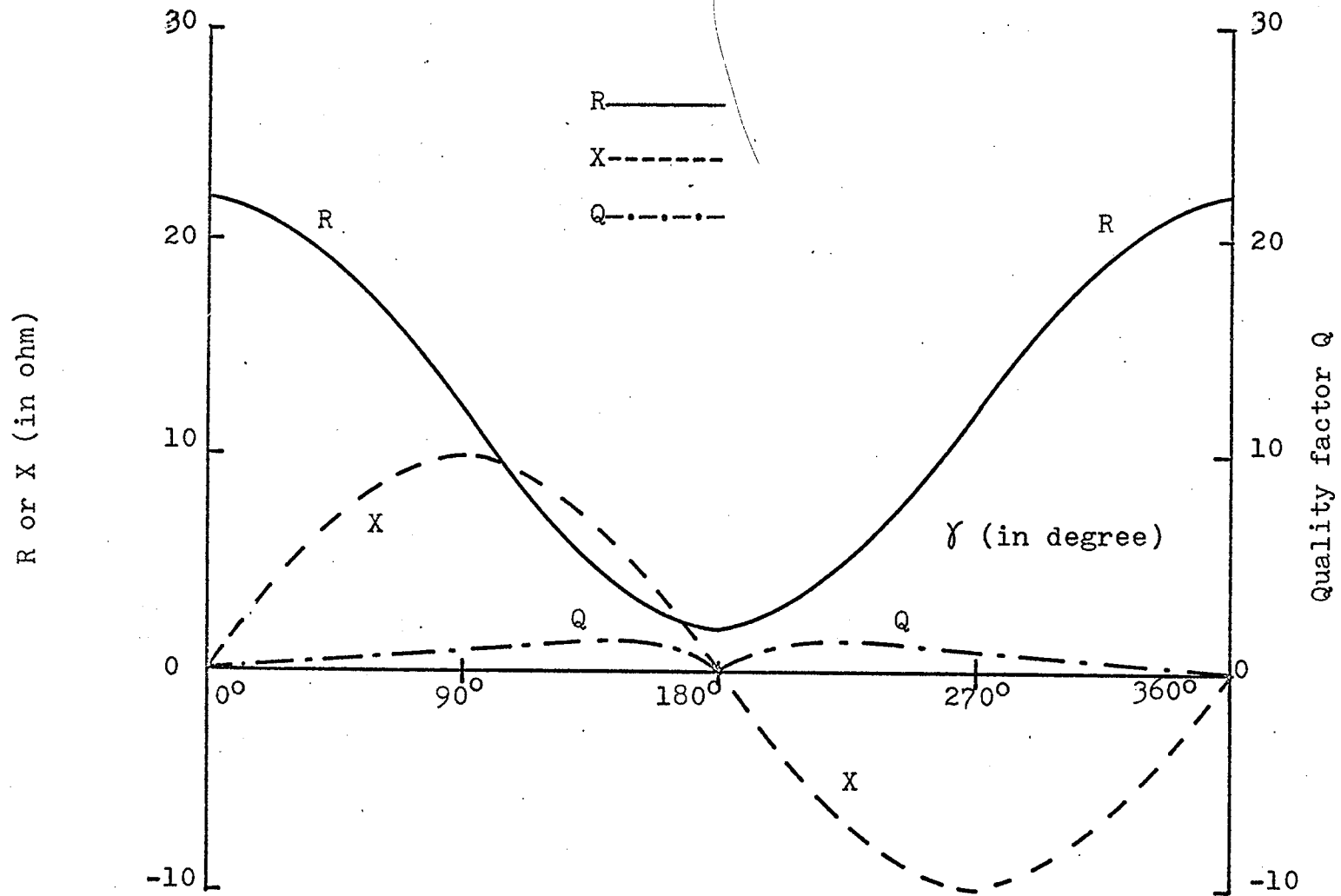


Fig. (4.7) R, X and Q as functions of  $\gamma$  for  $H = 12 \Omega$   $|p(\omega)|G = 10$ .

$H = 6 \Omega$ ,  $H = 10 \Omega$  and  $H = 12 \Omega$ . In all cases  $|P(\omega)| G(\omega)$  is set equal to 10. It can be seen that  $R$ ,  $X$ , and  $Q$  depends greatly on  $\gamma$  and theoretically  $Q$  can be made  $+\infty$  or  $-\infty$  by adjusting  $\gamma$ . The following are the phase shifts at which  $Q$  is a maximum.

H (ohm)	Q (max)	$\gamma$
0	$\pm \infty$	$90^\circ$ and $270^\circ$
6	$\pm \infty$	$126^\circ$ and $233^\circ$
10	$\pm \infty$	$\sim 180^\circ$
12	$\sim 1.5$	$150^\circ$ and $210^\circ$

Consider the effect of the phase shift  $\gamma$  on the frequency response of R.R.E.G., we refer to Fig. (4.8) which is part of Fig. (4.3). For a current source  $I_{A1}$  which is taken as a reference current and is proportional to  $I$ , the input current to second stage of amplifier  $i_{A2}$  is

$$i_{A2} = \frac{\frac{1}{j\omega C_p}}{\frac{1}{j\omega C_p} + R_{I2}} I_{A1} \quad (4.17)$$

There are two ways to connect the output terminals of the amplifier to the Hall terminals. They either are  $e \rightarrow c$  and  $f \rightarrow d$ , or are  $e \rightarrow d$  and  $f \rightarrow c$ , the differ-

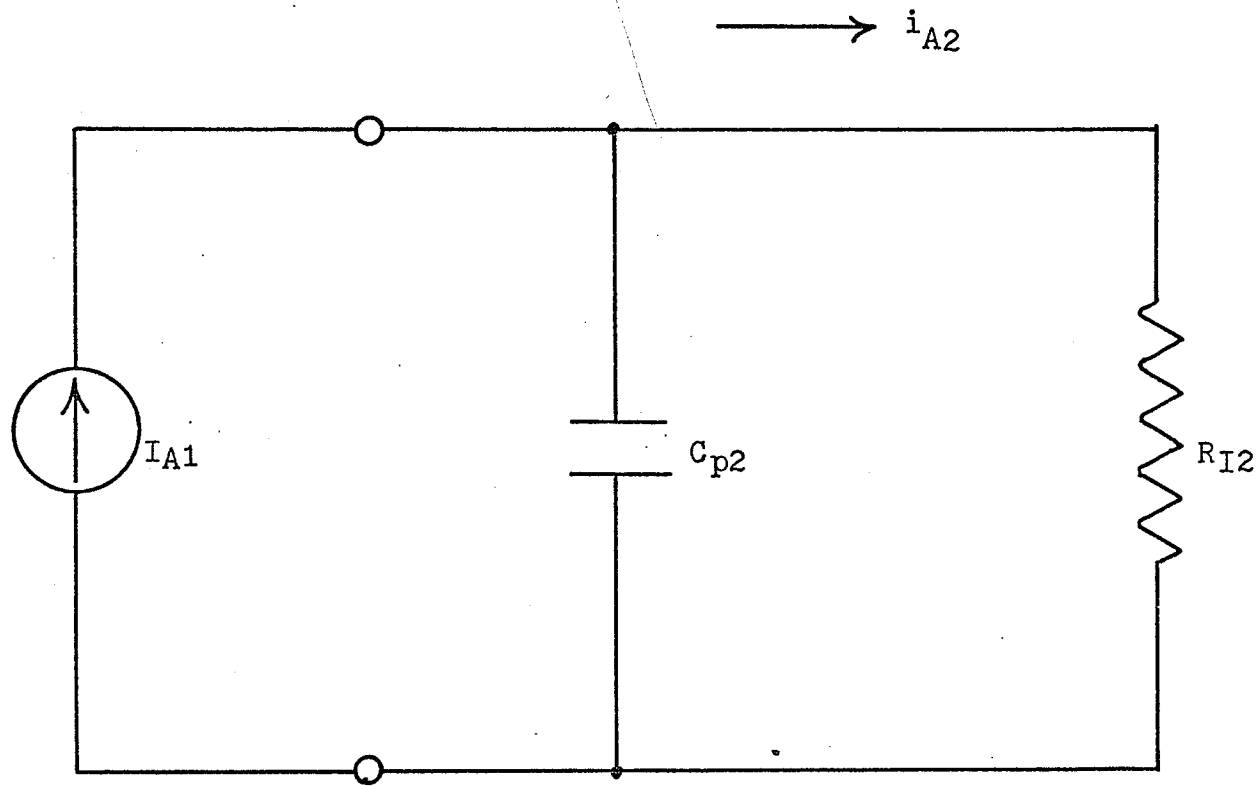


Fig. (4.8) Simple phase shifter for current source.

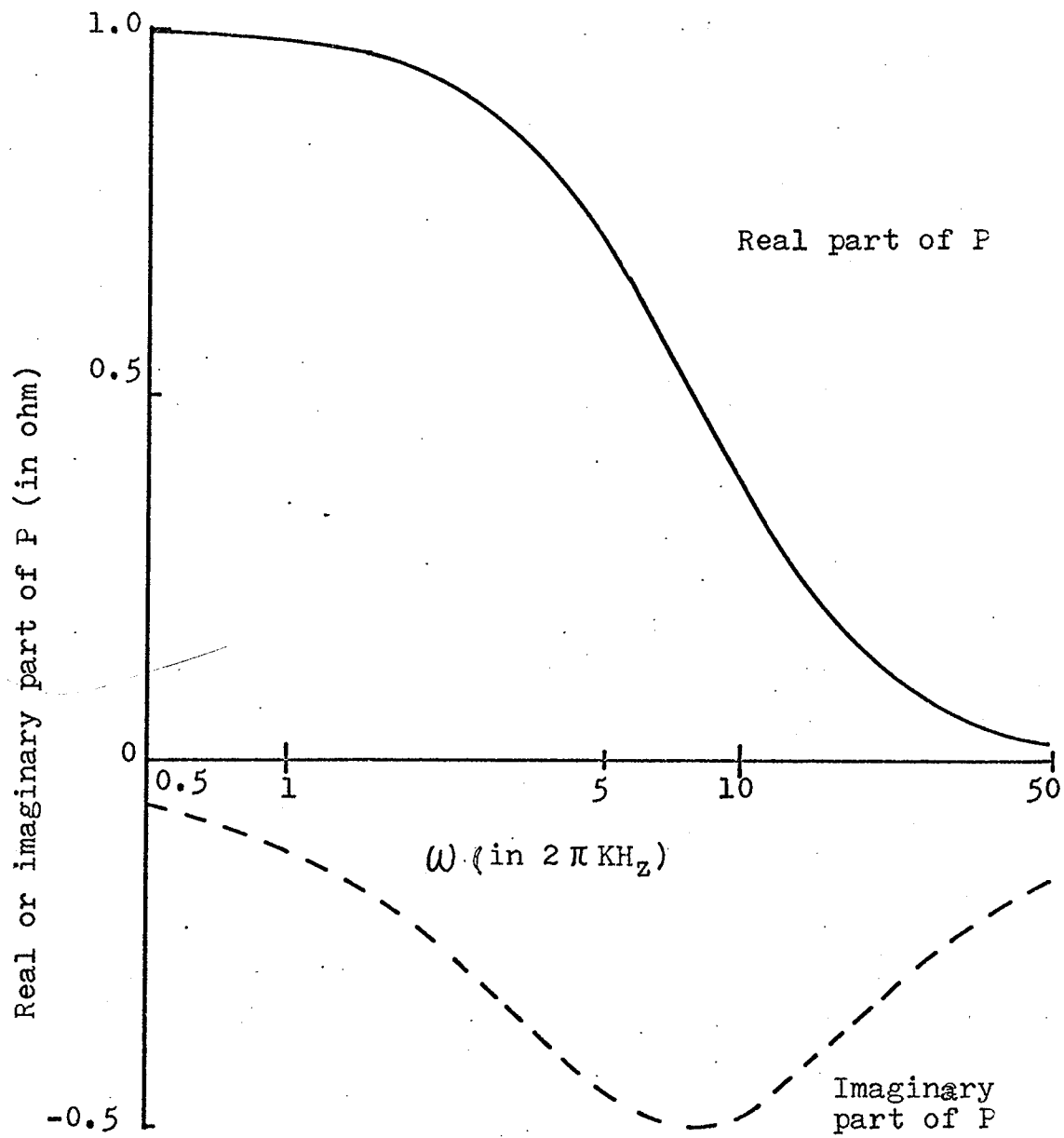


Fig. (4.9) Frequency dependence of real and imaginary parts of  $P(\omega)$  for current source.

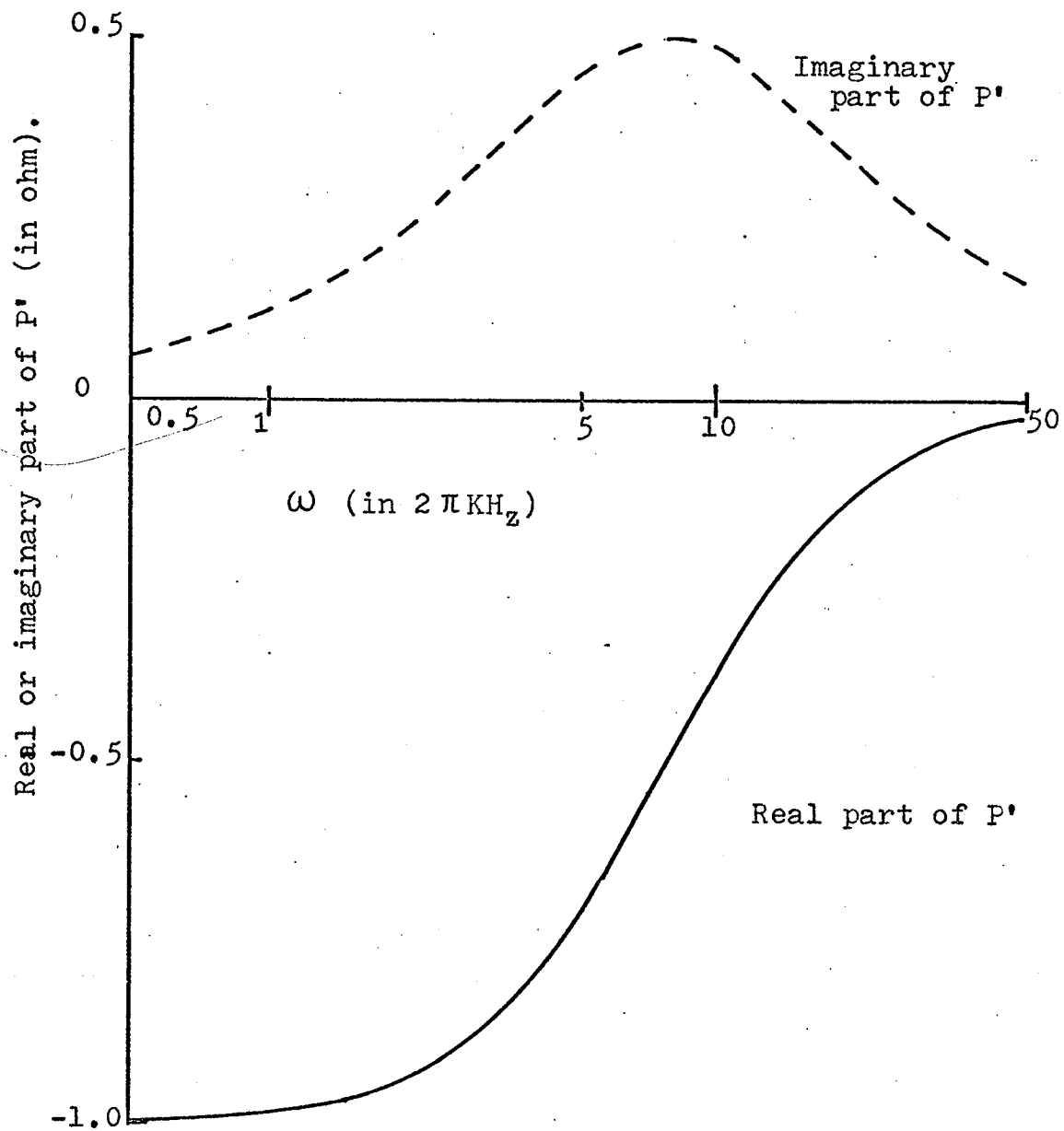


Fig. (4.10) Frequency dependence of real and imaginary parts of  $P'(\omega)$  for current source.

ence between those two cases being only  $180^\circ$  phase difference. For these two cases, the phase-shift and attenuation factors are

$$\begin{aligned}
 P(\omega) &= \frac{\frac{1}{j\omega C_p}}{\frac{1}{j\omega C_p} + R_{12}} \\
 &= \frac{1}{1 + (\omega C_p R_{12})^2} - j \frac{\omega C_p R_{12}}{1 + (\omega C_p R_{12})^2} \quad (4.18)
 \end{aligned}$$

or

$$P'(\omega) = - \frac{1}{1 + (\omega C_p R_{12})^2} + j \frac{\omega C_p R_{12}}{1 + (\omega C_p R_{12})^2} \quad (4.19)$$

The real and the imaginary parts of  $P(\omega)$  and  $P'(\omega)$  as functions of frequency  $\omega$  are shown in Fig. (4.9) and Fig. (4.10).

Fig. (4.11) shows a simple phase shifter for a voltage source  $V_{A1}$  which is considered to be proportional to  $I$ . For this case the input current  $i_{A2}$  into the second stage is given by

$$i_{A2} = \frac{V_A}{R_{12} + \frac{1}{j\omega C_p}} \quad (4.20)$$

Again, there are two possible ways of connection as in the cases for a current source. For these two connections the phase shift and attenuation factors are

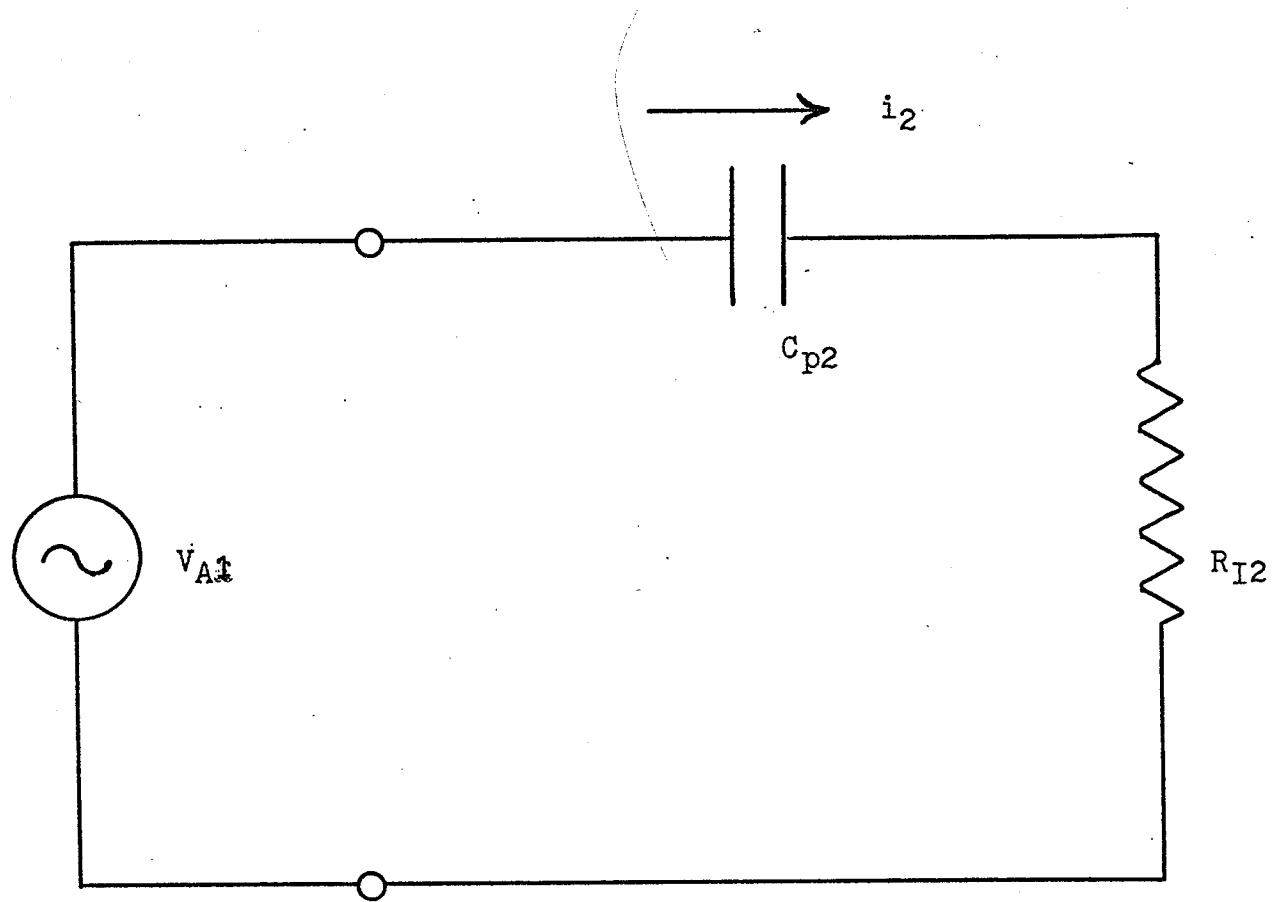


Fig. (4.11) Simple phase shifter for voltage source.

$$\begin{aligned}
 P(\omega) &= \frac{1}{R_{I2} + \frac{1}{j\omega C_p}} \\
 &= \frac{(\omega C_p)^2 R_{I2}}{1 + (\omega C_p R_{I2})^2} + j \frac{\omega C_p}{1 + (\omega C_p R_{I2})^2} \quad (4.21)
 \end{aligned}$$

or

$$P'(\omega) = -\frac{(\omega C_p)^2 R_{I2}}{1 + (\omega C_p R_{I2})^2} - j \frac{\omega C_p}{1 + (\omega C_p R_{I2})^2} \quad (4.22)$$

The real and the imaginary parts of  $P(\omega)$  and  $P'(\omega)$  as functions of  $\omega$  are shown in Fig. (4.12) and Fig. (4.13).

Having known the  $P(\omega)$  or  $P'(\omega)$  as function of frequency, we now can determine  $R(\omega)$  and  $X(\omega)$ . Figs. (4.14) and (4.15) show the frequency dependence of  $R(\omega)$  and  $X(\omega)$  for several values of  $G$  with  $H$  as a constant. Figs. (4.16) and (4.17) show the frequency dependence of  $R(\omega)$  and  $X(\omega)$  for several values of  $H$  with  $G$  as a constant.

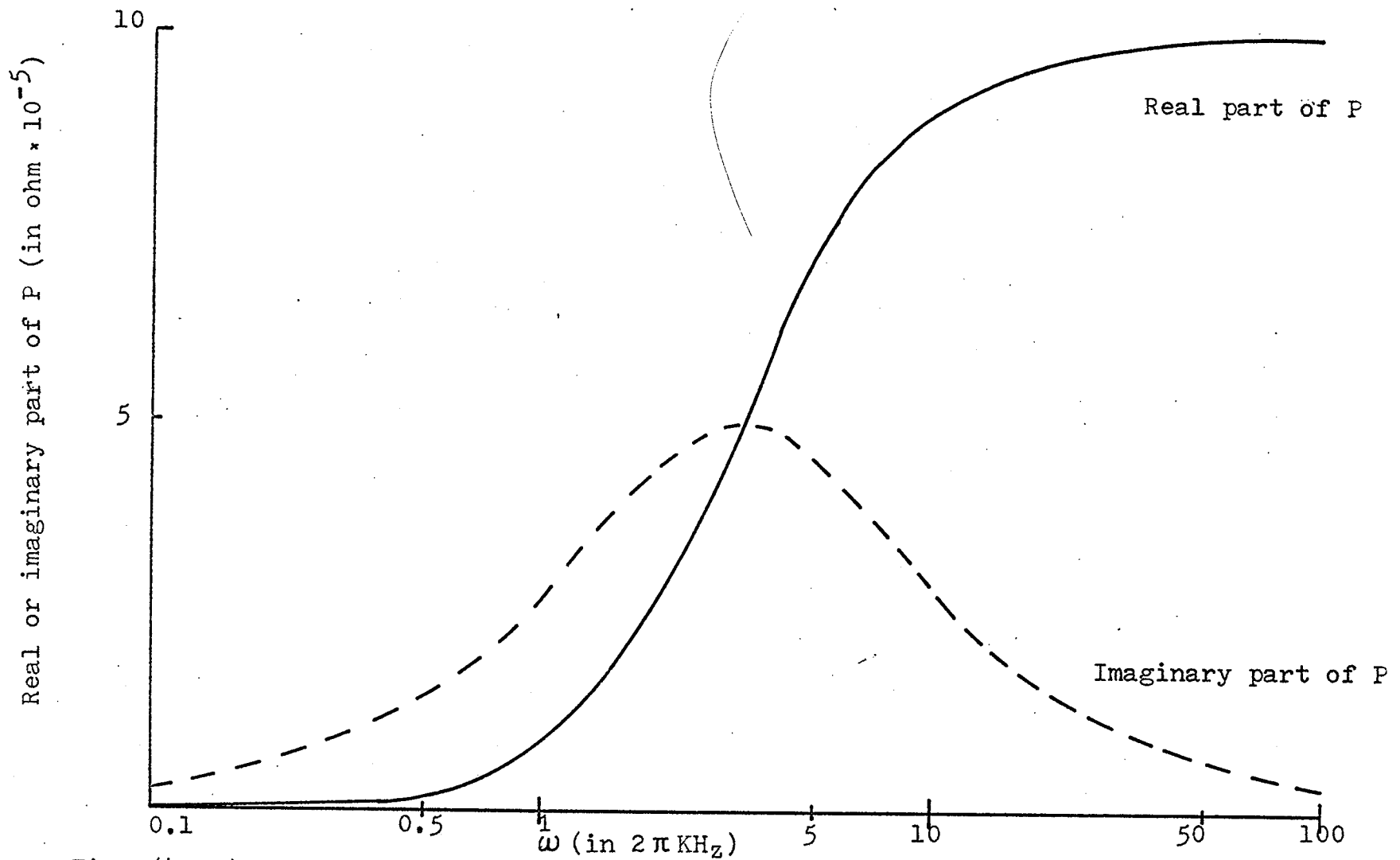


Fig. (4.12) Frequency dependence of real and imaginary parts of  $P'(\omega)$  for a voltage source.

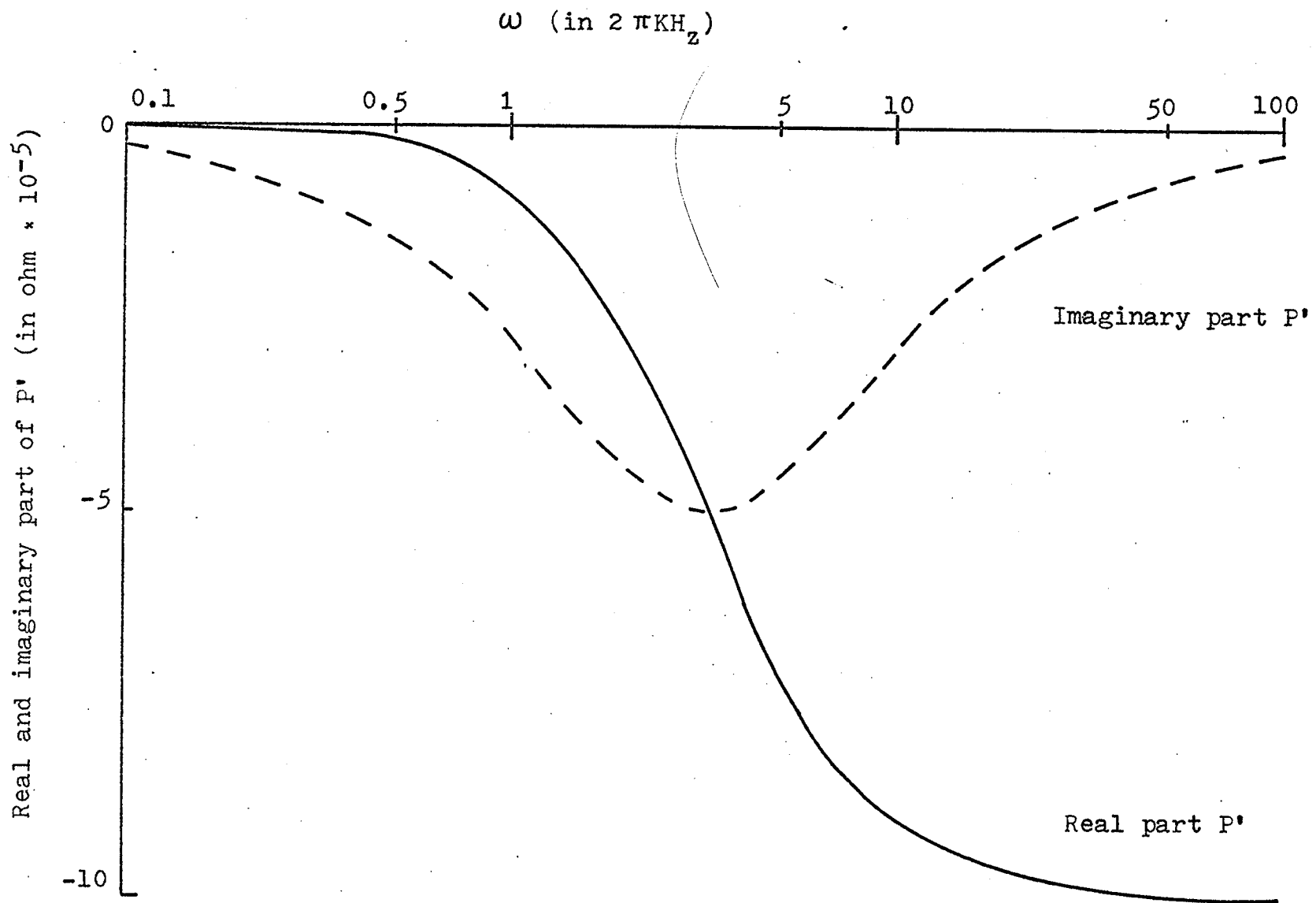


Fig. (4.13) Frequency dependence of real and imaginary parts of  $P'(\omega)$  for a voltage source.

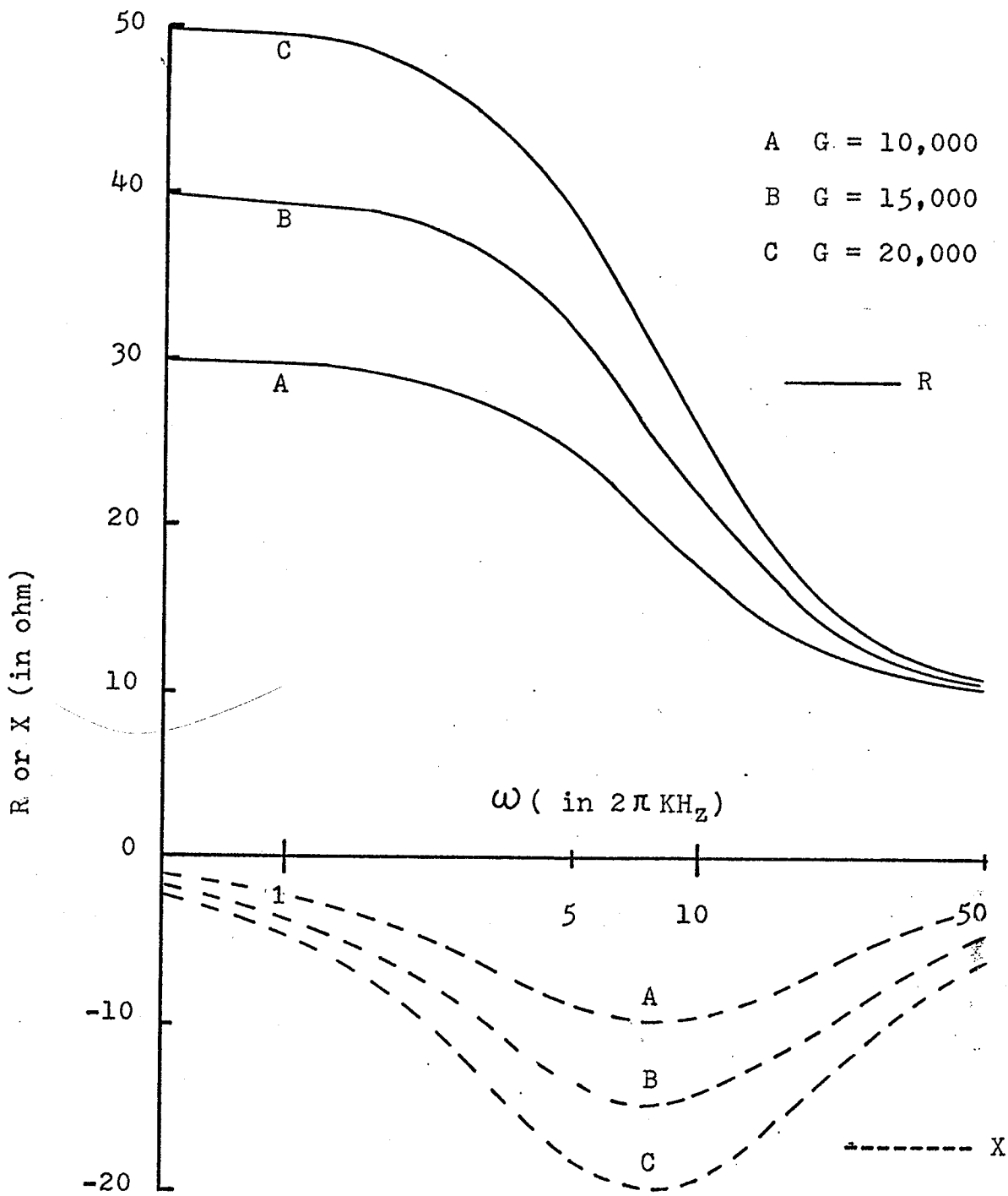


Fig. (4.14) Frequency dependence of  $R$  and  $X$  for various  $G$  with  $H = 10 \Omega$

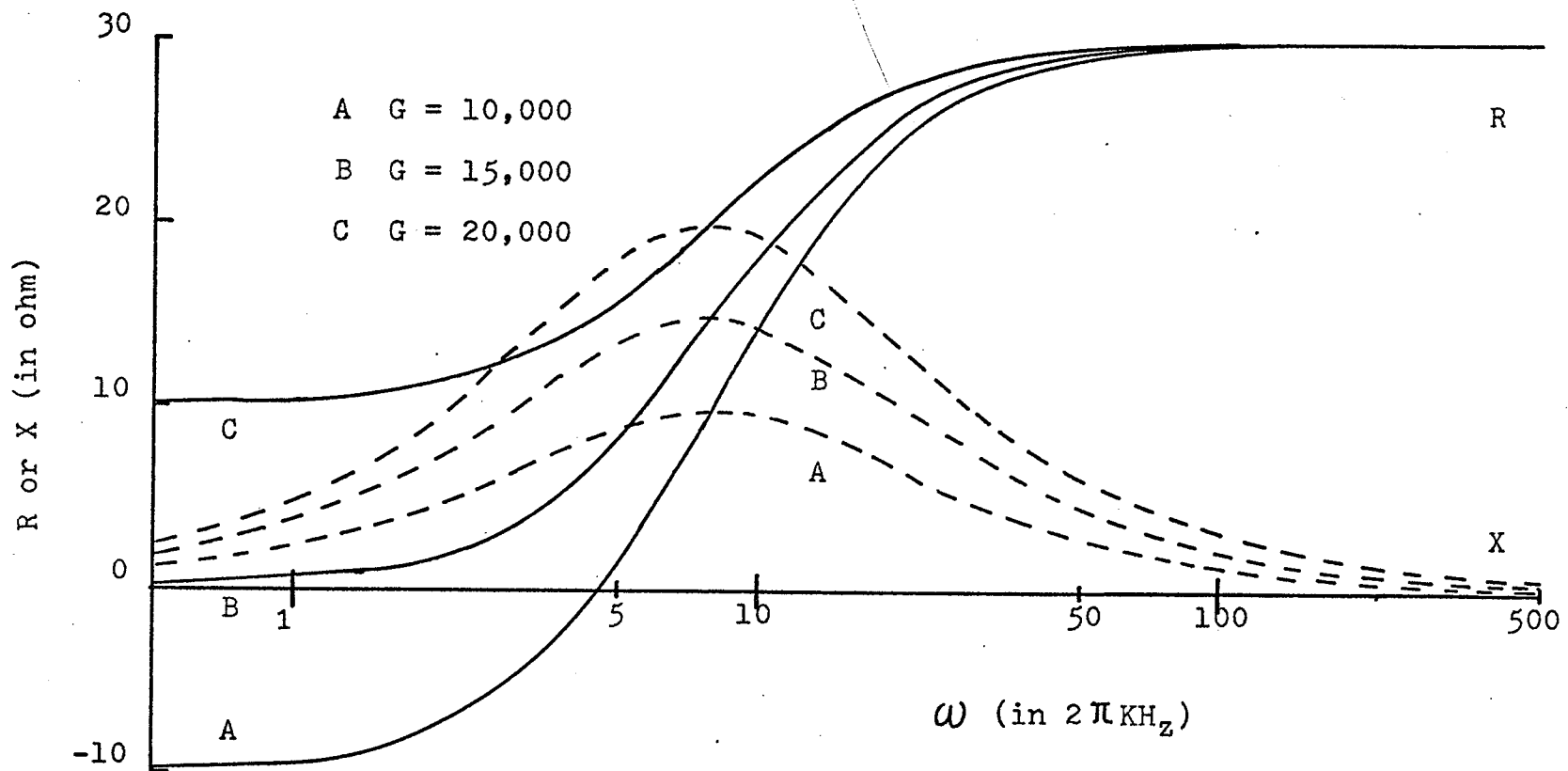


Fig. (4.15) Frequency dependence of R and X for various G with  $H = 30 \Omega$

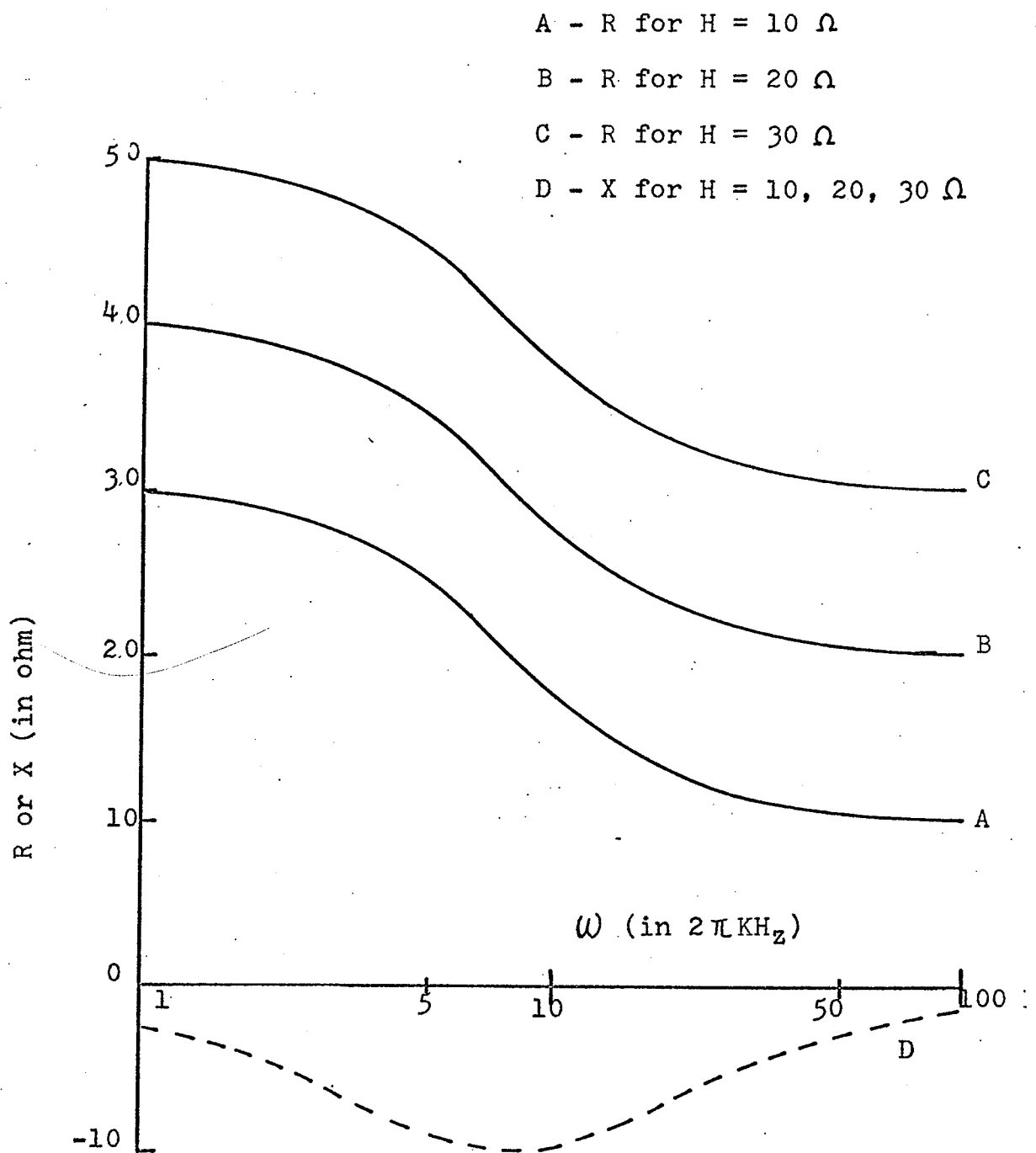


Fig. (4.16) Frequency dependence of R and X for  $H = 10, 20$  and  $30 \Omega$  with  $G = 10,000$ .

A - R for  $H = 10 \Omega$

B - R for  $H = 20 \Omega$

C - R for  $H = 30 \Omega$

D X for  $H = 10, 20, 30 \Omega$

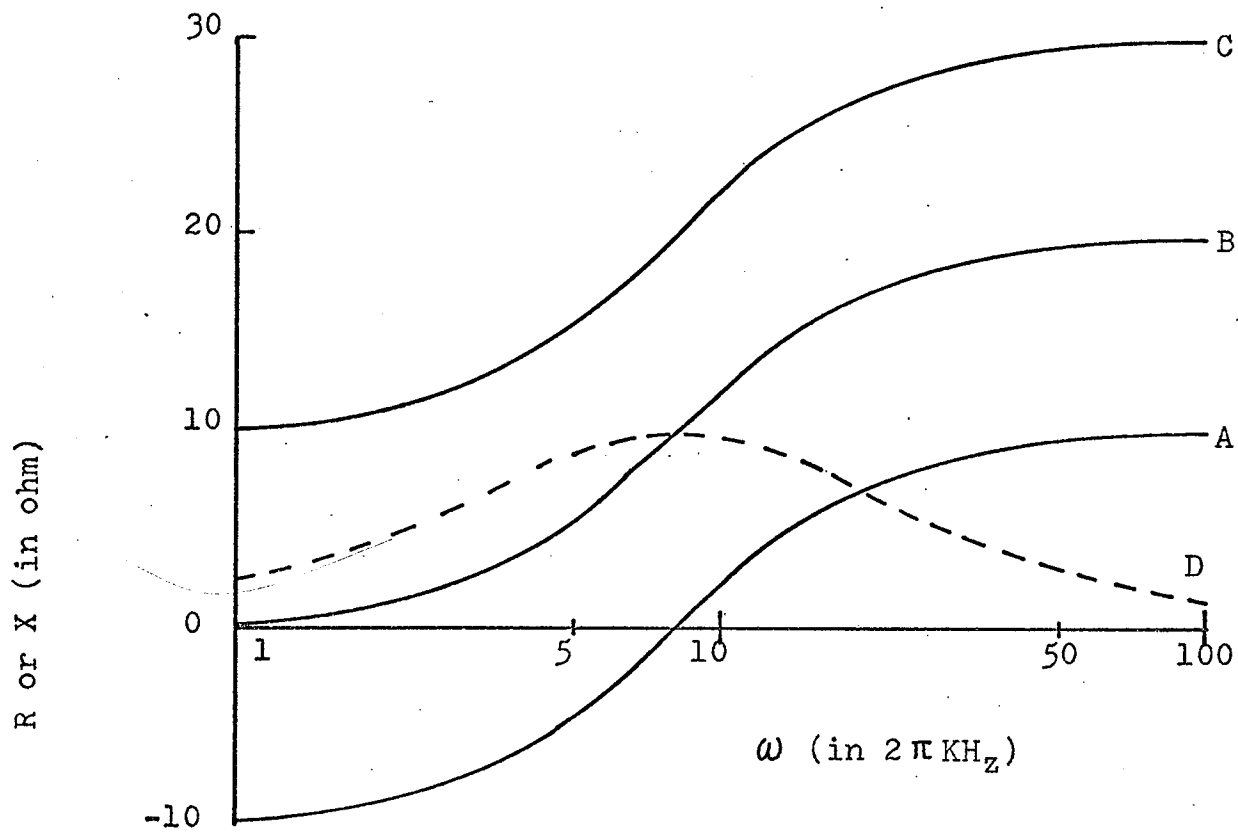


Fig. (4.17) Frequency dependence of R and X for  $H = 10, 20$  and  $30 \Omega$  with  $G = 10,000$ .

## CHAPTER V

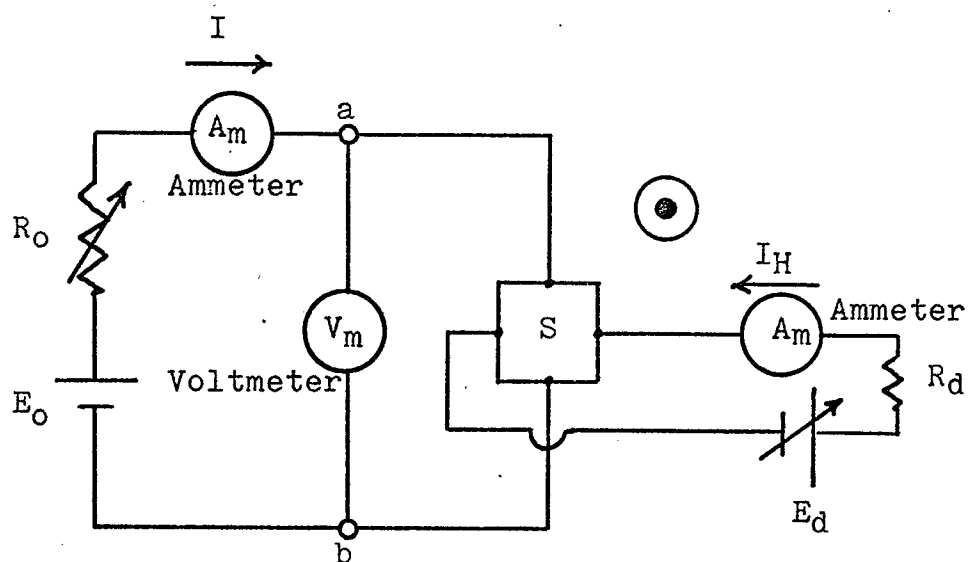
## EXPERIMENTAL RESULTS AND DISCUSSION

In this chapter we shall describe the experiments designed to prove the theory given in Chapter IV and to show the use of the R.R.E.G. as an element in simple oscillator and tuned circuits. We shall discuss step by step as follows:

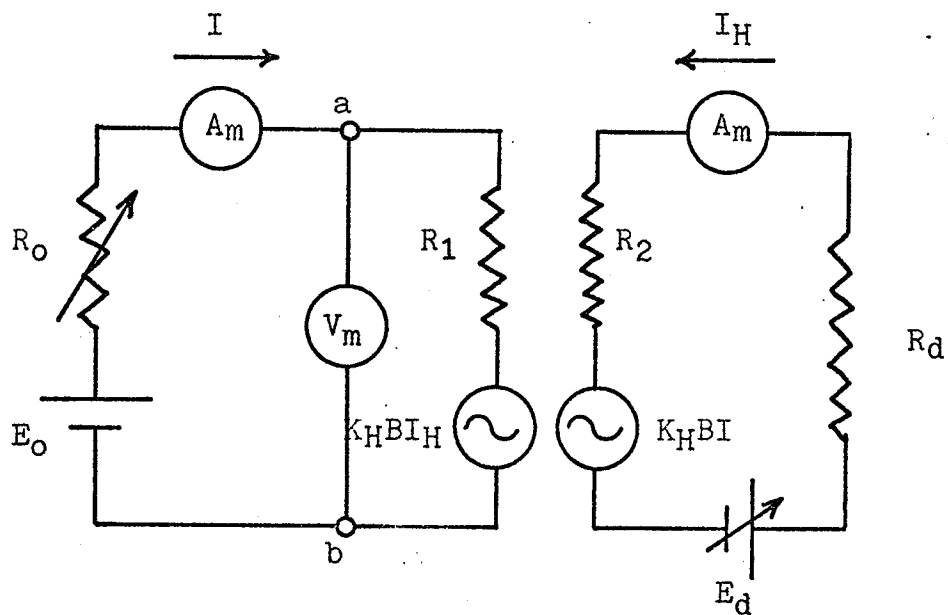
### 5.1 Equivalent Impedance with D.C. Power Source and D.C. Active Hall Load

In order to show how an active source connected across the Hall terminals causes the change of the equivalent impedance looking at the current terminals, we use the experimental set-up as shown in Fig. (5.1) in which  $R_1$  and  $R_2$  are the internal resistance of the Hall specimen across the current terminals and the Hall terminals respectively. The Hall specimen is an n-type  $I_n A_5$  of which  $R_1 = 3.3 \Omega$  and  $R_2 = 3.0 \Omega$  in the absence of magnetic field, and  $R_1 = 6.2 \Omega$  and  $R_2 = 6.0 \Omega$  when  $B = 10$  kilogauss.  $R_0$  and  $R_d$  are resistance which are connected in series to the sources  $E_0$  and  $E_d$ .

Referring to Fig. (5.1) we can write



(a)



(b)

Fig. (5.1) Experimental set-up (a) and its equivalent circuit (b).

$$V = \frac{R_1 E_o}{R_1 + R_o} + K_H B I_H \frac{R_o}{R_1 + R_o} \quad (5.1)$$

$$I = \frac{E_o - K_H B I_H}{R_1 + R_o} \quad (5.2)$$

Thus the equivalent impedance looking at the terminals a and b is

$$\begin{aligned} Z &= \frac{V}{I} \\ &= R_1 + \frac{K_H B I_H (R_1 + R_o)}{E_o - K_H B I_H} \end{aligned} \quad (5.3)$$

To visualize the characteristics of  $Z$ , we have the following three cases:

(a) when  $R_o \gg R_1$  and  $E_o \gg K_H B I_H$  then  $I \sim \frac{E_o}{R_o}$ .

In this case the power source can be considered as a constant current source, and the voltage  $V$  becomes

$$V = R_1 I + K_H B I_H \quad (5.4)$$

and the equivalent impedance becomes

$$Z = R_1 + K_H B \frac{I_H}{I} \quad (5.5)$$

Since  $R_1$ ,  $I$  and  $K_H B$  are constant for a given magnetic field, the values of  $V$  and  $Z$  should increase linearly with increasing  $I_H$  which can be adjusted to any value and to either positive or negative direction. Fig. (5.2) shows that the experimental results are in

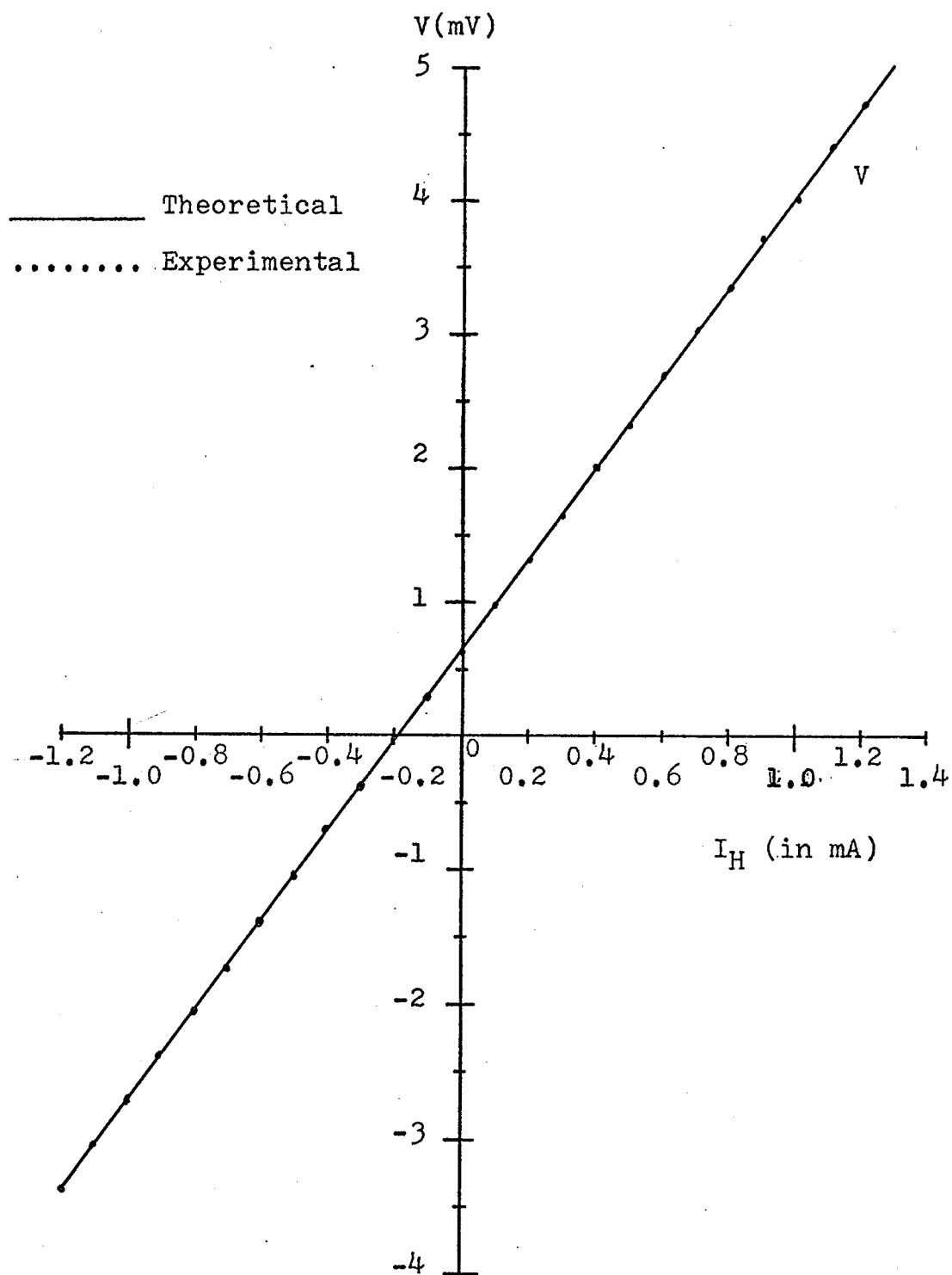


Fig. (5.2)  $V$  as a function of  $I_H$  for the case  $R_0 \gg R_1$  and  $E_0 \gg K_H B I_H$ .

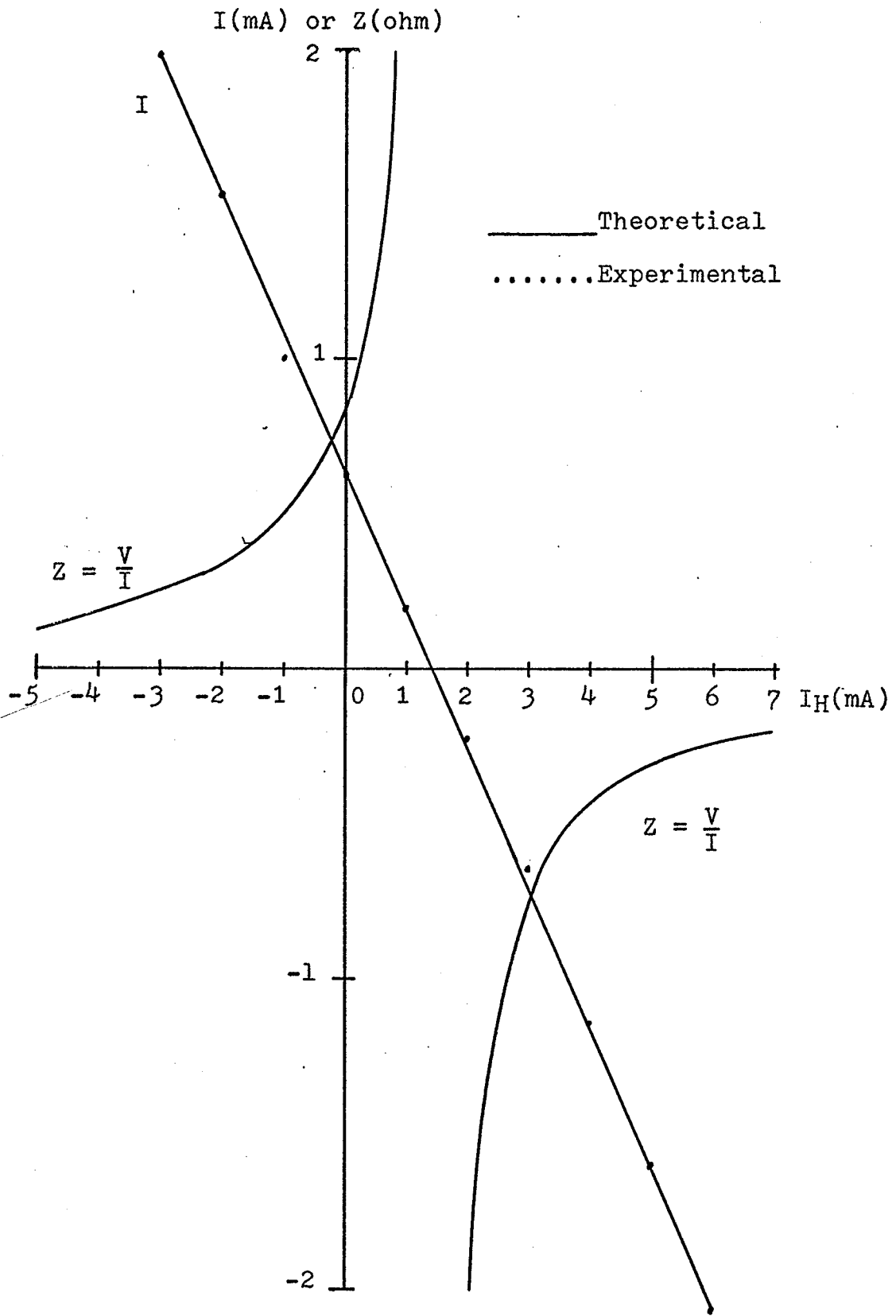


Fig. (5.3) I and Z as functions of  $I_H$  for the case  $R_0 \sim 0$  and  $V = E_0$ .

excellent agreement with the theoretical prediction. The experiment was performed with  $E_o = 10 \text{ V}$ ,  $R_o = 100 \text{ K}\Omega$ ,  $I = 0.1 \text{ mA}$  and  $B = 10 \text{ K}$  gauss.

(b) when  $R_o \sim 0$  the power source can be considered as a constant voltage source. In this case, we have

$$V = E_o \quad (5.6)$$

$$I = \frac{E_o - K_H B I_H}{R_I} \quad (5.7)$$

$$\text{and } Z = \frac{E_o R_I}{E_o - K_H B I_H} \quad (5.8)$$

$I$  increases linearly with  $I_H$  but  $Z$  increases with decreasing  $|I_H|$  and becomes infinite when  $E_o = K_H B I_H$ . Fig. (5.3) shows some experimental results for  $R_o = 0$ ,  $E_o = 5 \text{ mV}$  and  $B = 10 \text{ Kilogauss}$ . Again, the experimental results are in excellent agreement with the theoretical prediction.

(c) when  $R_o$  is of such a value that the power source can neither be treated as a constant current source, nor a constant voltage source. In this case we used  $E_o = 5 \text{ mV}$ ,  $R_o = 10$  and  $B = 10 \text{ Kilogauss}$  for the experiment. The results shown in Fig. (5.4) are in good agreement with the

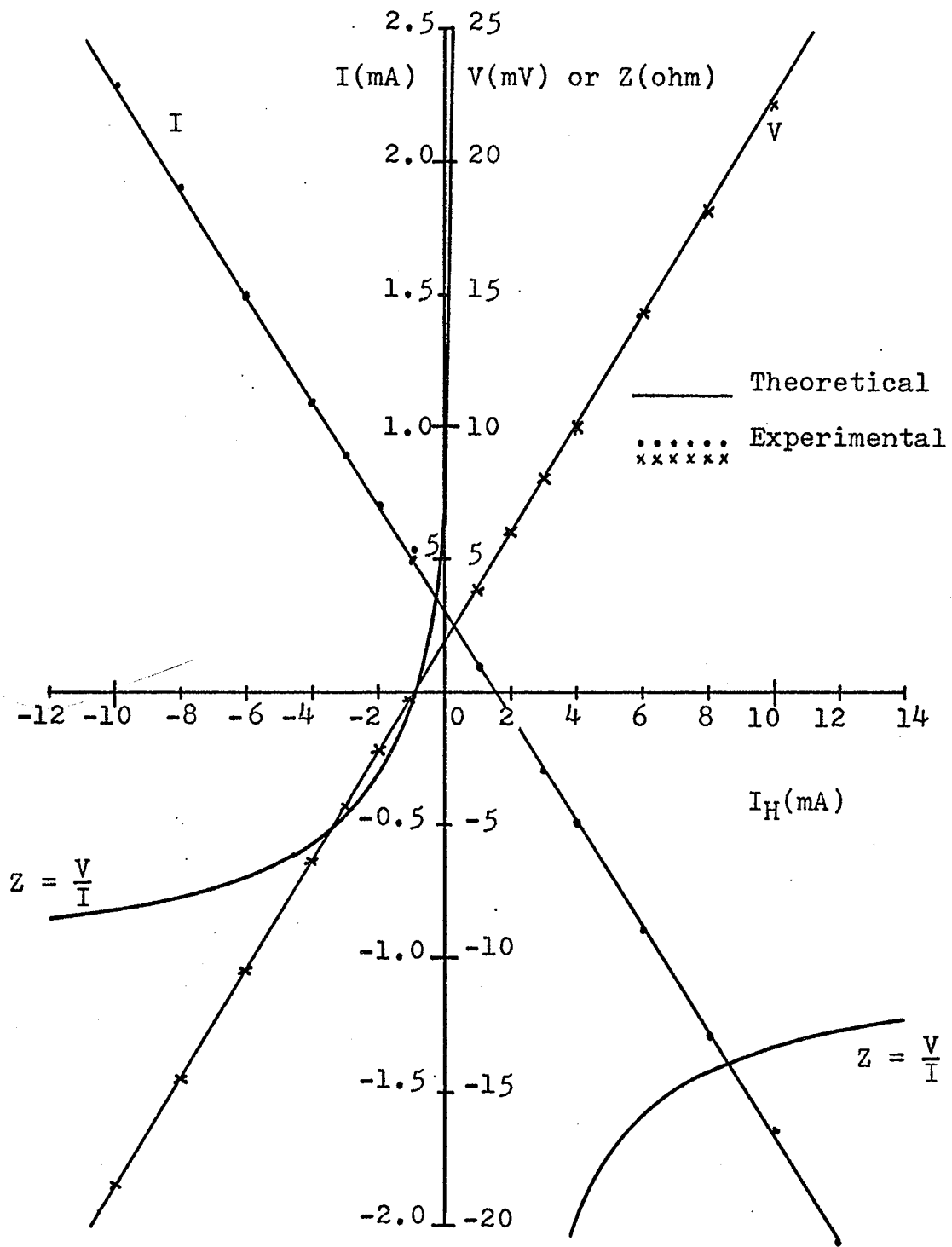


Fig. (5.4)  $V$ ,  $I$  and  $Z$  as functions of  $I_H$  for  $R_0$  having the same order of the value of  $R_1$ .

theoretical prediction.

## 5.2 Equivalent Impedance with A.C. Source and A.C.

### Active Hall Load

When the frequency of an a.c. power source and that of an a.c. active Hall load are different, the equivalent impedance of the a.c. active Hall load is given by Equation (3.3). We rewrite this equation as follows:

$$Z(\omega_0, \omega_1, t) = Z_1(\omega_0) + \frac{E_1(\omega)}{I(\omega_0, \omega_1, t)} \left\{ \frac{Z_1(\omega_0) + Z_0(\omega_1)}{Z_0(\omega_1) + Z_1(\omega_1)} \right\} \quad (5.9)$$

For simplicity, we use pure resistance  $R_0$  and  $R_1$ , which are independent of frequency, to represent  $Z_0$  and  $Z_1$ ; then Equation (5.9) becomes

$$Z(\omega_0, \omega_1, t) = R_1 + \frac{E_1(\omega_1)}{I(\omega_0, \omega_1, t)} \quad (5.10)$$

in which  $E_1(\omega_1)$  is the Hall potential produced by  $I_H$ ,

$$E_1 = K_H B I_H \quad (5.11)$$

Suppose we take  $I$  as reference

$$I = |I| \angle 0 \quad (5.12)$$

and write

$$\begin{aligned}
 I_H &= |I_H| \angle (\omega_0 - \omega_1)t + \gamma_0 \\
 &= |I_H| \angle \gamma(\omega_0, \omega_1, t)
 \end{aligned}
 \tag{5.13}$$

in which  $t \leq \frac{2\pi}{\omega_0 - \omega_1}$ . The phase angle  $\gamma$  is time dependent, the physical meaning of which is given in the Appendix I. Introducing Equations (5.11), (5.12) and (5.13) into Equation (5.10) we obtain

$$Z(\omega_0, \omega_1, t) = R(\omega_0, \omega_1, t) + jX(\omega_0, \omega_1, t)
 \tag{5.14}$$

in which

$$R(\omega_0, \omega_1, t) = R_1 + \frac{K_H B |I_H|}{|I|} \cos \gamma(\omega_0, \omega_1, t)
 \tag{5.15}$$

and

$$X(\omega_0, \omega_1, t) = \frac{K_H B |I_H|}{|I|} \sin \gamma(\omega_0, \omega_1, t)
 \tag{5.16}$$

The quality factor is therefore

$$\begin{aligned}
 Q(\omega_0, \omega_1, t) &= \frac{|X(\omega_0, \omega_1, t)|}{R(\omega_0, \omega_1, t)} \\
 &= \frac{|K_H B |I_H| \sin \gamma(\omega_0, \omega_1, t)}{R_1 + K_H B |I_H| \cos \gamma(\omega_0, \omega_1, t)}
 \end{aligned}
 \tag{5.17}$$

and the phase angle  $\phi(\omega_0, \omega_1, t)$  which indicates the relative magnitude of  $X(\omega_0, \omega_1, t)$  and  $R(\omega_0, \omega_1, t)$  is given by

$$\begin{aligned}\phi(\omega_0, \omega_1, t) &= \tan^{-1} \frac{X(\omega_0, \omega_1, t)}{R(\omega_0, \omega_1, t)} \\ &= \tan^{-1} Q(\omega_0, \omega_1, t) \quad (5.18)\end{aligned}$$

The absolute value of  $Z(\omega_0, \omega_1, t)$  is thus

$$\begin{aligned}|Z(\omega_0, \omega_1, t)| &= \sqrt{\{R(\omega_0, \omega_1, t)\}^2 + \{X(\omega_0, \omega_1, t)\}^2} \\ &= \sqrt{R_i^2 + \left(K_H B \left|\frac{I_H}{I}\right|\right)^2 + 2 K_H B R_i \left|\frac{I_H}{I}\right| \cos \gamma(\omega_1, \omega_0, t)}\end{aligned} \quad (5.19)$$

Using the experimental set-up as shown in Fig. (5.5), we obtained a series of results for  $|Z(\omega_0, \omega_1, t)|$  as a function of  $\phi(\omega_0, \omega_1, t)$  for  $\left|\frac{I_H}{I}\right| = 0.5, 1, 1.5$  and  $2$  at  $f_0 = \frac{\omega_0}{2\pi} = 10 \text{ KHz}$  and  $f_0 - f_1 = \frac{\omega_0 - \omega_1}{2\pi} = 0.1 \text{ Hz}$  and they are shown in Fig. (5.6). For this case both  $\phi(\omega_0, \omega_1, t)$  and  $|Z(\omega_0, \omega_1, t)|$  are time dependent as shown in Fig. (5.7). The rate of the change of  $|Z(\omega_0, \omega_1, t)|$  and  $\phi(\omega_0, \omega_1, t)$  depends upon the frequency difference between  $\frac{\omega_0}{2\pi}$  and  $\frac{\omega_1}{2\pi}$ .

When  $\omega_0$  and  $\omega_1$  are identical or derived from

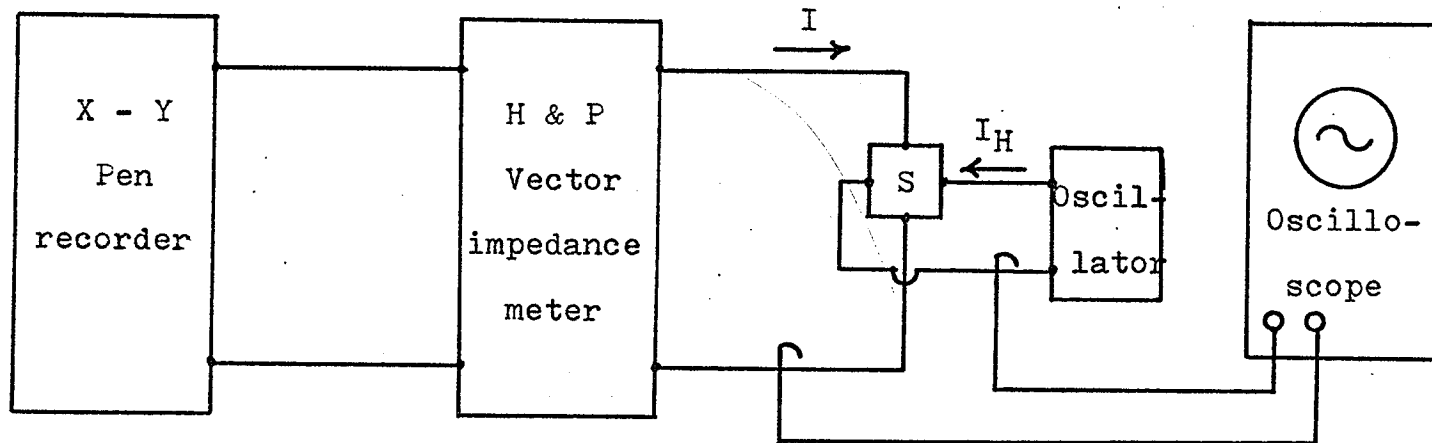


Fig. (5.5) Experimental set-up for measuring the values of  $Z$  as a function of  $\phi$  ( $= \tan^{-1} \frac{X}{R}$ ) and  $\frac{I_H}{I}$  for  $\omega_0 = 2\pi \cdot 10\text{KHz}$  and  $\omega_0 - \omega_1 = 0.2\pi\text{Hz}$ .

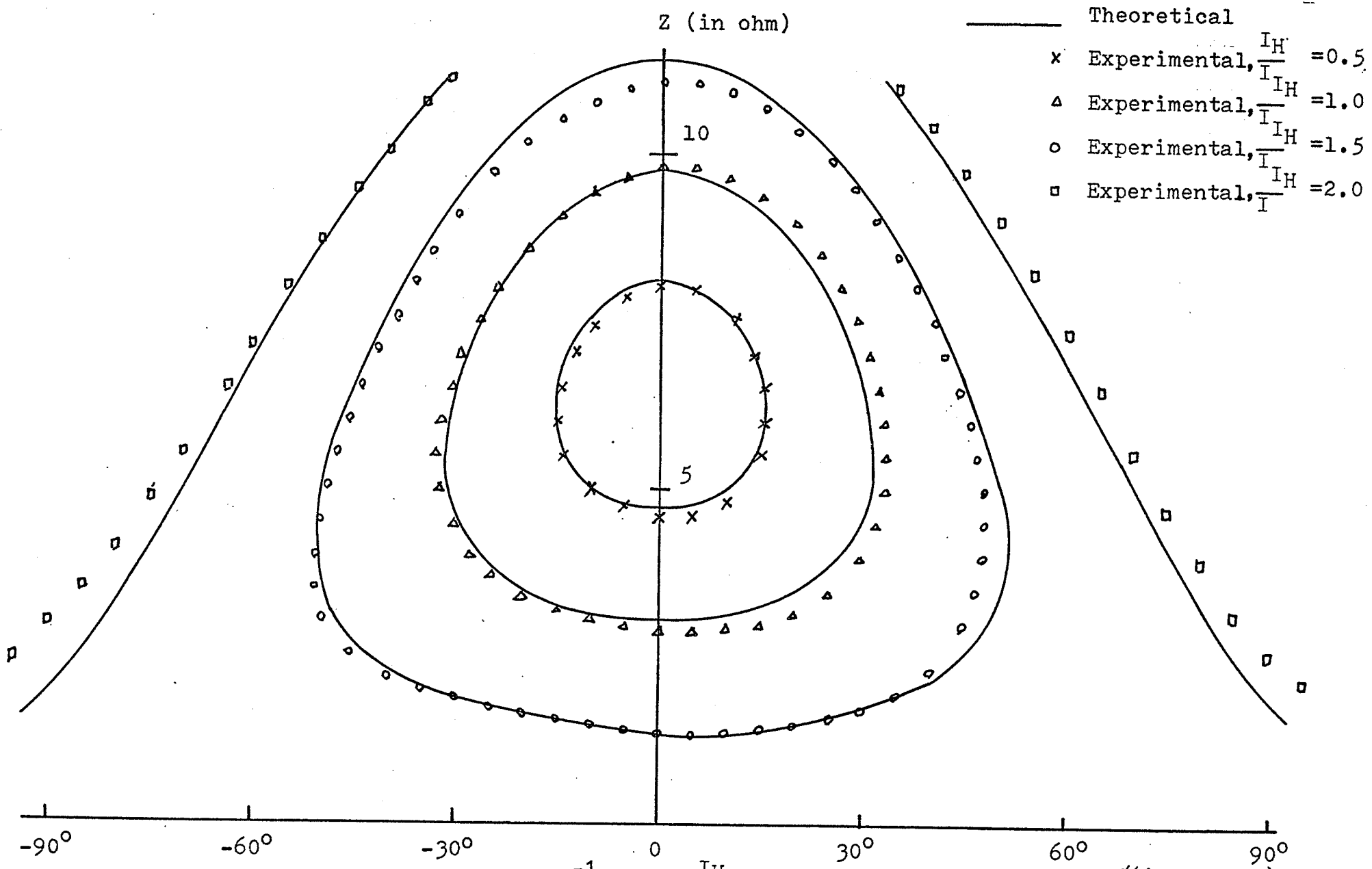


Fig. (5.6) Z as a function of  $\phi = \tan^{-1} \frac{X}{R}$  and  $\frac{I_H}{I}$  for  $\omega_0 = 2\pi \text{ 10KHz}$  and  $\omega_0 - \omega_1 = 0.2\pi \text{ Hz}$ .

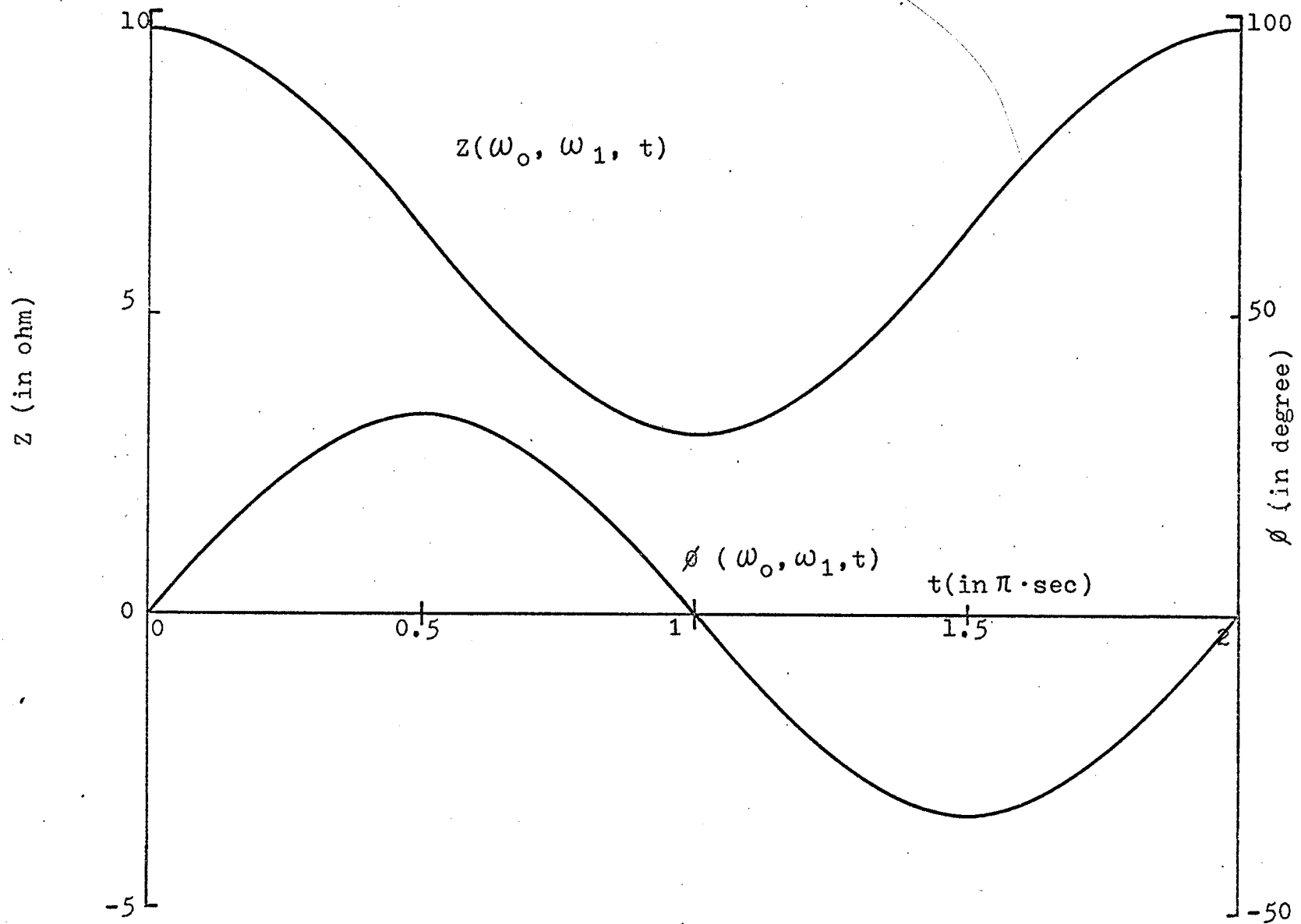


Fig. (5.7)  $Z$  and  $\phi$  as functions of time.

the same source, both  $\phi$  and  $Z$  are independent of time. In this case the value of  $Z$  depends mainly on  $\left| \frac{I_H}{I} \right|$  and the phase angle  $\gamma$  between  $I$  and  $I_H$ . Using the experimental set-up shown in Fig. (5.8)  $I_H$  was derived from the same source - the test oscillator of the Hewlett Packard vector impedance meter, which was also used to produce  $I$ , therefore the frequency of  $I$  and that of  $I_H$  are identical. Fig. (5.9) shows the value of  $|Z|$  and  $\phi (= \tan^{-1} \frac{X}{R})$  as functions of  $\gamma$  and  $\left| \frac{I_H}{I} \right|$ . For this experiment Hall specimen has  $K_H = 3.86$  ohm/weber  $R_1 = 4.41 \Omega$ ,  $R_2 = 4.4 \Omega$  with  $B = 5$  Kilogauss. The experimental results are in good agreement with the theoretical prediction. It is interesting to note that when  $I_H$  is large, the value of  $\phi$  becomes closer to the value of  $\gamma$ , and that  $Z$  has an inductive component when  $\gamma$  is positive and a capacitive component when  $\gamma$  is negative.

### 5.3 Resistive and Reactive Elements Based on Galvanomagnetic Effect (R.R.E.G.).

Referring to Fig. (4.2) and Equation (4.5) the equivalent impedance of the R.R.E.G. is given by

$$Z(\omega) = R_s + R_1 + \frac{R_b (R_{I1} - jX_{P1})}{R_b + R_{I1} - jX_{P1}} + K_H B A_1 A_2 \left( \frac{R_b}{R_b + R_{I1} - jX_{P1}} \right) \left( - \frac{jX_{P2}}{R_{I2} - jX_{P2}} \right)$$

$$\begin{aligned}
 &= H + G P \\
 &= R + jX \qquad (5.20)
 \end{aligned}$$

where

$$X_{p1} = \frac{1}{\omega C_{p1}} \qquad (5.21)$$

$$X_{p2} = \frac{1}{\omega C_{p2}} \qquad (5.22)$$

$$H = R_s + R_1 + \frac{R_b (R_{I1} - jX_{p1})}{R_b + R_{I1} - jX_{p1}} \qquad (5.23)$$

$$G = K_H B A_1 A_2 \qquad (5.24)$$

$$P = \left( \frac{R_b}{R_b + R_{I1} - jX_{p1}} \right) \left( - \frac{jX_{p2}}{R_{I2} - jX_{p2}} \right) \qquad (5.25)$$

$$\begin{aligned}
 R &= R_s + R_1 + \frac{R_b R_{I1} (R_b + R_{I1}) + R_b X_{p1}^2}{(R_b + R_{I1})^2 + X_{p1}^2} \\
 &+ \frac{K_H B A_1 A_2 X_{p2} R_b \{X_{p2} (R_b + R_{I1}) + X_{p1} R_{I2}\}}{\{(R_b + R_{I1}) R_{I2} - X_{p1} X_{p2}\}^2 + \{X_{p2} (R_s + R_{I1}) + X_{p1} R_{I2}\}^2} \\
 &\qquad (5.26)
 \end{aligned}$$

$$X = - \frac{R_b^2 X_{p1}}{(R_b + R_{I1})^2 + X_{p1}^2}$$

$$+ \frac{K_H B A_1 A_2 [X_{P2} R_b \{X_{P2} (R_b + R_{I1}) + X_{P1} R_{I2}\} - R_{I2} X_{P2} R_b (R_b + R_{I1})]}{\{R_{I2} (R_b + R_{I1})\}^2 + \{X_{P2} (R_b + R_{I1})\}^2} \quad (5.27)$$

If  $C_{P1} \rightarrow \infty$  i.e.  $C_{P1}$  is replaced with a short circuit, then Equations (5.23), (5.25), (5.26) and (5.27) become

$$H = R_s + R_1 + \frac{R_b R_{I1}}{R_b + R_{I1}} \quad (5.28)$$

$$P = \left( \frac{R_b}{R_b + R_{I1}} \right) \left( \frac{-j X_{P2}}{R_{I2} - j X_{P2}} \right) \quad (5.29)$$

$$R = R_s + R_1 + \frac{R_b R_{I1}}{R_b + R_{I1}} + \frac{K_H B A_1 A_2 X_{P2}^2 R_b (R_b + R_{I1})}{\{R_{I2} (R_b + R_{I1})\}^2 + \{X_{P2} (R_b + R_{I1})\}^2} \quad (5.30)$$

$$X = \frac{K_H B A_1 A_2 \{R_b X_{P2}^2 (R_b + R_{I1}) - R_b R_{I2} X_{P2} (R_b + R_{I1})\}}{\{R_{I2} (R_b + R_{I1})\}^2 + \{X_{P2} (R_b + R_{I1})\}^2} \quad (5.31)$$

Using the circuit of Fig. (4.2) and 2N4125 transistors, we obtained a series of results for R and X as functions of frequency under various conditions and they are shown in Figs.(5.10)-(5.17).

These results indicate the following features;

- (a) The shape of the frequency dependance of equivalent impedance curves is not altered

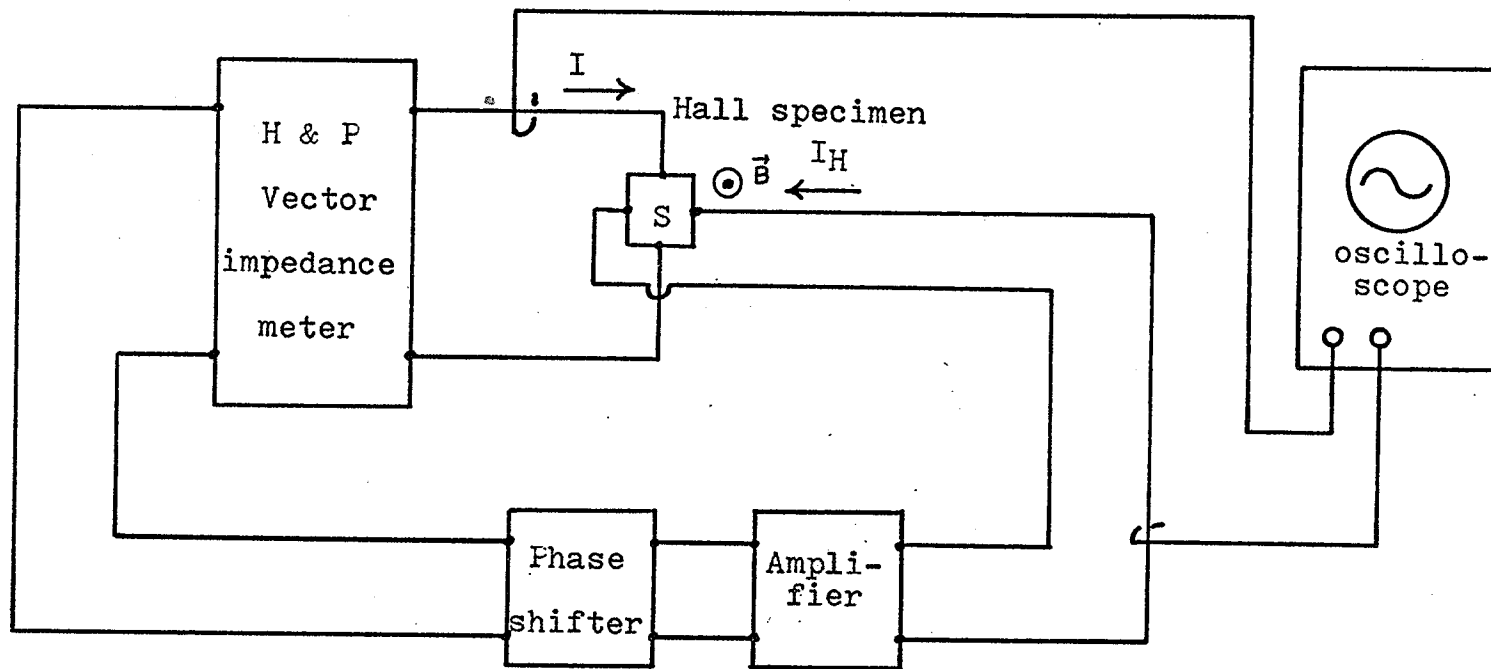


Fig. (5.8) Experimental set-up for measuring  $Z$  as a function of  $\gamma$  between  $I$  and  $I_H$ .

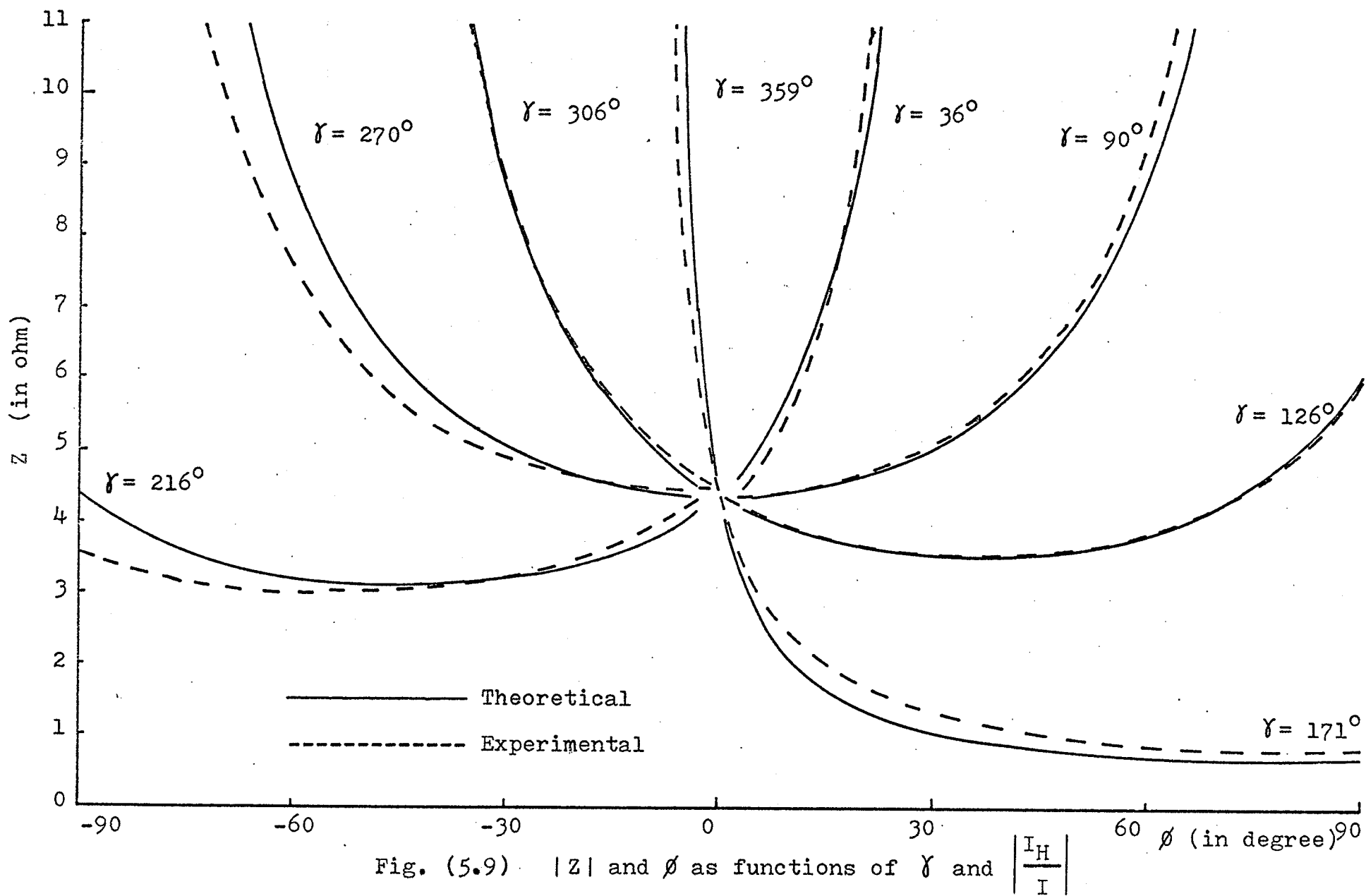


Fig. (5.9)  $|Z|$  and  $\phi$  as functions of  $\gamma$  and  $\left| \frac{I_H}{I} \right|$

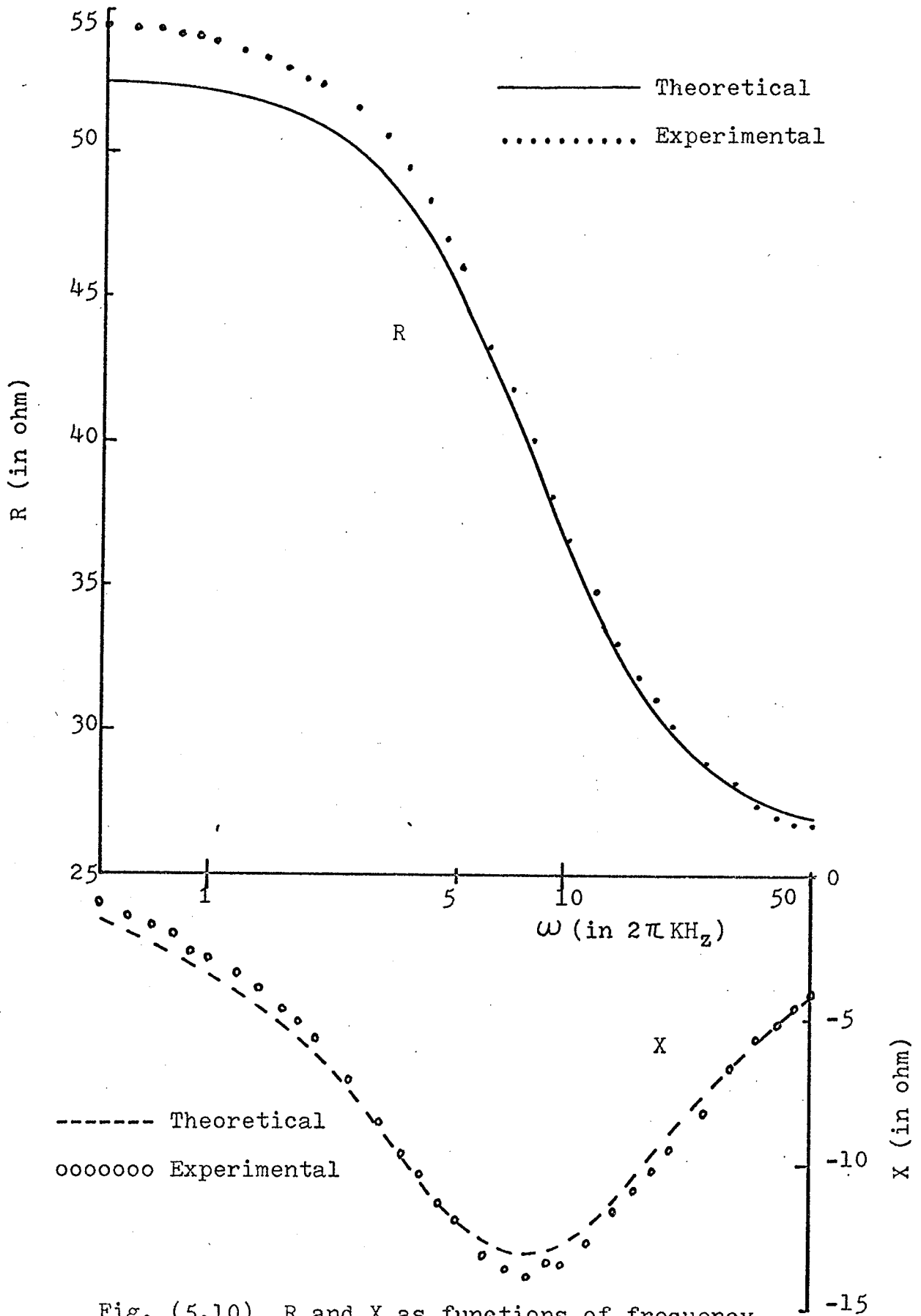


Fig. (5.10) R and X as functions of frequency.

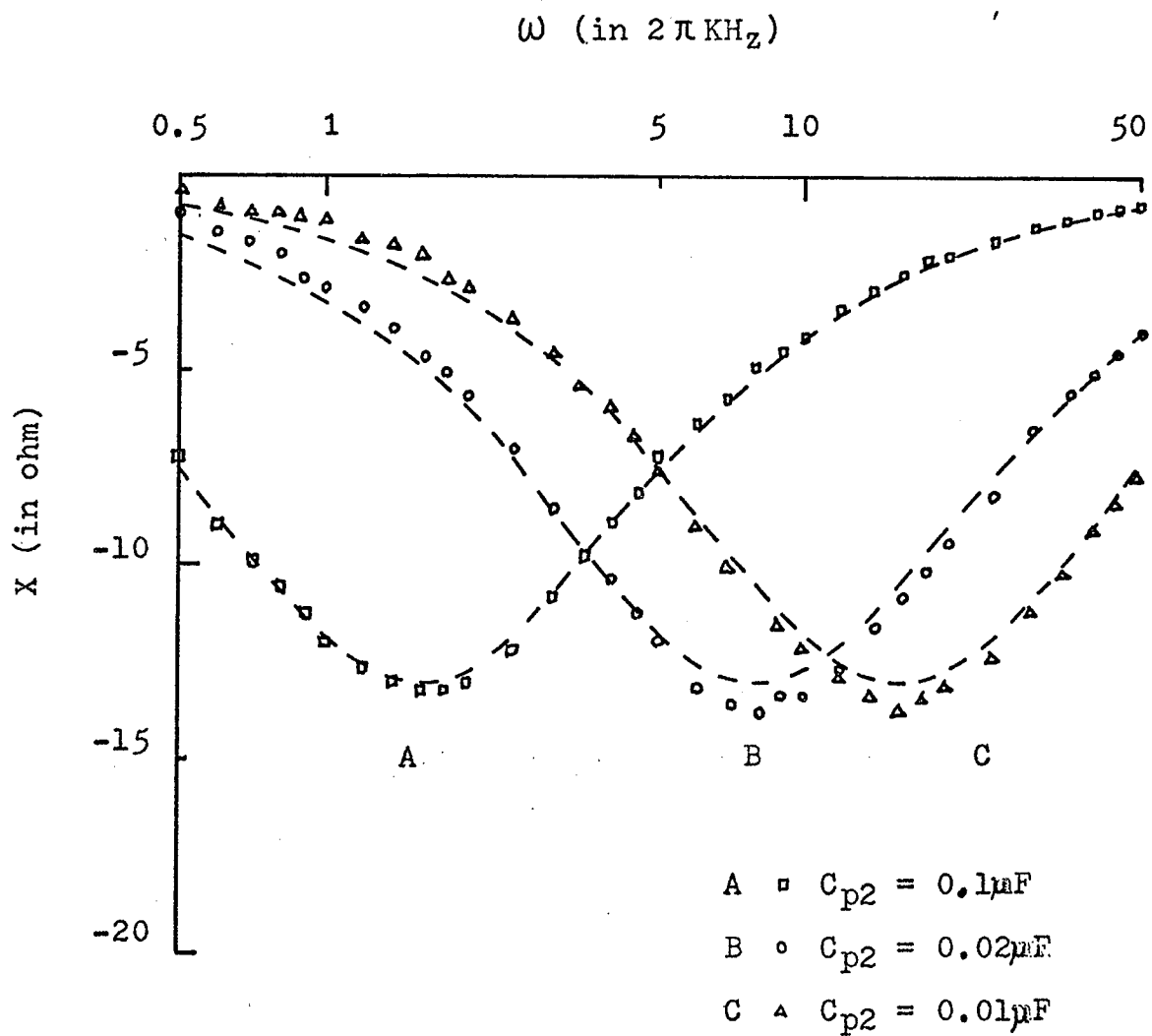


Fig. (5.11) X as a function of frequency and phase shifter capacitance.

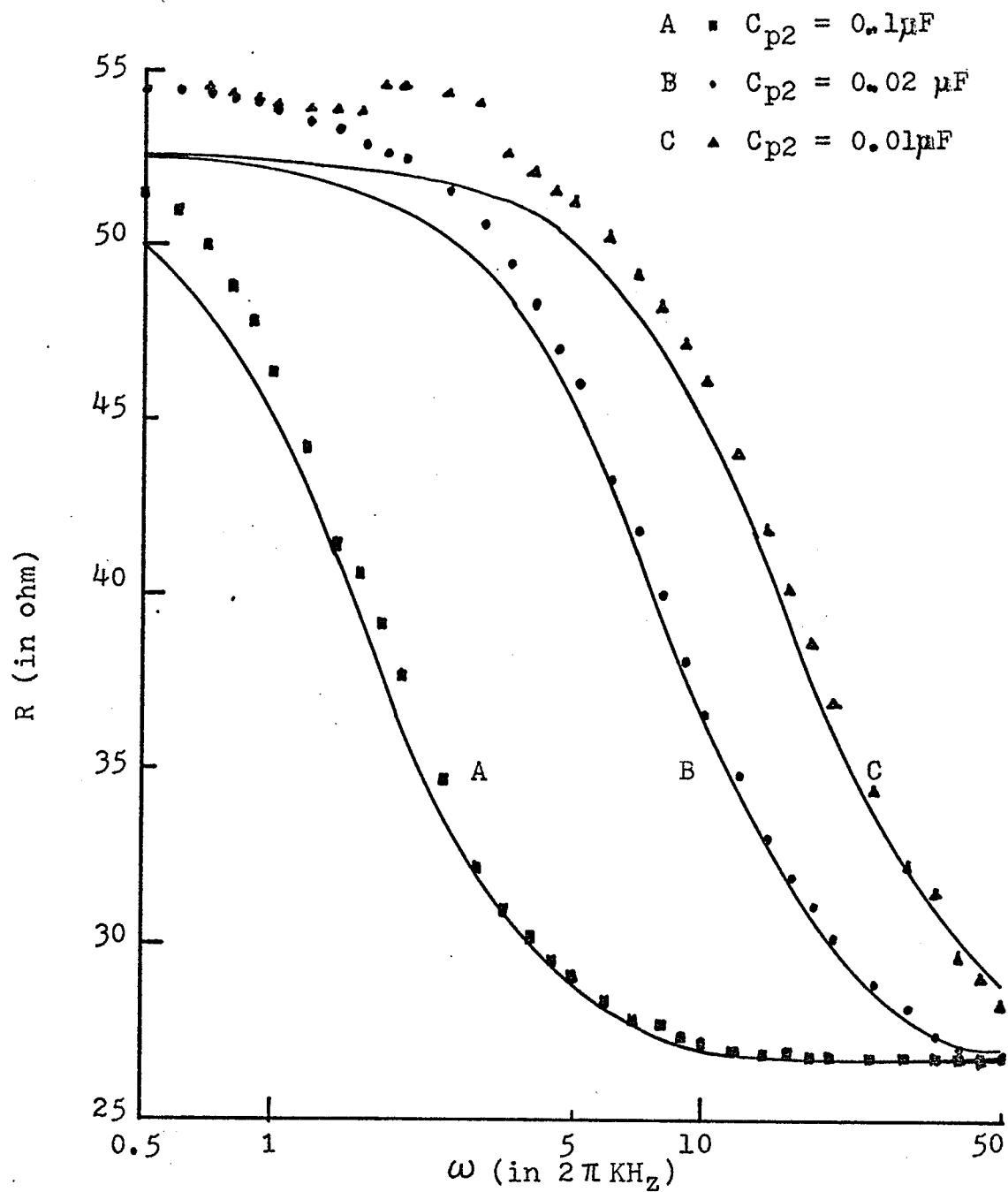


Fig. (5.12) R as a function of frequency and phase shifter capacitance.

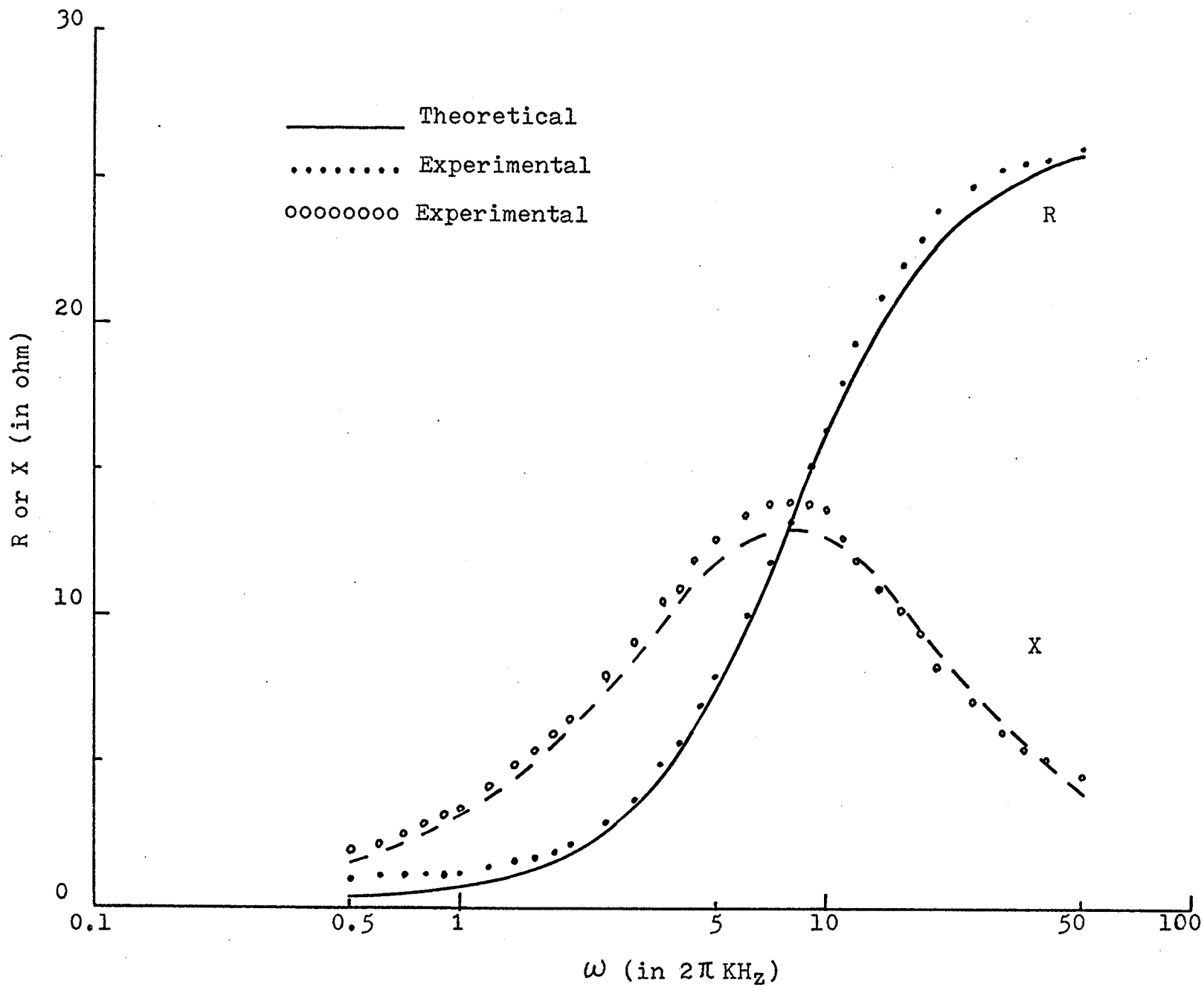


Fig. (5.13) R and X as functions of frequency.

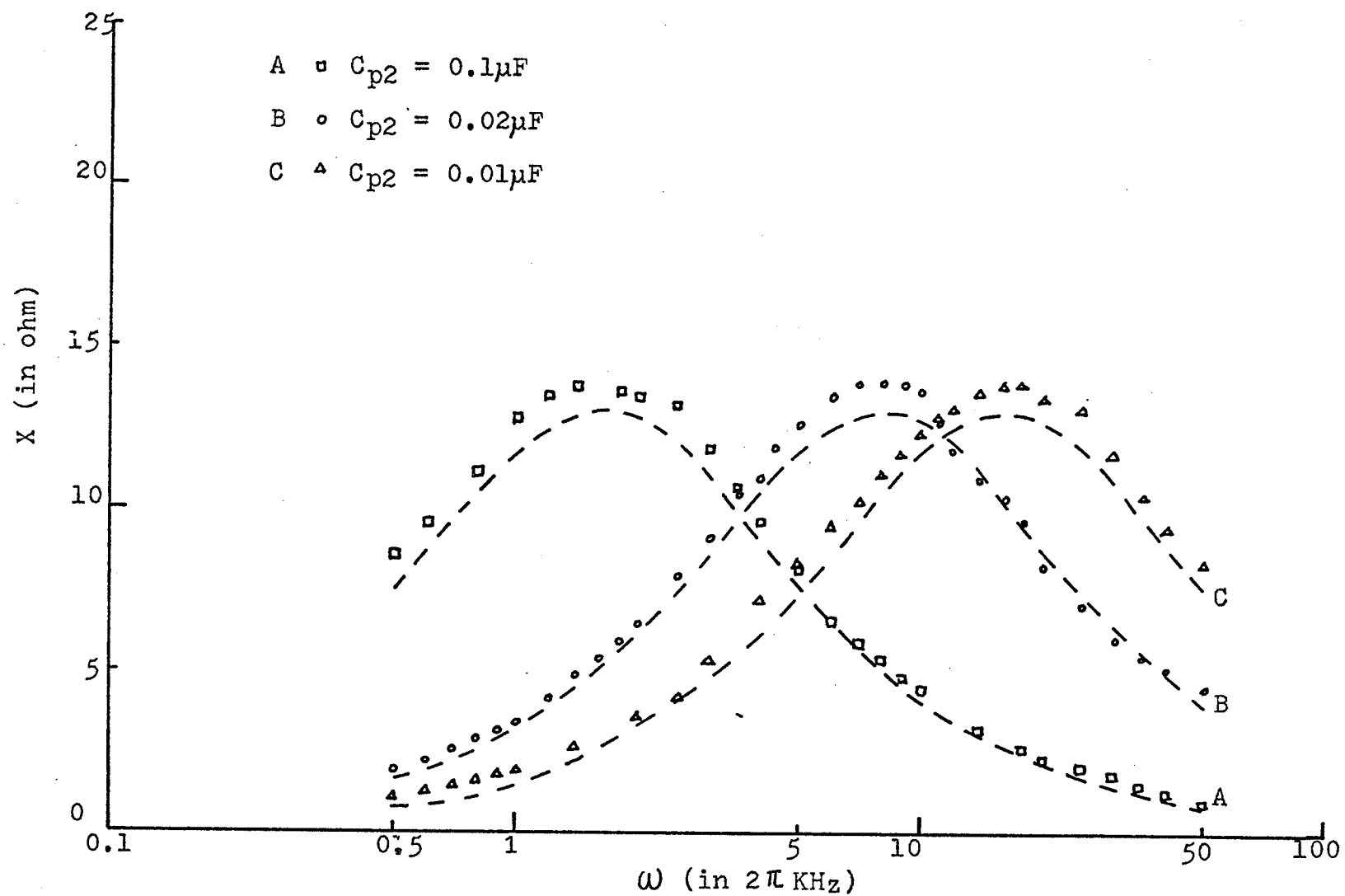


Fig. (5.14) X as a function of frequency and phase shifter capacitance.

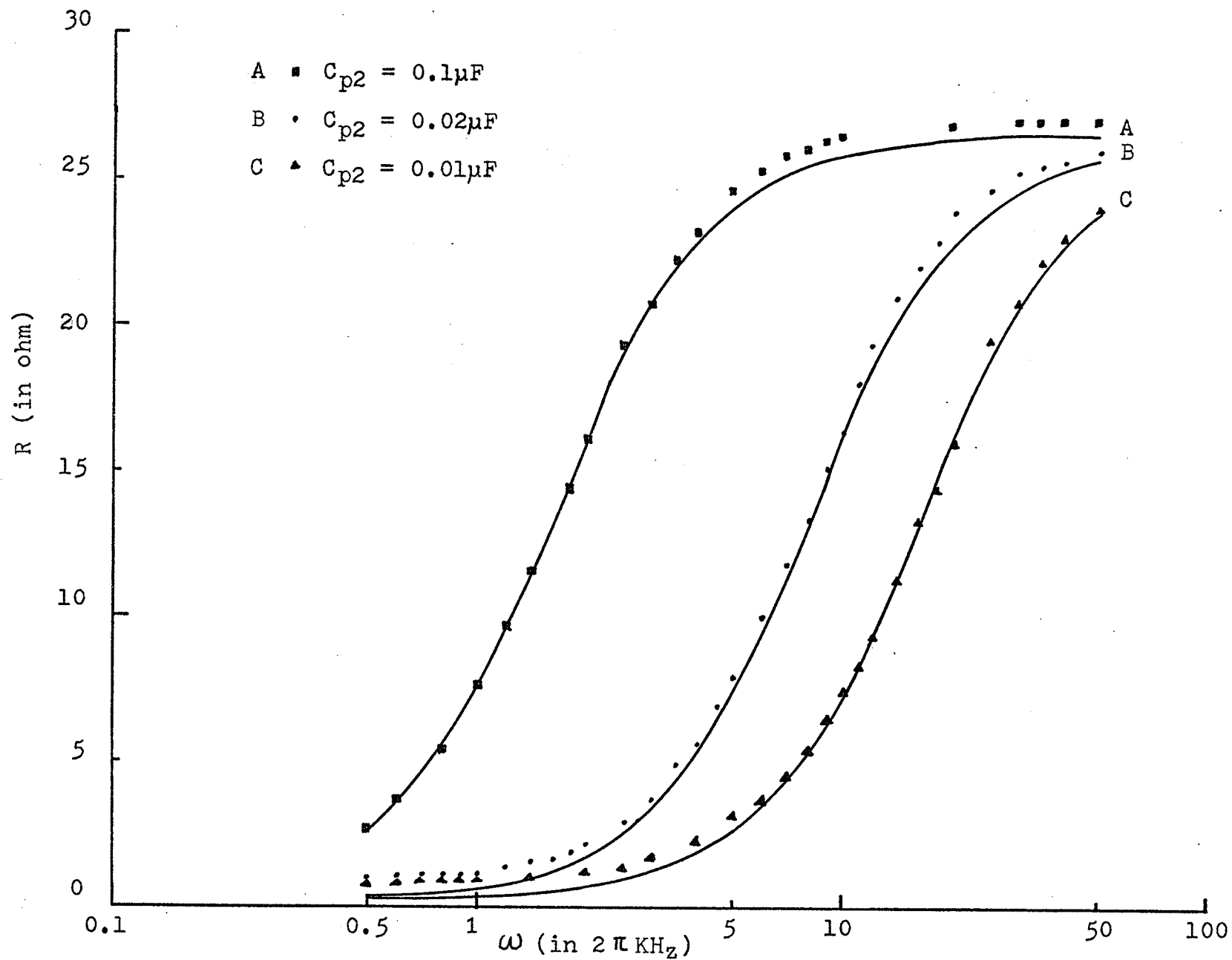
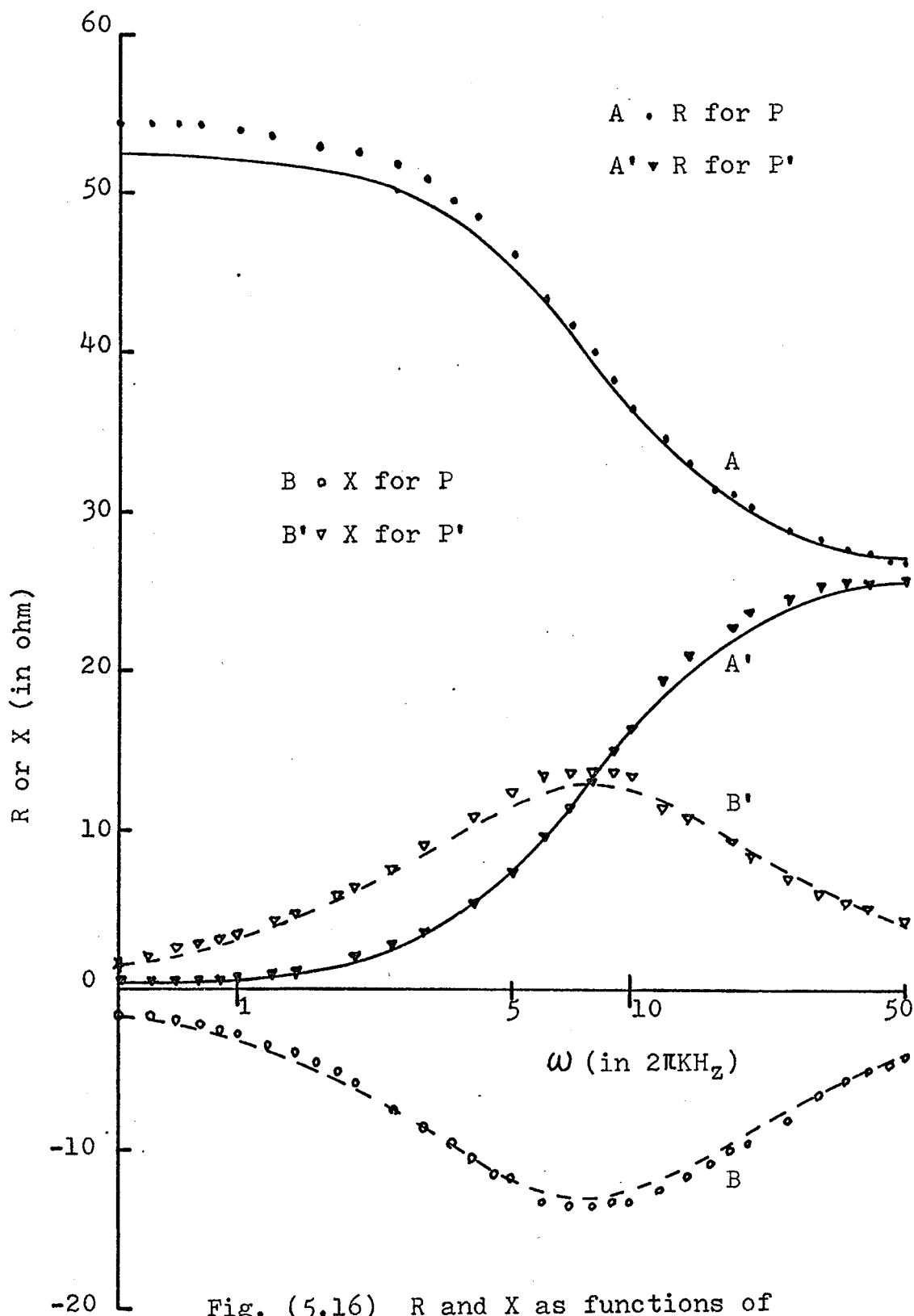


Fig. (5.15)  $R$  as a function of frequency and phase shifter capacitance.



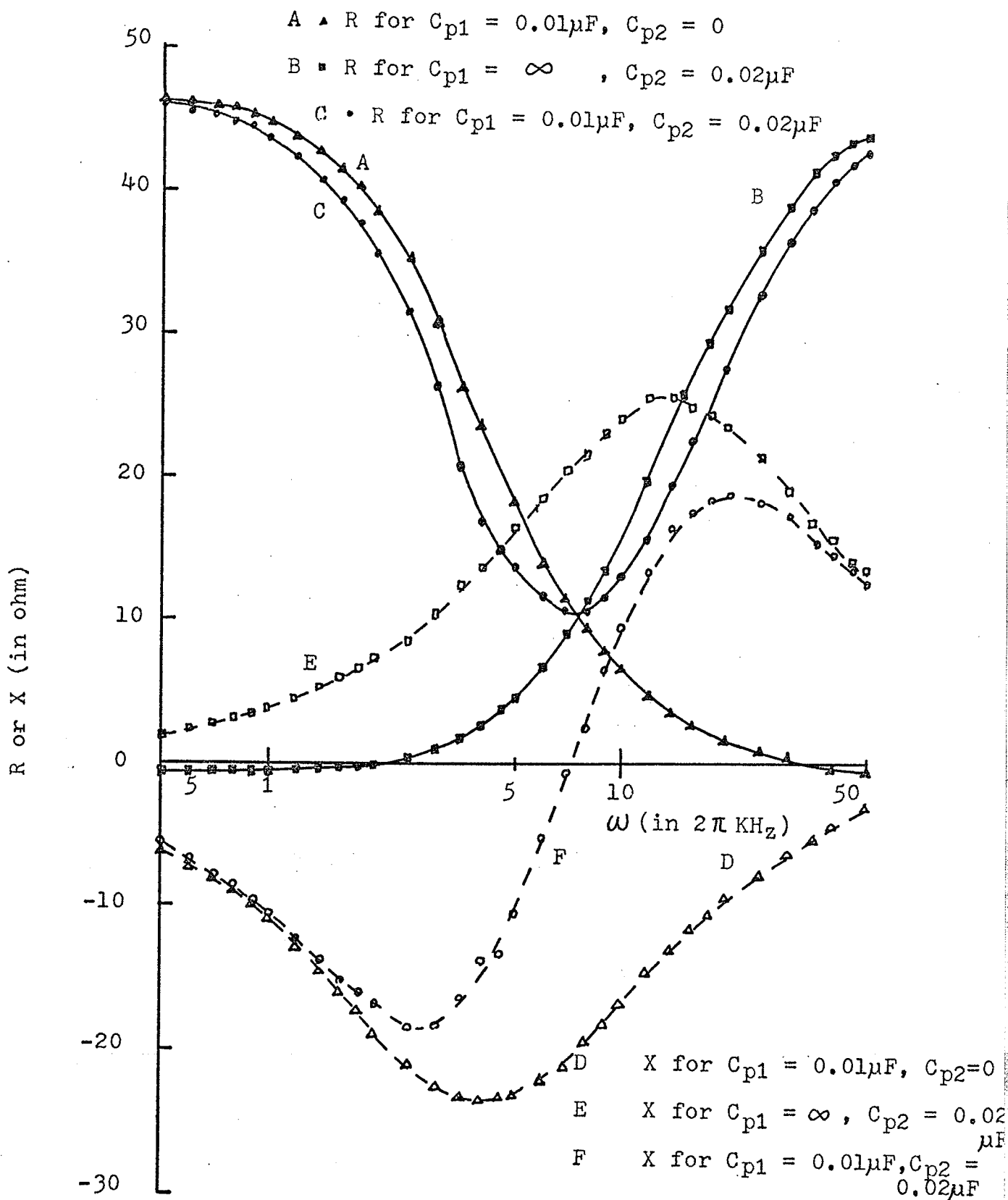


Fig. (5.17) R and X as functions of frequency and phase shifter capacitance.

by changing the value of phase shifter capacitance.

(b) The curves tend to shift toward a higher frequency range when  $C_{p2}$  is changed to a smaller value.

(c) For fine control it is better to use two phase shifters, one for coarse control and the other for fine control.

The magnitude of equivalent impedance depends on the current gain and generation constant  $G$ . The experimental results for  $G_1 = 0.583 \times 10^4$  and  $R_{I2} = 1 \text{ k}\Omega$  and  $G_2 = 1.23 \times 10^4$  and  $R_{I2} = 567 \Omega$  are shown in Fig. (5.18). The frequency ranges of the impedance for both conditions are different because the input impedance  $R_{I2}$  was changed by changing the gain of the amplifier.

#### 5.4 The Use of R.R.E.G. in An Experimental Tuned Circuit

We have shown in previous sections that R.R.E.G. can be made as a pure resistance element with positive or negative values, or a pure inductive reactance, or a pure capacitive reactance, or the combination of both. In this section we shall show how such an element can be used in an oscillator circuit and a tuned circuit. The experimental circuit for oscillation is shown in Fig. (5.19). For this case when

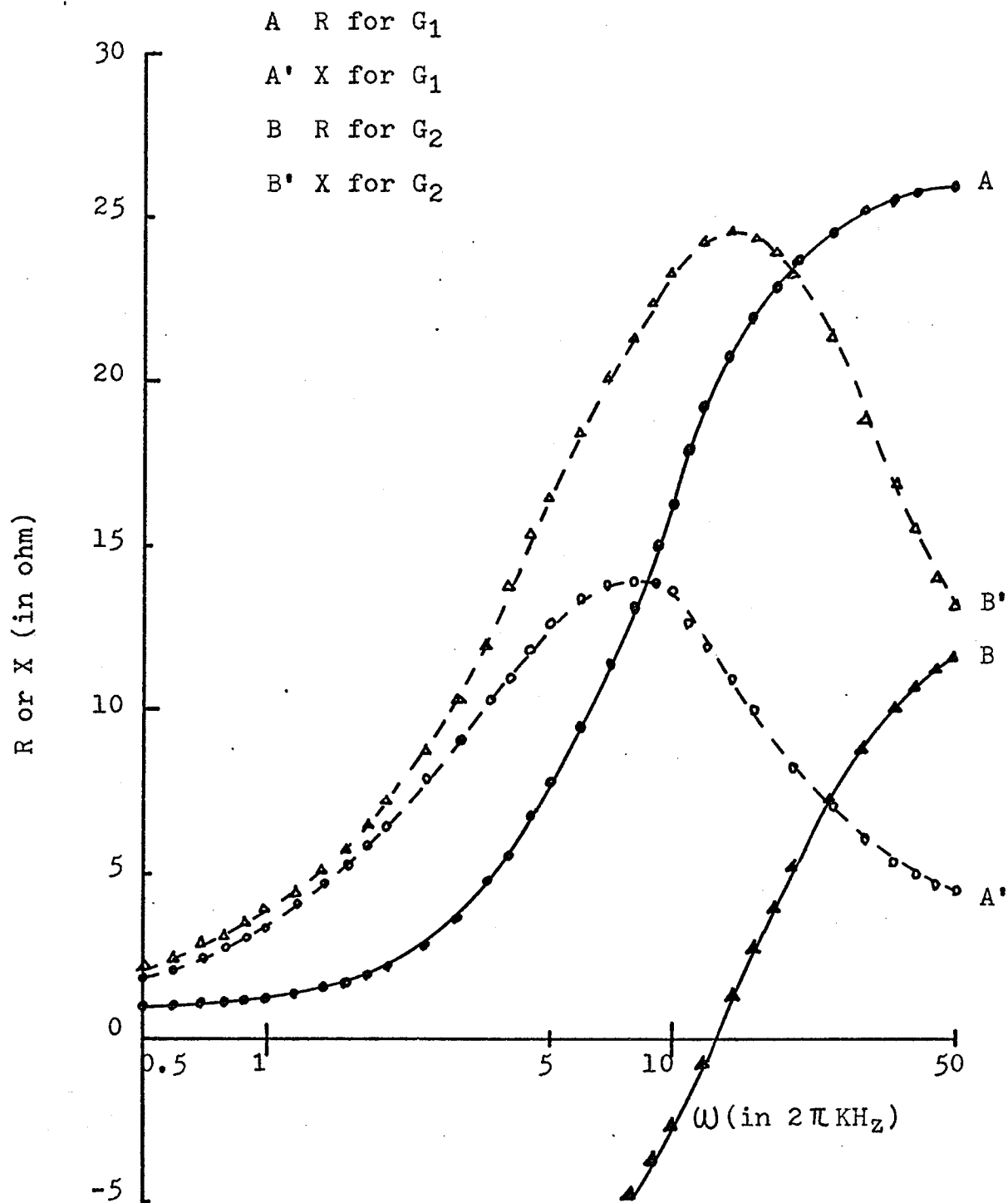
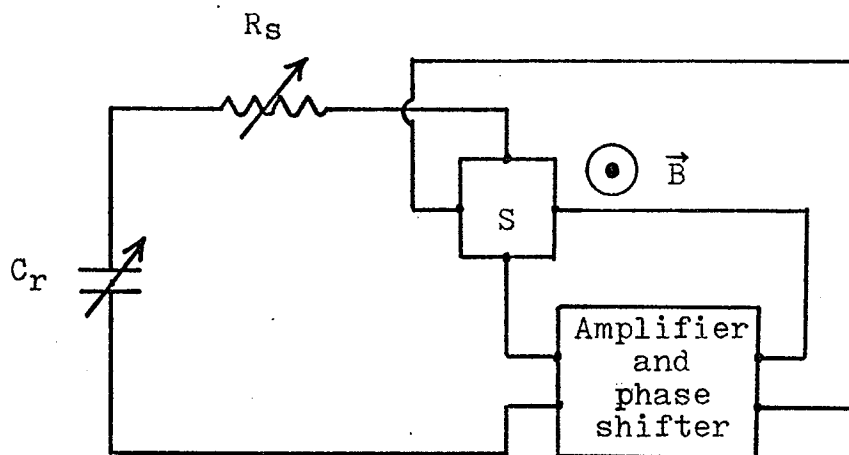
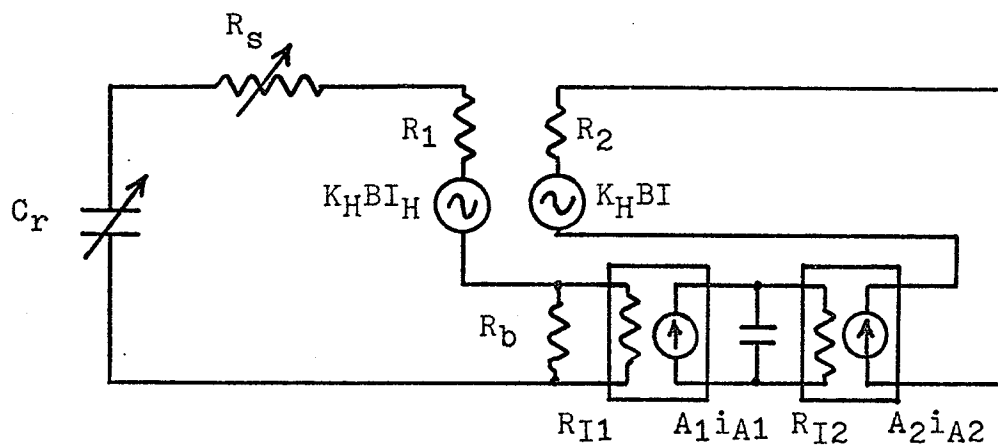


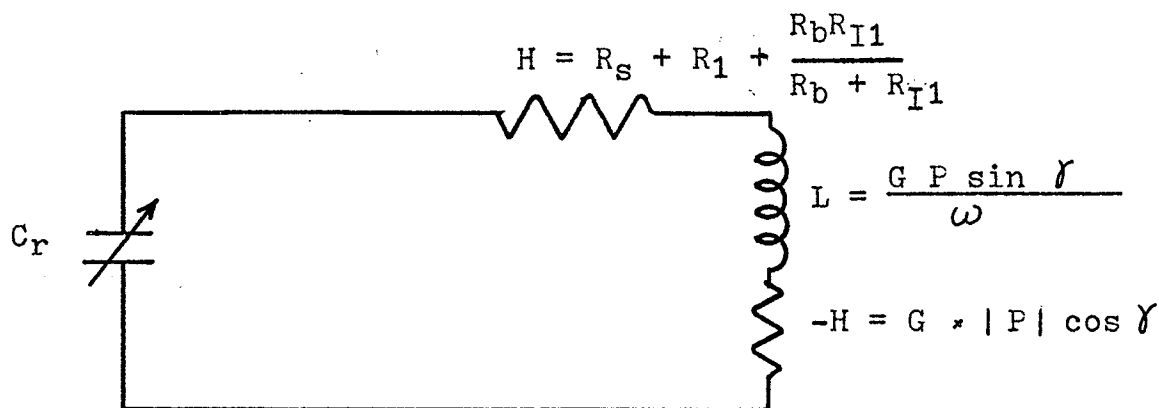
Fig. (5.18) Z for  $G_1 = 0.583 \times 10^4$   
 ( $R_{I2} = 1\text{K}\Omega$ ) and  $G_2 = 1.23 \times 10^4$  ( $R_{I2} = 567\Omega$ ).



(a) Experimental circuit



(b) Equivalent circuit of (a)



(c) Equivalent circuit

Fig. (5.19) The use of a R.R.E.G. in an oscillator circuit.

$I_H = 0$ , we have

$$Z = H = R_s + R_i + \frac{R_b R_{zi}}{R_b + R_{zi}} \quad (5.32)$$

and when  $I_H \neq 0$ , we have

$$\begin{aligned} Z &= H + GP \\ &= H + G|P| \cos \gamma + jG|P| \sin \gamma \\ &= R + jX \end{aligned} \quad (5.33)$$

The oscillation occurs when  $R = 0$  and  $X = X_{C_r}$  i.e. when  $H = -G|P| \cos \gamma$  and  $X_{C_r} = G|P| \sin \gamma$ . For different values of phase shifter, we can adjust  $C_r$  and  $R_s$  to meet the conditions for oscillations. Fig. (5.20) shows the values of  $X (= X_{C_r})$  and  $H (= -G|P| \cos \gamma)$  as functions of frequency.

We also use this element in a tuned circuit as shown in Fig. (5.21) for parallel resonance and Fig. (5.22) for series resonance. The experimental results are shown in Fig.(5.23) to(5.26) for  $C_r = 0.91 \mu F$ ,  $0.74 \mu F$ ,  $0.555 \mu F$ ,  $0.355 \mu F$  and  $0.185 \mu F$ . The higher the resonance frequency, the broader is the bandwidth of the resonance and the lower is the value of the quality factor  $Q$ .

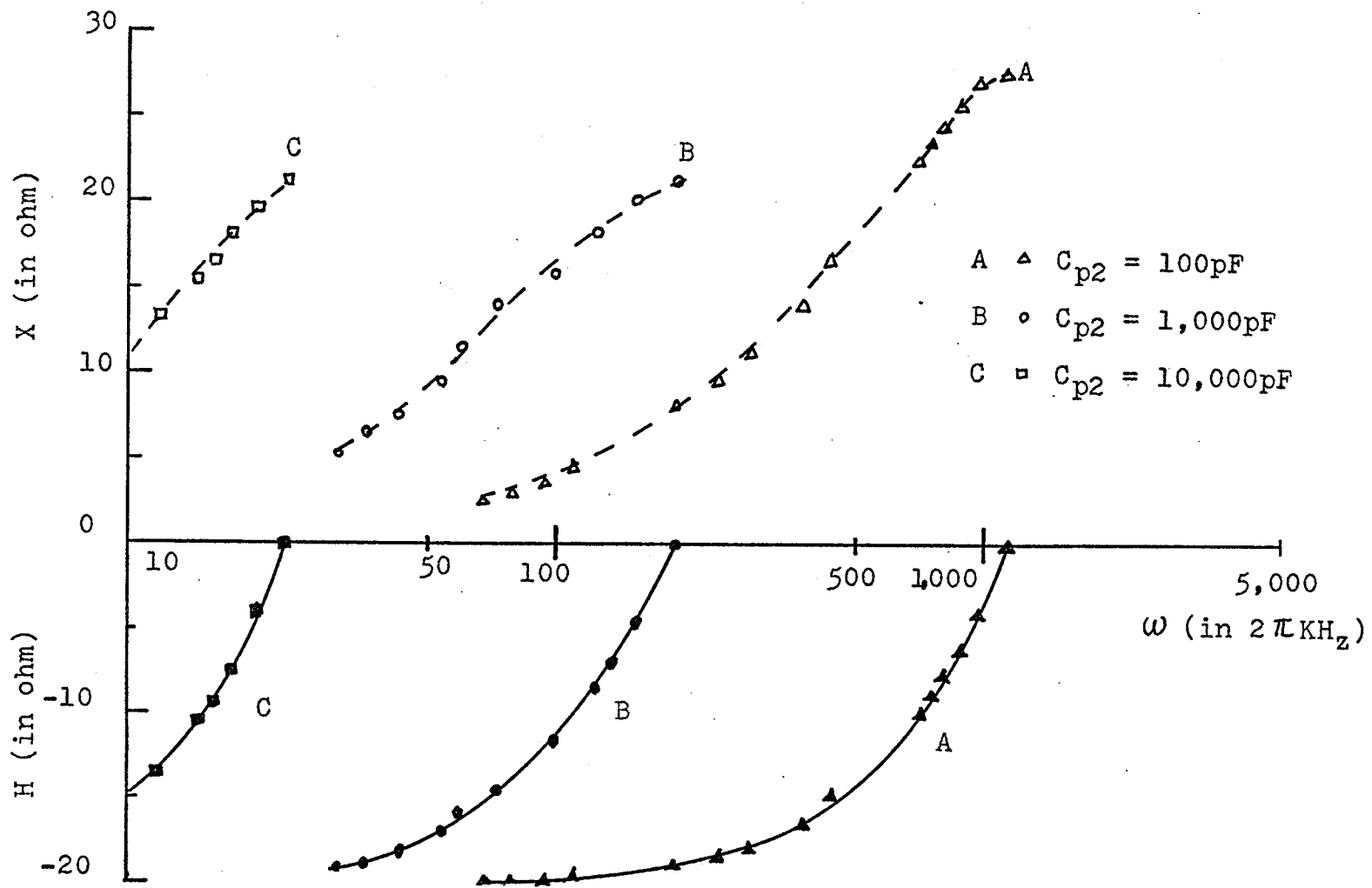
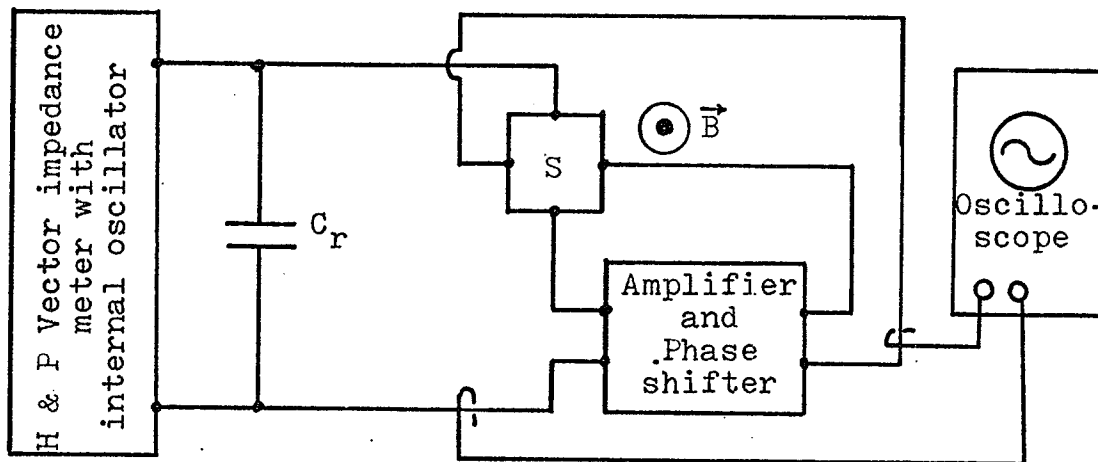
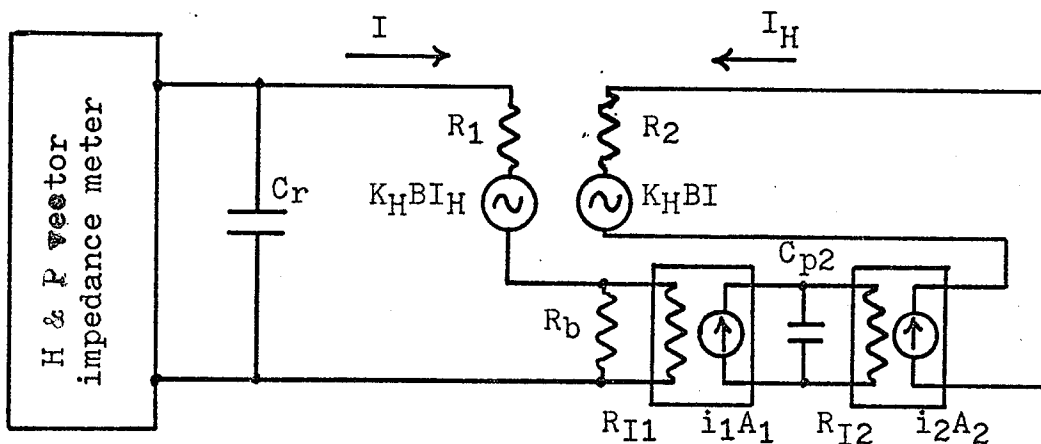


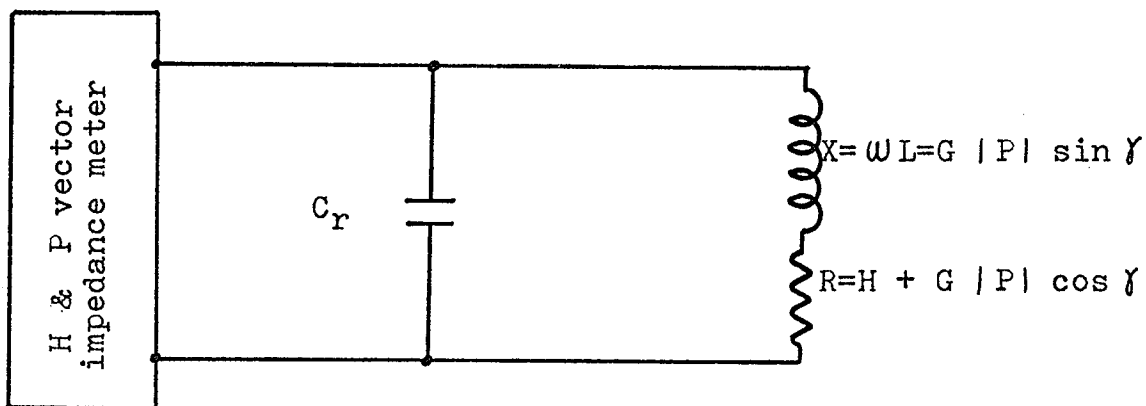
Fig. (5.20) Experimental results of current oscillation



(a) Experimental circuit

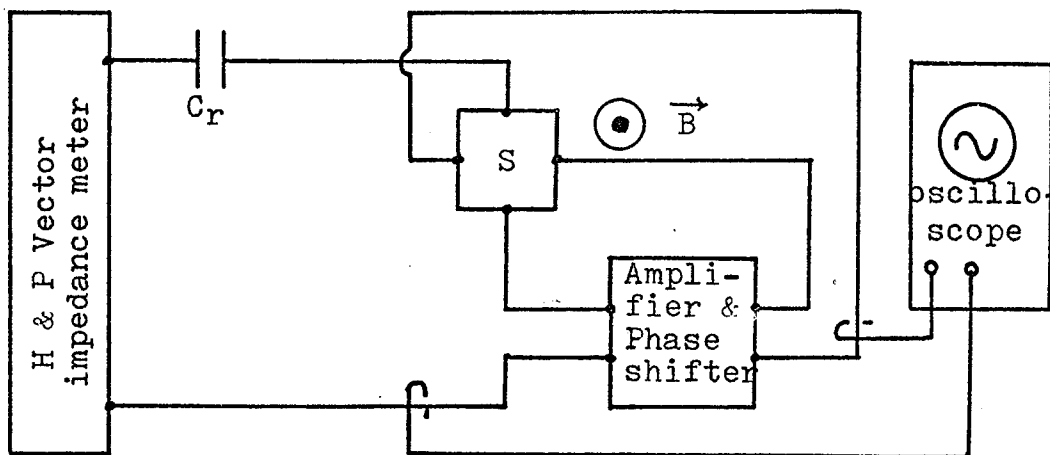


(b) Equivalent circuit of (a)

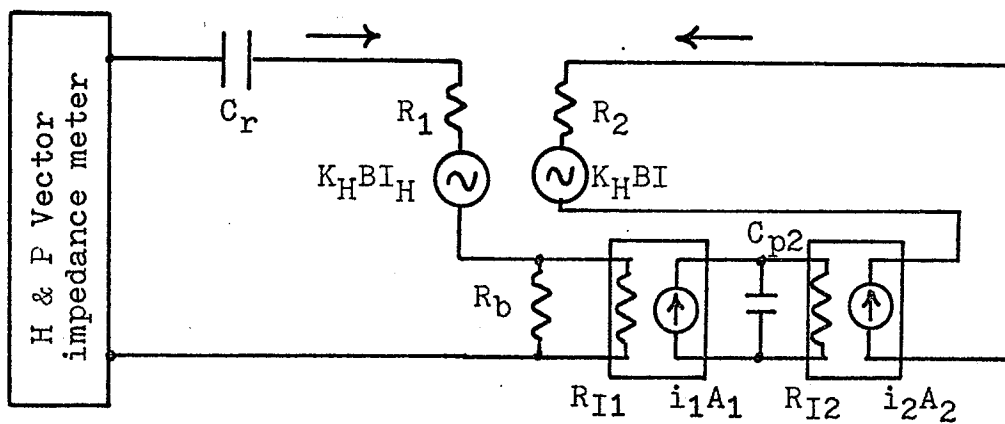


(c) Parallel resonance circuit

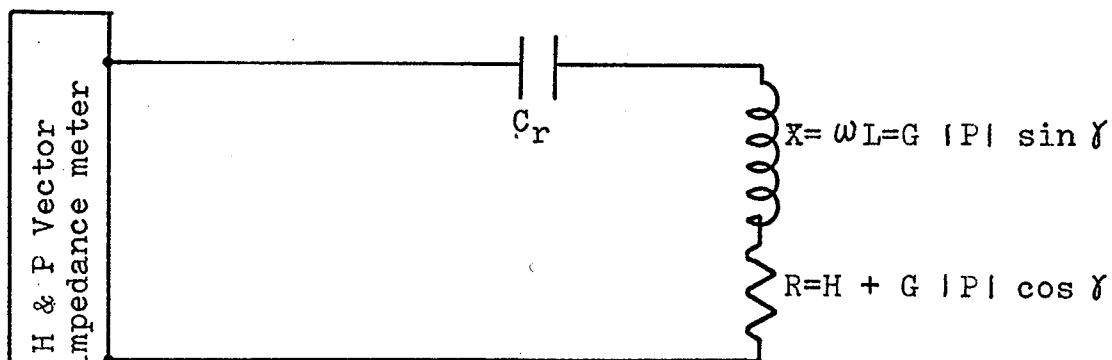
Fig. (5.21) The use of R.R.E.G. in a tuned circuit (parallel resonance)



(a) Experimental circuit



(b) Experimental circuit of (a)



(c) Series resonance circuit

Fig. (5.22) The use of R.R.E.G. in a tuned circuit (series resonance).

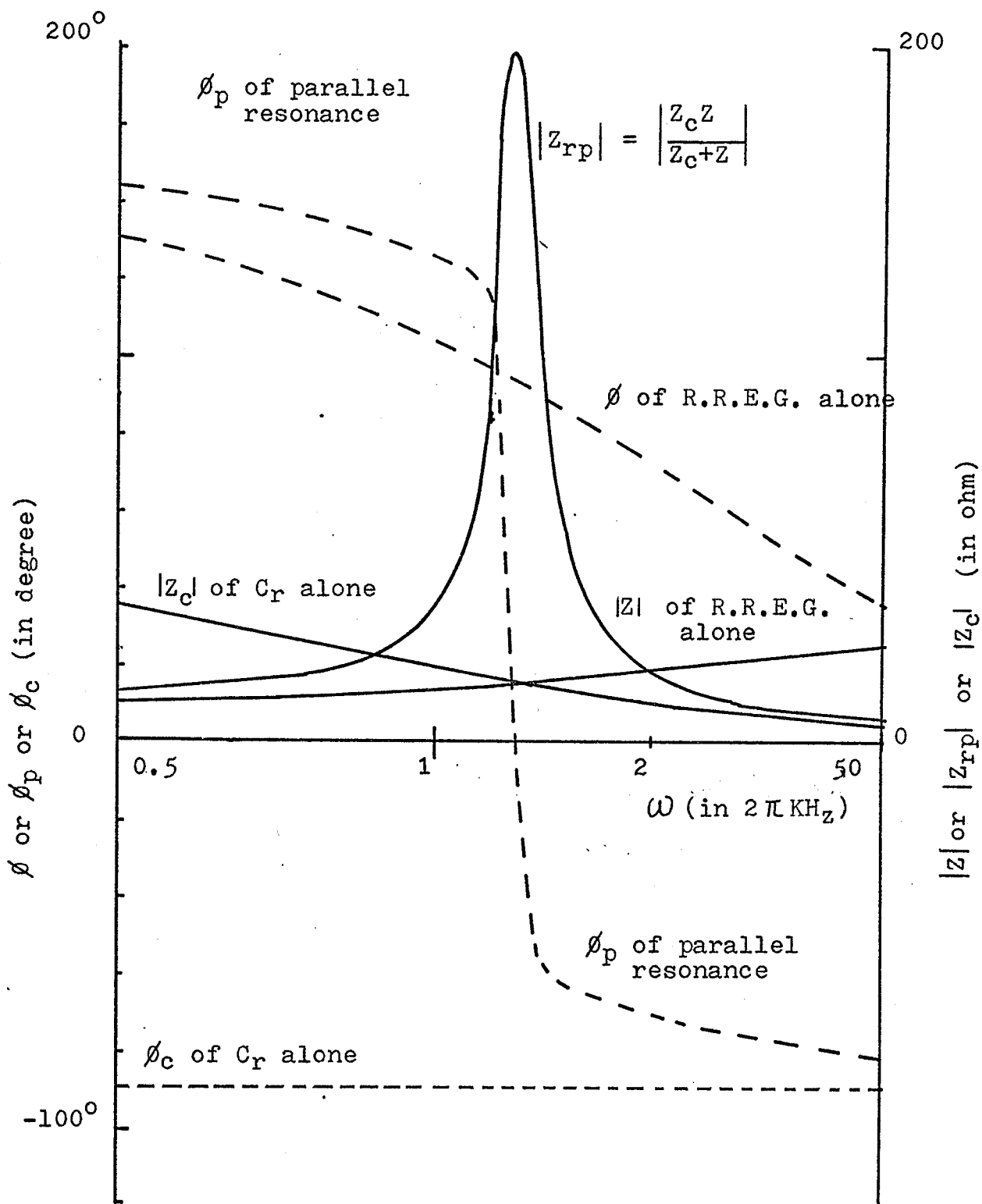


Fig. (5.23) Experimental result of parallel resonance.

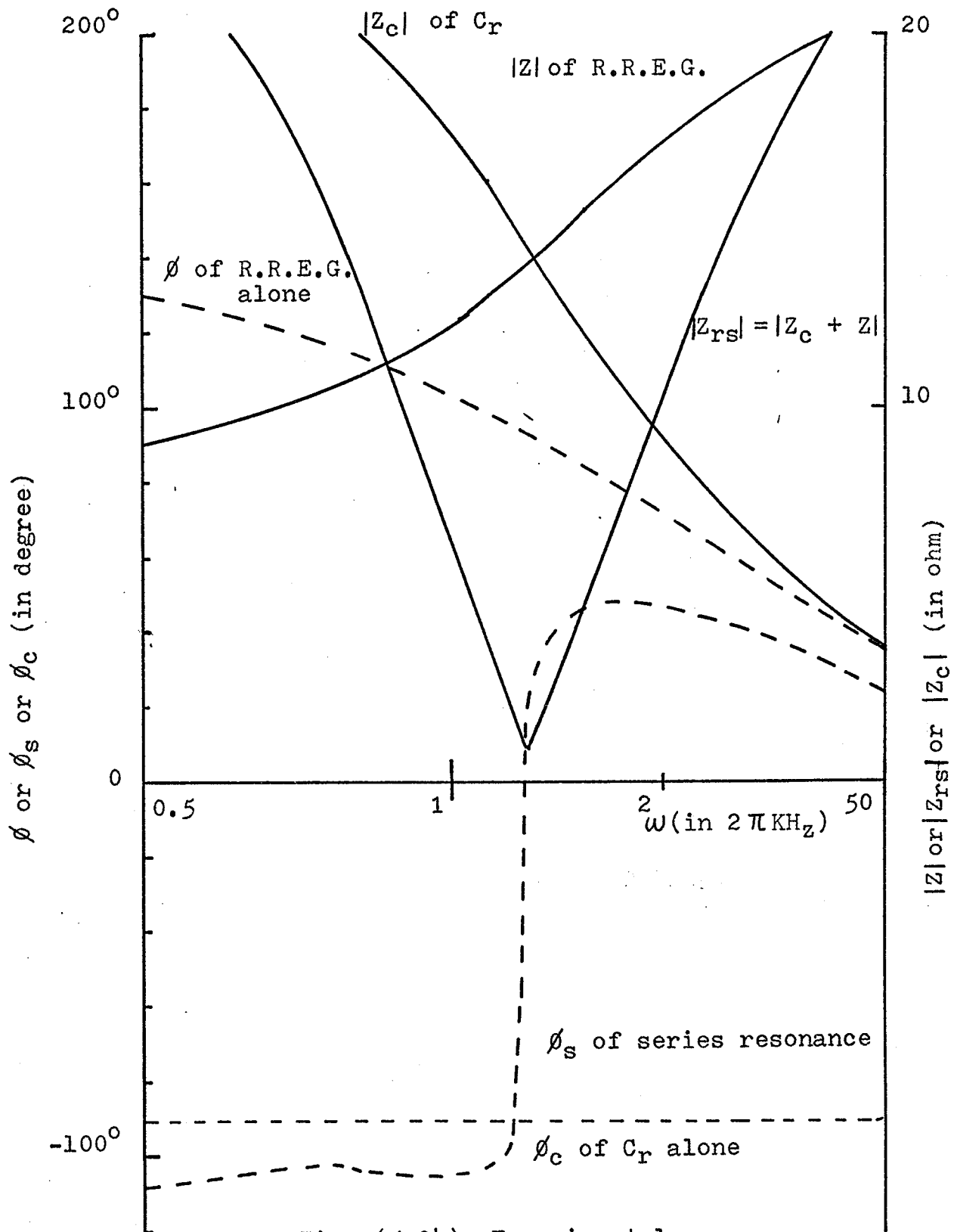


Fig. (5.24) Experimental result of series resonance.

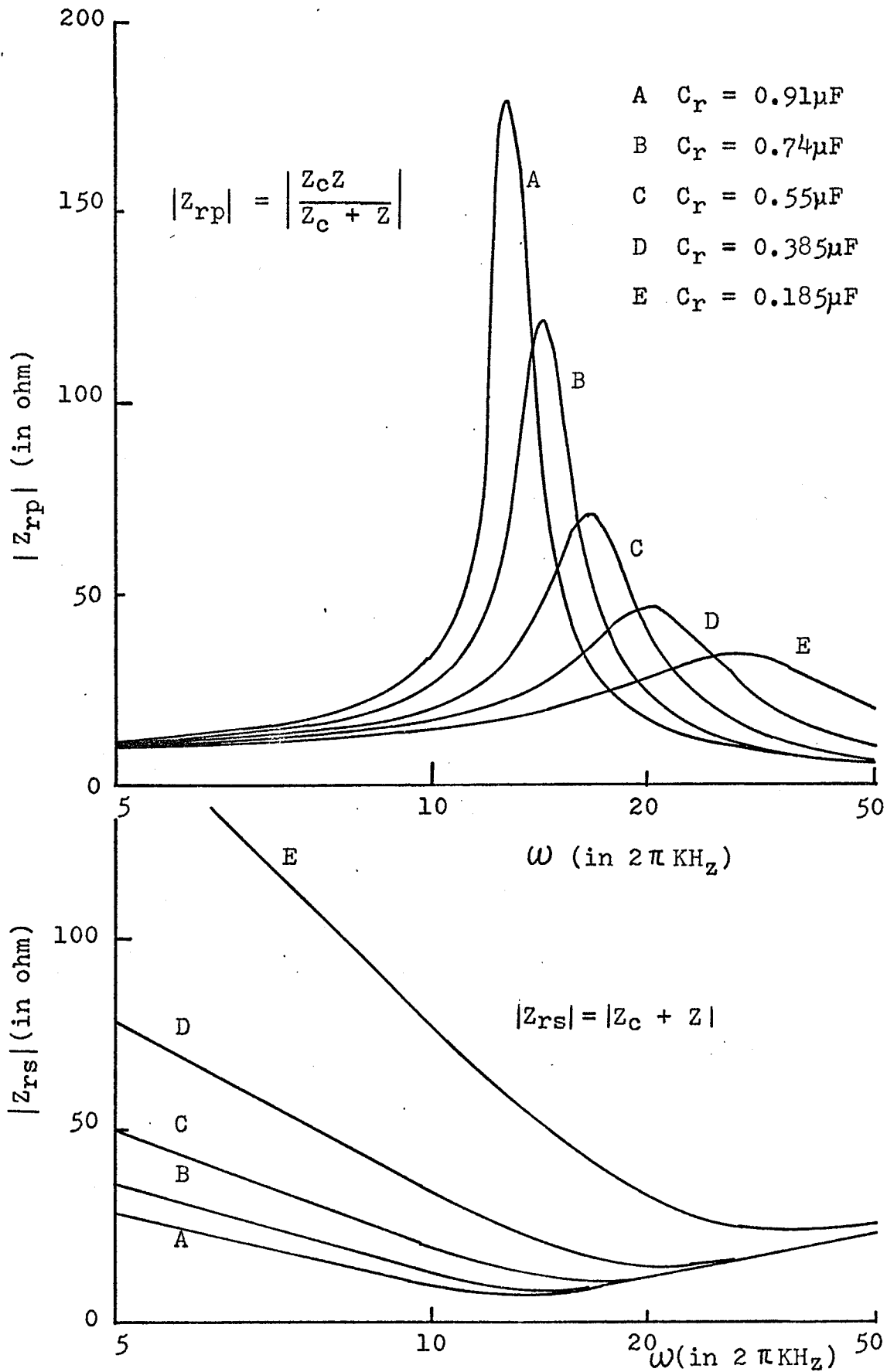


Fig. (5.25) Parallel resonance and series resonance for different values of capacitance  $C_r$  ( $C_r = 0.91\mu\text{F}$ ,  $0.174\mu\text{F}$ ,  $0.555\mu\text{F}$ ,  $0.385\mu\text{F}$  and  $0.185\mu\text{F}$ )

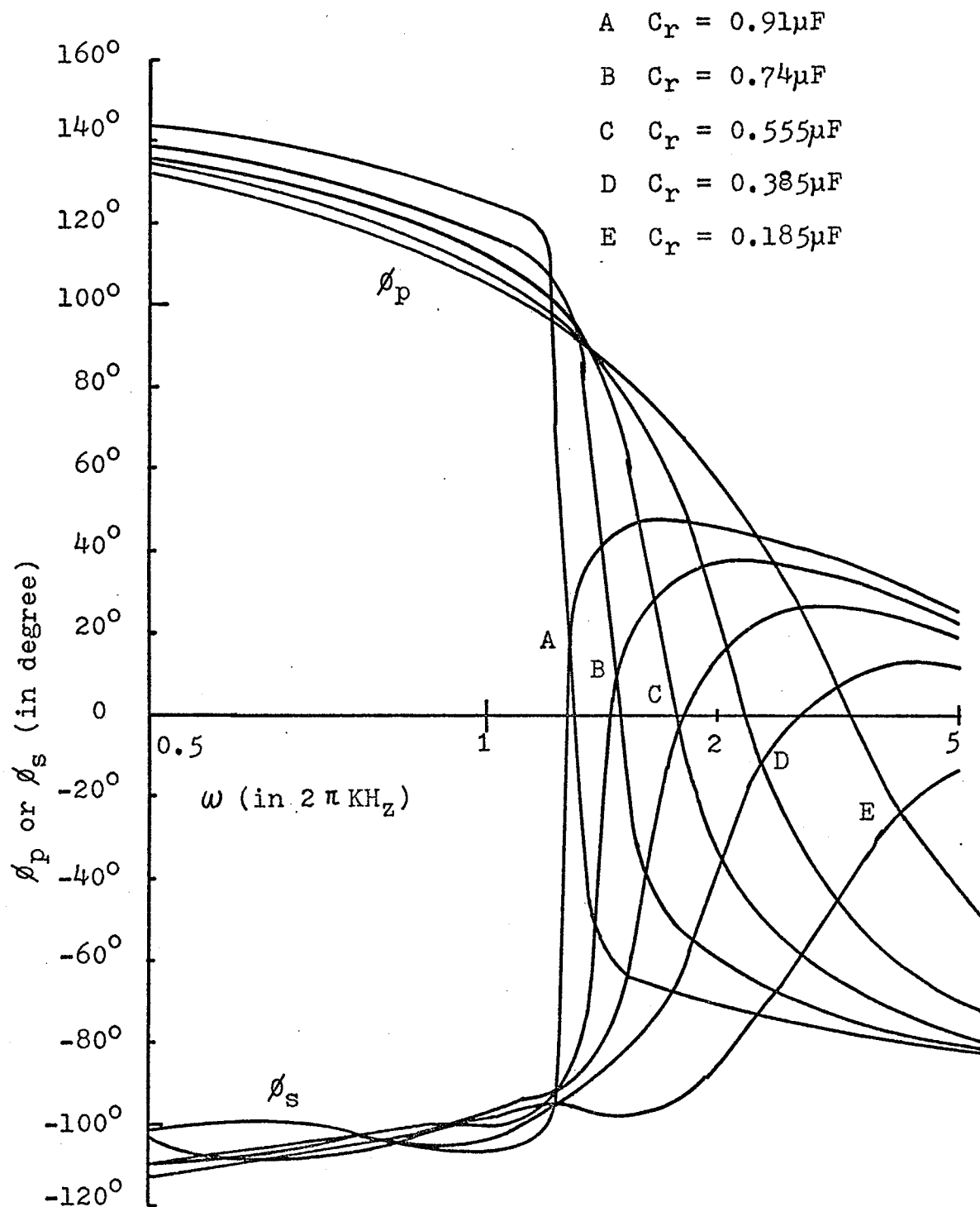


Fig. (5.26)  $\phi_p$  for parallel resonance and  $\phi_s$  for series resonance for different values of capacitance  $C_r$ .

## CHAPTER VI

## CONCLUSIONS

The experimental results on the electrical characteristics of the proto-type resistive and reactive elements based on galvanomagnetic effects (R.R.E.G.) are in good agreement with theoretical prediction. From the results we can conclude that

- (1) The R.R.E.G. can be made either as an inductance, a capacitance, a positive or a negative resistance, or a combination of them. The magnitude and the characteristics of the R.R.E.G. depend upon the magnetic field, the ratio of the Hall current to the current flowing through the current terminals and the phase angle between these two currents, and the operating frequency range.
- (2) If frequency of the exciting source connected to the Hall terminals is different from that of the active network to be connected to the current terminals, the equivalent impedance of the R.R.E.G. will be time-dependent. The rate of change of the impedance depends upon the difference between the two frequencies.

(3) If the whole system involves only one frequency, the equivalent impedance becomes time-independent, but it depends upon the relative magnitudes and phase angles of the Hall current  $I_H$  at the Hall terminals and the current  $I$  at the current terminals.

(4) In order to make the equivalent impedance independent of  $I$ , the ratio  $\left| \frac{I_H}{I} \right|$  must be kept constant. To do so, the amplifier must be linear and the phase shifter must be stable.

(5) The behaviour of R.R.E.G. in the oscillator circuit and in the tuned circuit is similar to that of a conventional reactive element. The higher the value of the quality factor, the narrower is the band-width of the resonance.

(6) There are many possible applications of R.R.E.G. For example, the negative capacitance of R.R.E.G. can be used to eliminate the stray capacitance of any circuits, such as antenna circuits. Similarly, the negative resistance or the negative inductance can be used to eliminate the unwanted resistance or inductance in a circuit. As such elements

can be easily miniaturized, they can be used to represent any parameters for microelectronic circuits.

## APPENDIX A

## THE TIME DEPENDENCE OF EQUIVALENT IMPEDANCE

The impedance of a network looking at two terminals is usually defined as the ratio of the voltage between the two terminals to the current flowing into the network and it is time-independent because it usually involves not more than one frequency at a time. If the impedance involves two different sources of two different frequencies, then it becomes time-dependent. From Equation (3.4) we can write

$$Z(\omega_0, \omega_1, t) = f \left\{ \frac{E_0(\omega_0, t)}{E_1(\omega_1, t)} \right\}$$

If we write

$$E_0(\omega_0, t) = |E_0| e^{j\omega_0 t}$$

and

$$E_1(\omega_1, t) = |E_1| e^{j(\omega_1 t + \varphi_0)}$$

where  $\varphi_0$  is the phase angle between  $E_0$  and  $E_1$  at  $t=0$  then

$$\begin{aligned} \mathcal{E} = \frac{E_0(\omega_0, t)}{E_1(\omega_1, t)} &= |\mathcal{E}| \cos \{ (\omega_0 - \omega_1)t - \varphi_0 \} \\ &+ j |\mathcal{E}| \sin \{ (\omega_0 - \omega_1)t - \varphi_0 \} \end{aligned}$$

where  $t \leq \frac{2\pi}{\omega_0 - \omega_1}$

It can be seen that if  $\omega_0 = \omega_1$ ,  $Z$  becomes time-independent. Fig. (A.1) shows the time-dependent phase relation between  $E_0$  and  $E_1$  for  $|E_0| = |E_1|$  and Fig. (A.2) shows the variation of  $\xi$  with time. Since  $\xi$  is a function of time,  $Z$  depends upon time.

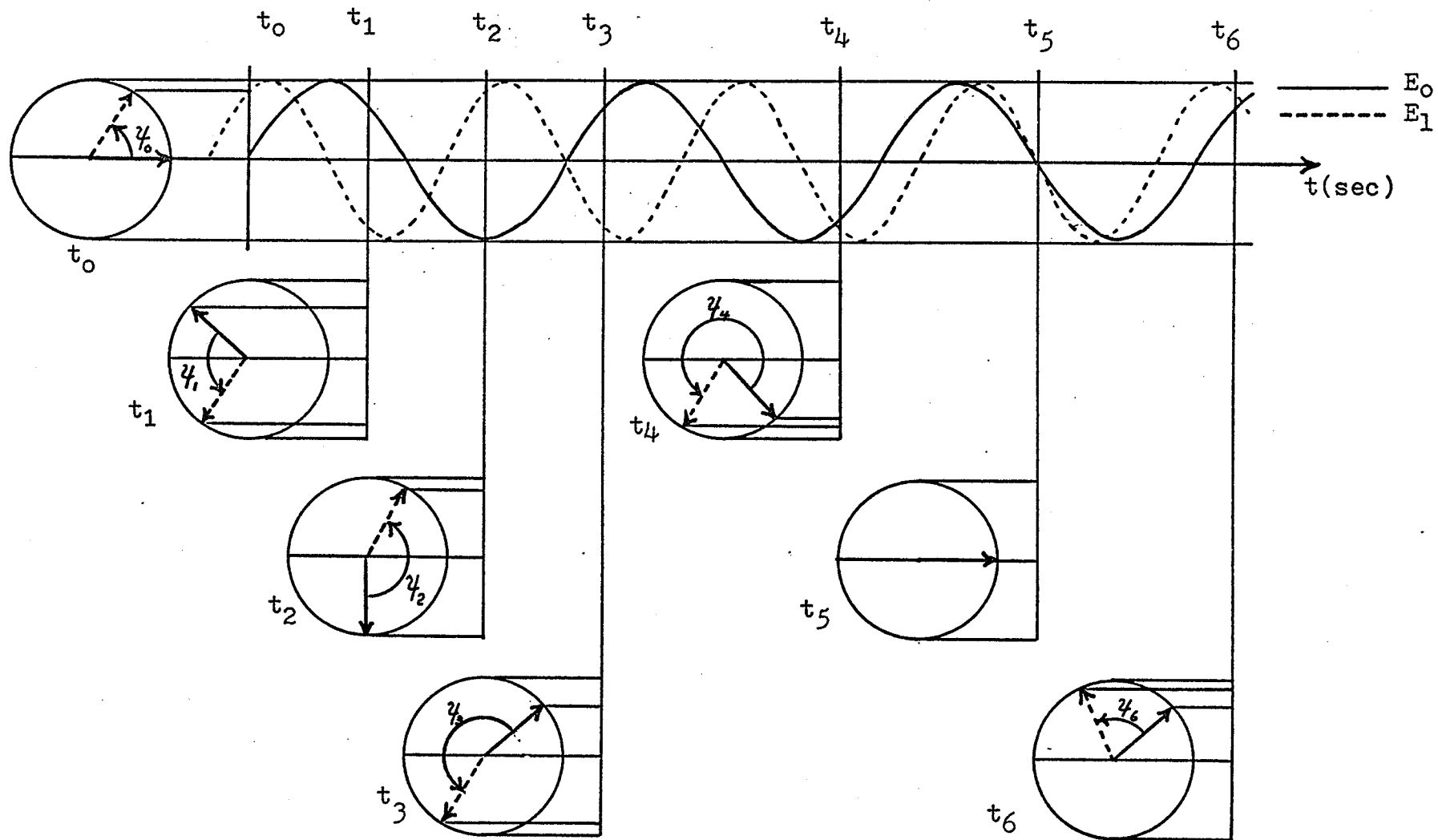


Fig. (A.1) Phase relation between  $E_0$  and  $E_1$  for the case  $|E_0| = |E_1|$ .

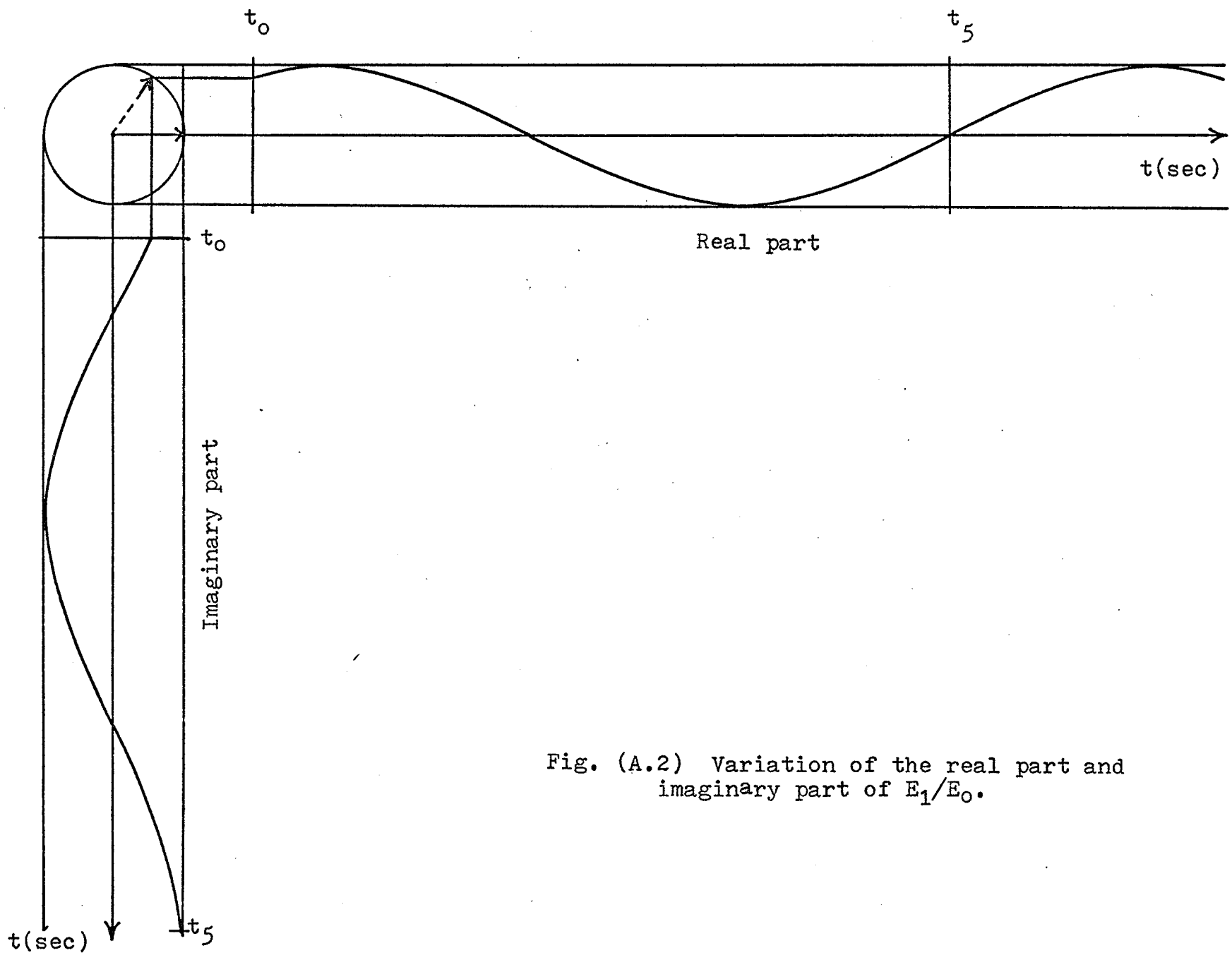


Fig. (A.2) Variation of the real part and imaginary part of  $E_1/E_0$ .

## APPENDIX B

THE PHYSICAL MEANING OF  $Q$ 

The quality factor  $Q$  is usually defined as

$$Q = \frac{|X|}{R}$$

$X = \omega L$  for the impedance consisting of an inductive reactance and  $X = \frac{1}{\omega C}$  for the impedance consisting of a capacitive reactance. The quality factor at resonance is given by

$$Q_0 = \omega_0 \frac{\text{energy stored}}{\text{average power dissipated}}$$

In our resistive and reactive elements based on galvanomagnetic effects (R.R.E.G.) the value of  $R$  can be negative. Under this condition  $Q$  is negative. The negative  $Q$  indicates that the impedance element does not dissipate energy, but rather, generates energy. Generally the higher the value of  $Q$ , the lower is the energy dissipation when  $Q$  is positive, and the lower is the energy generation when  $Q$  is negative. Thus the element having a negative  $Q$  can be used to compensate the energy dissipation of the element having a positive  $Q$ .

## BIBLIOGRAPHY

- Barnwell, P.G., "Thick-Film Inductors at VHF",  
Electronic Components, pp 681 - 684,  
June (1970).
- Barlow, H.M., "Hall Effect and Its Application to  
Microwave Power Measurement," Proceedings  
of the IRE, vol. 46, pp 1411-1413, (1958).
- Barlow, H.M., "A Proposed New Method of Measuring  
Microwave Power and Impedance Using Hall  
Effect in a Semiconductor", Proceedings  
IEEE, vol. 109B, pp 286-289, (1962).
- Barlow, H.M. and Kataoka, S., "The Hall Effect and  
Its Application to Power Measurement at  
10 Gc/s", Proceedings of IEEE, vol. 105B,  
pp 53-60, (1958).
- Beer, A.C., "The Hall Effect and Related Phenomena",  
Solid State Electronics, vol. 9, pp 339-  
351, (1966).
- Capparelli, F., "Simulatore di Induttanze ad Elevato  
per circuiti in Microminiatura", Alta  
Frequenza, vol. 36, pp 226-232, (1966).
- Champlin, K.S., "Hall Field Relaxation in Semi-  
conductors at High Frequency", J. appl.  
Phys., vol. 31, pp 1770-1771, (1960).
- Debye, P.P. and Conwell, E.M., "Electrical Proper-  
ties of N-Type Germanium", Phys. Rev.,  
vol. 93, pp 693-696, (1954).
- Ghandi, S.G., "The Theory and Practice of Micro-  
electronics", John Wiley and Sons Ltd.,  
(1968).
- Haeusler, J., "Die Geometriefunktion Vierelektro-  
diger Hallgeneratoren", Archiv für  
Elektrotechnik, vol. 52, pp 11-19, (1968).
- Harman, T.C., Goering, H.L. and Beer, A.C.,  
"Electrical Properties of N-Type InAs",  
Phys. Rev., vol. 104, pp 1562-1564, (1956).

- Josephs, H.C., George, R.I. and Billette, R., "Solid State Inductors", Solid-State Electronics, vol. 8, pp 775-788, (1965).
- Kataoka, S. and Hashizume, N., "A Variable Impedance Device Using Galvanomagnetic Effects in Semiconductors", Proceedings IEEE (correspondence), vol. 53, pp 2138-2139, (1965).
- Kataoka, S. and Hashizume, N., "Variable Reactance Element Using Galvanomagnetic Effect in Semiconductors", Bul. Electrotech. Lab. (Tokyo, Japan), vol. 30, No. 8, pp 716-722, (1966).
- Kataoka, S., Hashizume, N. and Iida, S., "Magnetoreactive Element and New Solid-State Inductor", Solid State Electronics, vol. 11, pp 155-162, (1968).
- Laxpati, S. and Mittra, R., "Antenna Impedance Matching by Means of Active Networks", Antenna Lab. Tech. Report No. 64 (University of Illinois), (1962).
- Lin, H.C., "Integrated Electronics" Holden-Day (1967).
- Morin F.J. and Maita, J.P., "Electrical Properties of Silicon Containing Arsenic and Boron", Phys. Rev., vol. 96, pp 28-35, (1954).
- Morin, F.J. and Maita, J.P., "Conductivity and Hall Effect in the Intrinsic Range of Germanium", Phys. Rev., vol. 94, pp 1525-1529, (1954).
- Motto, J.W., "Developing the Hall Generator Equivalent Circuit", Electronics, vol. 35, 1190-1192, (1962).
- Nishina, Y. and Spry, W.J., "Measurement of the Hall Mobility in N-Type Germanium at 9121 Megacycles", J. Sppl. Phys., vol. 29, pp 230-231, (1958).
- Toda, M., "Solid-State Inductive Element Using Magnetoresistance", Proc. IEEE (corresp.), vol. 54, pp 1456-1457, (1966).
- Valkenburg, M.E.V., "Network Analysis", Prentice-Hall, (1955).

Weiss, H., "Galvanomagnetic Devices", IEEE Spectrum, pp 75-82, Jan. (1968).

Wick, R.F., "Solution of the Field Problem of the Germanium Gyrator", J. App. Phys., vol. 25, pp 741-756, (1954).